Delft University of Technology
Faculty of Electrical Engineering, Mathematics and Computer Science
Delft Institute of Applied Mathematics

Using futures in yield curve calibration

A thesis submitted to the
Delft Institute of Applied Mathematics
in partial fulfillment of the requirements

for the degree

MASTER OF SCIENCE
in
APPLIED MATHEMATICS

by

Alexander Lee
Delft, The Netherlands
September 2019

MSc thesis in Applied Mathematics

Financial Engineering

"Using futures in yield curve calibration"

Alexander Lee, 4345983

Delft University of Technology

Daily supervisor

Ir. Marko Iskra

Responsible professor

Prof.dr.ir. C.W. Oosterlee

Other thesis committee members

Dr.ir. Lech Grzelak

Dr.ir. Robbert Fokkink

September, 2019

Delft

Abstract

The yield curve represents market supply and demand implied expectations of future interest rates and is calibrated from the most liquidly traded interest rate derivatives like cash deposits, forward rate agreeents, swaps and futures. Due to the daily margining mechanism of futures contracts, interest rate futures require the substraction of a convexity adjustment in order for them to be used in curve calibration. It is common practice to use externally computed convexity adjustments, which treats the convexity adjustment as a black-box parameter. We will argue the inherent relationship between the convexity adjustment and cap/floor volatility smiles and derive a nested calibration algorithm for the simultaneous calibration of the yield curve to futures and the convexity adjustment to cap/floor volatility surfaces. This introduces dependencies of the yield curve to to option volatilities and we will argue that for simple interest rate derivatives the implied vegas are negligible.

Keywords: Futures, Interest rates, Yield curve, Volatility smile, Calibration, Greeks

Acknowledgements

This thesis has been written for the receival of the degree of Master of Science in Applied Mathematics at Delft University of Technology. First and foremost I would like to thank Erik van Raaij, head of the Pricing Model Validation team for providing me with a welcoming and stimulating environment at Rabobank International in Utrecht to do my thesis work. I would like to thank my daily supervisor Ir. Marko Iskra for introducing and guiding me through the subject and providing me with a lot of help through moments of hardship. Special thanks goes to Prof. C.W. Oosterlee and Dr. Ir. Lech Grzelak for providing me with useful feedback in writing of the thesis and the members of the Pricing Model Validation team for helping me answer questions related to the underlying mathematics and programming involved. Finally, I would like to thank my mother Ljoedmila van Vyve and my girlfriend Camila Arizpe for supporting me throughout the process.

Glossary

$(\mathbb{Q}, D)$ Risk neutral numeraire pair.

$(\mathbb{Q}^M, P(\cdot, M))$ M-forward measure numeraire pair.

$C_t^{(i)}$ Convexity adjustment corresponding to the spot Libor rate with accruing period $[T_i, T_{i+1}]$. When used individually (without superscript), the accruing period is $[T, M]$.

$F_t^{(i)}$ Forward overnight rate with accruing period $[T_i, T_{i+1}]$. When used individually (without superscript), the accruing period is $[T, M]$.

$F_{T_i}^{(i)}$ Spot overnight rate with accruing period $[T_i, T_{i+1}]$. When used individually (without superscript), the accruing period is $[T, M]$.

$Fut_t^{(i)}$ Eurodollar Futures rate with accruing period $[T_i, T_{i+1}]$. When used individually (without superscript), the accruing period is $[T, M]$.

$L_t^{(i)}$ Forward Libor rate with accruing period $[T_i, T_{i+1}]$. When used in the context of caplets, the accruing period is $[T_i', T_{i+1}']$. When used individually (without superscript), the accruing period is $[T, M]$.

$L_{T_i}^{(i)}$ Spot Libor rate with accruing period $[T_i, T_{i+1}]$. When used in the context of caplets, the accruing period is $[T_i', T_{i+1}']$. When used individually (without superscript), the accruing period is $[T, M]$.

$P(t, T)$ Libor curve discount factor, single-curve framework.

$P^{(O)}(t, T)$ Overnight curve discount factor, multi-curve framework.

$P^{(\tau)}(t, T)$ Libor curve discount factor, multi-curve framework, tenor $= \tau$.

S_t Libor forward swap rate at time t defined over a Libor swap over n floating payments of the spot Libor over time structure $T_0 < ... < T_n$ and m fixed payments of the swap rate over $T_0' < ... < T_m'$..

T_i' Fixed leg or caplet maturity time structure.

T_i Curve calibration instrument maturities and settlements, $[T, M]$ used when talking about one accruing period.

$\mathbf{C}$ Fixed convexity adjustments or convexity adjustment vector used in curve calibration. .

$\sigma_{\mathbf{P}}^{(\theta)}$ θ-shifted at the money caplet volatility vector used in convexity adjustment calibration..

$\sigma^{(\theta)}(K)$ Caplet volatility spine point vector, used in absolute strike volatility stripping. Given $T_1' < ...T_n'$ the maturities of the underlying caplets $\sigma_{T_i'}^{(\theta)}(K)$ corresponds to the caplet with underlying spot Libor having accruing period $[T_i', T_{i+1}']$.

$\sigma^{(\theta)}$ θ-shifted at the money caplet volatility surface..

$\sigma^{(\theta_{\mathbf{flat}})}(K)$ Flat cap volatility spine point vector, used in absolute strike volatility stripping..

τ_i' Tenor corresponding to loan period $[T_i', T_{i+1}']$, when used in the context of caplets.

τ_i Tenor corresponding to accruing period $[T_i, T_{i+1}]$., τ is used for accruing period $[T, M]$. .

$\mathbf{P}^{(O)}$ Overnight spine point vector.

$\mathbf{P}^{(\tau)}$ Libor spine point vector, multi-curve framework, tenor $= \tau$.

$\mathbf{P}$ Libor spine point vector, single-curve framework.

$\mathbf{Q}$ Rate quote vector in a curve calibration context.

θ_{flat} Cap flat implied volatility shifting parameter.

θ Caplet implied volatility shifting parameter.

t_i Daily marking to market time structure, used in the context of Futures or overnight rate enrollment dates.

Acronyms

ARRC Alternative Reference Rates Committee.

ATM At the money.

CMS Constant maturity swap.

CSA Credit support annex.

ETP Exchange traded product.

EUR Euro.

FRA Forward rate agreement.

FVA Funding valuation adjustment.

IBA ICE Benchmark Administration.

ICAP Name: ICAP. Description: Broker of interest rate options settled in London..

ICE Intercontinental Exchange Group.

ISDA International swaps and derivatives association.

Libor London interbank offered rate.

LMM Libor Market Model.

OIS Overnight indexed swaps.

OTC Over the counter.

SABR Stochastic alpha beta rho.

USD United States dollar.

Contents

Chapter 1

Introduction

In this chapter we will introduce the connection between interest rates, discounting and the yield curve. After which we introduce our research-topic about constructing the yield curve from interest rate futures.

1.1 Interest rates

When a loan is issued an interest rate is charged depending on the duration of the loan, the difficulty for the lender to obtain the funds and the risk profile the lender associates with the borrower. Interest rates determine market supply and demand for loan provision and on a fundamental level represent the cost of borrowing and lending. Because the cost of borrowing and lending affects all aspects of the economy a vast market exists in interest rate derivatives, traded for purposes ranging between hedging, speculation and arbitrage:

	Instruments	Outstanding notionals
OTC market	Forward rate agreements (FRAs)	$ 67 Trillion
	Swaps	$ 326 Trillion
	Options	$ 42 Trillion
Exchange	Futures	$ 38 Trillion
	Futures options	$ 55 Trillion

Table 1.1: Volumes on interest rate derivatives, H2 2018, source: bis.org

The bulk of interest rate derivatives is formed by *fixed-income* instruments like forward rate agreements and swaps[1] that serve the purposes of fixing future funding rates and converting a floating liabilities to a fixed ones. More generally these practices fall under the hedging of interest rate exposures.

Providing loans and issuing structured products like mortgages is the main business of banks for which they respectively either use capital provided by depositors/investors or loans from other banks. Because of this the rates charged for borrowing and lending between banks further translate into the average rate the banks charge for the funding of their clients. As a consequence benchmark interest rates have been created to serve as an estimate for the average interbank cost of borrowing and lending to be used as a reference in various traded interest rate derivatives.

The most used reference rate is given by the *Libor* rate[2]. It is produced once a day by the Intercontinental Exchange (ICE) and regulated by the Financial Conduct Authority. There are a total

[1] Structure of these instruments will be explained in Section 2.5.
[2] London interbank offered rate.

of 35 Libor rates posted each day; interest rates are compiled for loans with seven different maturities (or due dates) for each of 5 major currencies, including the Swiss franc, the euro, the pound sterling, the Japanese yen, and the U.S. dollar. Each morning, just before 11 a.m. Greenwich Mean Time, the ICE Benchmark Administration (IBA) asks a panel of contributor banks (usually 11 to 18 large, international banks) to answer the following question: "At what rate could you borrow funds, were you to do so by asking for and then accepting interbank offers in a reasonable market size just prior to 11 a.m. London time?" Only banks that have a significant presence in the London market are considered for membership on the ICE Libor panel, which is determined annually. Exact details about the different Libor-like indices can be found in [24]. We will use the accroym Libor for all Libor-like indices even though not all rate estimates are provided by the ICE Libor panel. The spot Libor rate, is quoted as a simply compounded rate over multiple *tenors*[3]: overnight, 1 week, 1 month, 2 months, 3 months, 6 months and 12 months, with a spot lag of 2 business days[4]. There are multiple Ibor-like benchmark rates like the Euribor, which is also a reference rate of average unsecured loans in the Euro currency next to the Euro Libor. The Euribor is provided by a panel of up to 49 reference banks computed by the European Banking Federation (EBF) and posted over 5 tenors: 1 week, 2 weeks, 3 months, 6 months and 12 months. We will refer to Ibor-like rates in general by the abbreviation Libor for the rest of the thesis.

Reflecting average interbank offered rates, it is not an unusual assumption to see the Libor rate as a proxy for the funding rates charged to AA-rated[5] companies. This assumption is not entirely true however due to lower credit quality banks being eliminated from the consortium of banks polled for Libor rate quotes, therefore Libor rates are in general lower than funding rates used to discount obligations issued by AA-rated companies, see [11] for more details on the credit spreads between yields of corporate bonds and treasury bonds[6] or for a more recent article see [15]. There are several more things one needs to be aware off when using the interpretation of the Libor rate as the average unsecured interbank offered lending/borrowing rate. Banks that default or have deteriorating credit-qualities can be eliminated from the consortium of banks in the Libor panel and replaced by better credit-quality banks, while high-credit quality banks stay. Therefore the trimmed average spot rate is biased negatively because lower credit-quality banks are left out in estimation, see [35] for more details.

Nevertheless, Libor rates are the arguably the most important interbank reference rates and derivatives indexed to the Libor rates are traded in the largest volumes and new contracts are still being issued today. There are other rates to be aware of. In the United States banks are required to hold a certain balance with the Federal Reserve and can charge them overnight from other banks with an excess, this rate is called the *Fed Funds rate*. The Euro and GBP markets do not have the same mechanism as the US does for Federal funds, but overnight rates that are proxies for riskfree borrowing in those currencies do exist as given in the Table below:

Currency	OIS-rate
EUR	Eonia
USD	Fed Funds
JPY	Tonar
GPB	Sonia
CHF	Saron

Table 1.2: Benchmark interbank offered interest rates

[3]Loan duration.

[4]For loans with periods longer than overnight the spot rate usually corresponds to the rate charged over the period starting 2 business days in the future for a length corresponding to the tenor.

[5]Standard & Poors rating, see `https://www.standardandpoors.com/en_US/web/guest/article/-/view/sourceId/504352`.

[6]Note that giving a fixed interest rate loan to a company is equivalent to buying a bond from them, given the same repayment agreements if the company defaults.

These rates are also called *overnight rates*. They are the bext proxies for 'risk-free' interest rates in their corresponding currencies and are also the rates paid over outstanding collateral in over the counter interbank deals as specified in the CSA as part of the ISDA master agreement[7].

Finally since the Libor scandal following the mortgage crisis of 2007 efforts have been put in place to find a replacement for the Libor in all currencies, due to its exposure to manipulation. In 2014 The Financial Stability Board (FSB) published a report about a major reform of reference rates[8]. In June 2017 the US Alternative Reference Rates Committee (ARRC) identied a treasuries repofinancing rate, which they called Secured Overnight Funding Rate (SOFR), as the best replacement for Libor. Similar decisions were made by regulators in other countries. In the UK, Libor will be replaced with reformed SONIA, while CHF OIS and swap markets have transitioned from TOIS to SARON, a secured overnight rate based on repo trades. More about these rates and consequences on the interest rate market in general will be discussed in Chapter 5.

1.2 Yield curve

Due to the opportunity cost of capital, interest rates determine the time dependent value of future cash flows, which can be visualized in a curve that maps maturity to a discount factor. This is also called the *discount curve*, used to discount the value of contracts containing future cash flows issued by specific entities. The relationship between discounting and interest rates is given in the following illustration. When entity 1 provides a loan to entity 2, the computation of the rate charged depends on several factors: The risk entity 1 assigns to entity 2 of no or lower payback (Credit risk). The difficulty for entity 1 to obtain funds for entity 2 (Liquidity risk). Rates for which entity 2 could obtain funds from other entities. (Supply and demand)

Credit and liquidity risk are the 2 main driving forces behind the supply and demand of loans and are generally summarized as a *credit-spread*, see Morini [35] for more details. When entity 2 issues an obligation to entity 3 then the value of this obligation is dependent on the rate that is charged by entity 1 for the following reason: Entity 2 can borrow from entity 1 to fund the obligation it owes to entity 3. Consequently, the present value of the obligation is the discounted payoff using the funding curve of entity 2. Otherwise, entity 2 or entity 3 is provided with an *arbitrage* opportunity[9].

If both entities 2 and 3 write each other obligations the netted present value is dependent on the funding curves of both. Direct discounting works when the obligation is some deterministic value, if it is not, then the its forward value must be used, which will be explained in Section 2.4.

In practice the funding rates of various entities that issue obligations are unknown and therefore are estimated from benchmarks like the Libor and the overnight rate. Resulting in the Libor and overnight curves. Figure 1.1 is an example of the 3-month EUR Libor curve:

[7] See `http://www.rbc.com/investorrelations/_assets-custom/pdf/covered-bonds-Program/covered-bond-swap-agreements/Credit_Support_Annex_covered_2015_05_19.pdf`.

[8] See `https://www.fsb.org/2014/07/r_140722/`.

[9] An opportunity to make risk free profit. Arbitrage will be formally explained in Section 2.1.

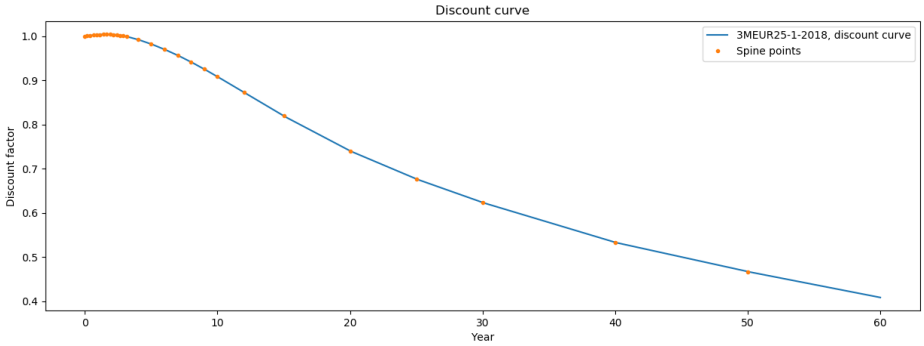

Figure 1.1: 3-month Euro Libor discount curve.

Bank issued fully collateralised derivatives are discounted using the overnight rate curve, though mentions are made about possibilities of using alternative reference rates to fund collateral, see [34]. Corporations need a rate that is more representative for their funding costs or credit quality. Therefore most fixed income instruments are issued referencing future Libor rates and are priced using the Libor curve. See Chapter 5 of [2] for more details.

Finally, one must denote the difference between borrowing and lending rates. In the context of bank issued derivatives the borrowing/investing problem should not be considered in isolation but globally. The banks are usually on the same side of the cash balance (lender or borrower) in a consistent way. Simplifying, the saving banks are permanently cash-rich from their customers' savings while the investment bank make investments and need to borrow cash also on a permanent basis. The cash needs of the derivative book are quite modest with respect to the general cash of the banks. The cash entering in the replication arguments for derivatives are small relative to the total cash borrowed or loaned. Consequently from a netting perspective an option desk of a cash rich bank will never borrow money, the bank is simply investing less cash. In an investment bank the desk never invests cash, but is simply borrowing less. We will not distinguish borrowing and lending rates for the rest of the thesis. See [23] for more details.

1.3 Research topic

Due to the large volume of Libor linked derivatives the Libor curve is important for pricing newly or already issued Libor rate derivatives. The Libor and overnight curves are constructed by stripping the implied discount factors from the most liquidly traded[10] overnight/Libor rate derivatives such as deposits, FRAs, swaps and futures[11], as visible in Table 1.1. Because these instruments only provide discount factors for a discrete number of maturities, an interpolation procedure is used to estimate the resulting discount factors in between, which will be explained in detail in Chapter 3.

The Libor rate underlying *Eurodollar futures* span the same time frame[12] of maturities as FRAs and therefore are an additional source of information for the inference of the Libor curve. Futures are in general more liquid and more transparent than FRAs. Even though in Table 1.1, FRAs are shown to have a higher outstanding notional than futures, futures trading volumes are concentrated among several standardized contracts, of which the 3 month futures contract (over Libor rates that have a loan period of 3 months) has starting date on the third Wednesday of every quarter month of the year is the most traded[13]. Furthermore, due to being exchange-traded futures rates are transparently visible at all times. FRA-rates do not have the same exposure to supply and demand due to being traded over the counter. Therefore, it can be argued that using futures for curve calibration gives a curve that is more aligned with supply and demand.

The convexity adjustment is the extra value that a futures contract on a rate has over a forward contract due to receiving intermediate margining payments effective in a futures contract over not receiving them. Due to the margining mechanism inherent in futures contracts[14] the values of can not be transformed into Libor rate discount factors without taking into account a *convexity adjustment*. Quantifying the adjustment requires one to have a notion about market expected benefit of receiving the underlying intermediate payments of the futures contract, which in turn requires a model for Libor forward rate dynamics. Several models have been developed in literature: A standard methodology in the single-curve setup was introduced by Kirikos and Novak [30], who calculated the risk-neutral expectation of Libor explicitly, using the Hull-White [27] one-factor model calibrated to ATM cap volatilities. More advanced approaches have then been proposed by Piterbarg and Renedo [39] and Jaeckel and Kawai [29], who investigated the impact of volatility skews on futures convexity adjustments in the context of the Libor Market Model (LMM), respectively using stochastic-volatility and shifted-lognormal dynamics. Mercurio considers 3 models for the convexity adjustment in the multi-curve framework using Gaussian overnight rate dynamics and the Libor market model with a fixed correlation. One where the overnight rate volatility is deterministic, 2 where the Libor-overnight forward rate basis spread is deterministic [33].

The single-curve and multi-curve frameworks will be addressed in Section 1.2. Because fast recalibration is important for a curve calibration algorithm we will limit our attention to simple short-rate models and calibrated to at the money caplet volatilities, after which we will study the influence of the smile using the replication method. We will not look into Libor market model or stochastic volatility approaches, for they require calibration of not only volatility but also correlation parameters. We will focus on answering the following 3 questions:

1. How can a curve and volatility-dependent convexity adjustments be integrated into a curve calibration algorithm?

2. How much do the convexity adjustments vary given stressed market scenarios?

[10] The best representation of market supply and demand for future interest rates.

[11] The instruments and the stripping procedure will be explained in detail in Section 2.5

[12] This will be further specified in 2.5.

[13] Second London bank business day before 3rd Wednesday of the contract month. Trading in expiring contracts terminates at 11:00 a.m. London time on the last trading day for CME traded Eurodollar futures, with underyling the 3-month USD Libor. See `https://www.cmegroup.com/trading/interest-rates/stir/eurodollar_contract_specifications.html` for more details.

[14] Which will be explained in Section 2.6.

3. Due to the dependence of the curve on option volatilities, how large are the vegas of linear instruments?

Our end result is an algorithm that allows for dual integration of volatility-dependent convexity adjustments and futures in curve calibration without the use of externally computed convexity adjustments.

1.4 Research outline

In Chapter 2 we will introduce the necessary pricing prerequisites like the no-arbitrage pricing framework that allows us to formally define the various yield curves, forward rates, futures rates and the convexity adjustment. We will also introduce the various calibration instruments, the intuition behind the convexity adjustment and the caplet volatility surface. In Chapter 3 we introduce the Libor curve calibration procedure in the single-curve framework using fixed convexity adjustments. In Chapter 4 we will start off by using short rate models (Ho-Lee and Hull-White, [27]), to calibrate convexity adjustments to at the money caplet volatilities and introduce the replication method to calibrate the convexity adjustment to the entire caplet volatility surface in the single-curve framework. We will compare the 2 models and stress test the resulting convexity adjustments under various market scenarios. Finally we will check whether the implied vegas of various instruments are worth hedging. In Chapter 5 we will look at what can be researched further like extension into the multi-curve framework including alternative reference rates.

Chapter 2

Prerequisites

In this chapter we will introduce several mathematical prerequisites to understand the pricing arguments made in later chapters. We start by recapping the no-arbitrage-pricing framework, the risk neutral measure, using the overnight rate as the proxy for the risk-free rate and in particular the change of numeraire technique. After this we will mathematically define the Libor/overnight curves and how the mortgage crisis of 2007 resulted in the adaptation of the multi-curve framework. We will specify how the Libor curve connects to Libor deposit, forward and swap rates used for calibration, we will leave out overnight curve calibration instruments. After this we will formally introduce futures and the convexity adjustment as the difference between expectations of the spot Libor under different measures. We will introduce the volatility smile and the caplet volatility surface, used for modelling of the convexity adjustments. The link between convexity adjustments and the volatililty surfaces will be explained in Chapter 4. We will work in the single-curve framework for the rest of the thesis.

2.1 No arbitrage pricing framework

Prices are driven by supply and demand, which in turn are driven by market participant expectations of both the future values of assets as well as the opportunity cost of capital. Because expectations require a notion of the future probability distributions of asset values, it makes sense to model asset movements as stochastic processes. No arbitrage pricing is about stripping implied probability distributions of asset derivatives from the prices of liquidly traded instruments, which requires assumption about dynamics[1] of the underlying assets. In 1976 Black and Scholes derived the Black-Scholes equation in order to price European call options under lognormal dynamics of the underlying asset, see [5], where both the volatility and the risk free interest rate are assumed to be constant. Since then the theory has been expanded drastically, continuous time market pricing is described in [42] or [7] in the context of interest rate derivatives. The most important tool in these market models is the risk neutral measure, as will be further defined further in this section. The following assumptions are made about the market:

Trading can happen at any time. There are $K+1$ traded assets $(A_t^{(0)}, ..., A_t^{(K)})$ in the market following some stochastic processes, with $\mathbb{P}$ the underlying probability measure. Furthermore, we assume that asset $A_t^{(0)}$ is positive and pays no dividend. There exists risk free continuously compounded rate r_t for which market participants can loan and borrow, also called the *risk-free rate*, which will be further specified in Section 2.3. Any multiple of any asset can be bought both long and short[2]. A trader can short an asset to a counter-party by having an agreement with a third party, like a bank, from which it can borrow funds to buy the underlying asset in order to

[1] Often parametric, where the dynamics are uniquely determined by some stochastic process like the Brownian-Motion and some finite set of parameters.

[2] Long means buying the asset and shorting means selling it.

sell it to the counter-party. The underlying agreement is that the trader owes the third party the value of the asset instead of the initially borrowed funds. There are no transaction costs. This assumption is made for computational convenience. In practice there are transaction costs but decrease as the market becomes more and more efficient, partially due to instruments like ETPs[3] which allow people to trade in commodities without physically buying the underlying. The final assumption is market completeness[4].

Without loss of generality we define the *discounted price process*:

$$Z_t^{(i)} = \frac{A_t^{(i)}}{A_t^{(0)}}, \tag{2.1}$$

with *numeraire* $A_t^{(0)}$. A martingale is specified by the underlying probability space $(\Omega, \Sigma, \mathbb{P})$, with $\{\mathscr{F}_t\}$ being a filtration of the underlying Brownian-Motion. See [28], [2] or [7] for more details. No-arbitrage pricing rests on the assumption that there exists some measure $\mathbb{Q}$ equivalent[5] to $\mathbb{P}$ such that any discounted asset is a martingale. This means for any $0 \leq t \leq T$:

$$Z_t^{(i)} = \mathbb{E}^{\mathbb{Q}}[Z_T^{(i)} | \mathscr{F}_t]. \tag{2.2}$$

Under given market assumption we can define the numeraire pair:

Definition 2.1.1 (Numeraire pair)**.** Given $A^{(0)}$ and $\mathbb{Q}$ as defined by Equation (2.2) we define $(\mathbb{Q}^A, A^{(0)})$ as a *numeraire pair*. Here $A^{(0)}$ is a strictly positive asset and $\mathbb{Q}$ the corresponding martingale measure.

This further defines the risk free numeraire pair rate r_t:

Definition 2.1.2 (Risk neutral numeraire pair)**.** Given $D_t = \exp\left(\int_0^t r_u du\right)$ and $\mathbb{Q}^D$ as defined by Equation (2.2) we define $(\mathbb{Q}, D)$ as the *risk neutral numeraire pair*.

Note that a continuously compounded risk free rate does not exist in the market. The best proxy is given by the overnight rate as has been specified in Section 1.1. Overnight rates are quoted on every business day as simply compounded rates, let $t > 0$ and $0 = t_0 < t_1 < ... < t_n$ such that $t \in [t_{n-1}, t_n]$, let F_i be the spot overnight rate with accruing period $[t_i, t_{i+1}]$. This gives the following defining property for the risk neutral numeraire:

$$D_{t_n} = \exp\left(\int_0^{t_n} r_u du\right) = \prod_{i=0}^{n-1}(1 + F_i(t_{i+1} - t_i)). \tag{2.3}$$

Note that this property underspecifies the risk-free rate for $t \in (t_i, t_{i+1})$. This gives us room for modelling, which will be further specified in Chapter 4, for now we will just assume its existence.

The following definitions are important:

Definition 2.1.3 (Self financing strategy)**.** A self financing strategy is given by a portfolio holding strategy θ such that $\theta_t = (\theta_t^{(0)}, ..., \theta_t^{(K)})$ and for $V_t^\theta = \sum_{i=0}^{K} \theta_t^{(i)} A_t^{(i)}$ the following holds:

$$dV_t^\theta = \sum_{i=0}^{K} \theta_t^{(i)} dA_t^{(i)} \tag{2.4}$$

[3]Exchange traded products.

[4]Completeness means that any contract with a future payoff can be replicated by a portfolio of assets traded in the market.

[5]This means that the 2 measures agree on which events they give 0 probability.

This means that movement in the portfolio is only caused by internal rebalancing of the assets and no money is added or removed from the portfolio. Market completeness can be translated to the statement that any payoff V_T is the result of some self financing strategy θ. We can now define arbitrage:

Definition 2.1.4 (Arbitrage)**.** An arbitrage is given by a self financing strategy θ where $V_t^\theta = 0$ but $\mathbb{P}(V_T^\theta \geq 0) = 1$ and $\mathbb{P}(V_T^\theta > 0) > 0$.

This means there exists a portfolio holding strategy that initially costs nothing, can not grow negative but can grow positive. The existence of the measure $\mathbb{Q}$ can be combined with the following fundamental results, see [22] or [42], we will not prove them here.

Theorem 2.1.5 (First fundamental theorem of asset pricing)**.** *Given the existence of a martingale measure $\mathbb{Q}$ as given in* (2.2)*, there is no arbitrage in the market.*

Theorem 2.1.6 (Second fundamental theorem of asset pricing)**.** *The market is complete if and only if the martingale measure is unique.*

The existence of the measure $\mathbb{Q}$ can intuitively be justified the following way, let $\{T_0, T_1, ..., T_n\}$ be some discretization of the interval $[0, T]$. We can reweigh the movement density functions $f_{\mathbb{P},i}$ of every asset at every time point to a density function $f_{\mathbb{Q}_n,i}$ with measure $\mathbb{Q}_n$ such that

$$\mathbb{E}^{Q_n}[Z^{(i)}(T_j)] = Z^{(i)}(T_{j-1}),$$

holds for every $i \in \{0, ..., K\}$ and $j \in \{1, ..., n\}$ and should always be possible because the movement upwards and downwards is always possible. Considering in practice trading can only happen at a discrete set of times[6], assuming existence of a continuous time martingale measure will not lead to problems in practice. The theorems show that given a complete market, if a martingale measure $\mathbb{Q}$ exists it is unique and there is no arbitrage. This leads to the following fundamental result:

Theorem 2.1.7 (Fundamental pricing formula)**.** *Let $(\mathbb{Q}, A^0)$ be a numeraire pair as given in Definition 2.1.1, for any contract with payoff V_T at time T its price at time t is given by $V_t = \mathbb{E}^{\mathbb{Q}}\Big[\frac{A_t^{(0)}}{A_T^{(0)}} V_T \Big| \mathscr{F}_t\Big]$.*

Proof. Assume that $\dfrac{V_t}{A_t^{(0)}} > \mathbb{E}^{\mathbb{Q}}\Big[\dfrac{V_T}{A_T^{(0)}}\Big|\mathscr{F}_t\Big]$ then one can sell the contract and take a self financing position in assets that replicates V_T[7] and pocket the difference[8] creating an arbitrage, the argument is analogous for $V_t < \mathbb{E}^{\mathbb{Q}}\Big[\dfrac{A_t^{(0)}}{A_T^{(0)}} V_T \Big| \mathscr{F}_t\Big]$. □

We will not introduce any cross currency instruments, therefore for the rest of the thesis we will work in a single currency market and look at Libor and overnight curves in one currency[9].

[6] Seperated by microseconds or less.

[7] Which exists because the market is complete.

[8] A discounted self financing strategy is a martingale under $\mathbb{Q}$, therefore its discounted value at time t is given by $\mathbb{E}^{\mathbb{Q}}\Big[\dfrac{V_T}{A_T^{(0)}}\Big|\mathscr{F}_t\Big]$, therefore $V_t > \sum_{i=0}^{K} \theta_t^{(i)} A_t^{(i)}$ for θ the corresponding self financing strategy.

[9] EUR and USD.

2.2 Measure change

Note that we only specified that the numeraire is some positive tradeable asset, therefore any strictly positive tradeable asset implies a unique numeraire pair. Using the theorem of Radon Nykodym, see [2], [28] or [7], this leads to the following fundamental result:

Theorem 2.2.1. *Let $t \leq T$. Given 2 numeraire pairs $(\mathbb{Q}^B, B)$ and $(\mathbb{Q}^A, A)$ given a $\mathscr{F}_T$-measurable, square integrable random variable V_T (defining a payoff at time T) the following results holds: $A_t\mathbb{E}^{\mathbb{Q}^A}\left[\frac{V_T}{A_T}|\mathscr{F}_t\right] = B_t\mathbb{E}^{\mathbb{Q}^B}\left[\frac{V_T}{B_T}|\mathscr{F}_t\right]$, which implies due to the theorem of Radon-Nikodym: $\frac{d\mathbb{Q}^V}{d\mathbb{Q}^A} = \frac{A_0}{A_T}\frac{B_T}{B_0}$. Such that: $\frac{d\mathbb{Q}^B}{d\mathbb{Q}^A}(t) = \mathbb{E}^{\mathbb{Q}^A}\left[\frac{A_0}{A_T}\frac{B_T}{B_0}|\mathscr{F}_t\right] = \frac{A_t}{A_T}\frac{B_T}{B_t}$*

Proof. See A.3. □

$\frac{d\mathbb{Q}^A}{d\mathbb{Q}^B}$ is also called a Radon-Nikodym derivative. We will use this results multiple times throughout the thesis to change between measures. Using Theorem 2.2.1 we will introduce 2 frequently used measures, dependent on the risk neutral measure, given by:

Definition 2.2.2 (Forward measure)**.** Let $M \geq T$. Let $(\mathbb{Q}, D)$ be the risk neutral numeraire pair, as given by Definition 2.1.2, and let $(\mathbb{Q}^M, P^{(O)}(\cdot, M)$ be the M-forward measure numeraire pair with the defining property $P^{(O)}(t, M) = \mathbb{E}^{\mathbb{Q}}[D_t/D_M|\mathscr{F}_t]$. By market completeness, given the risk neutral measure $(\mathbb{Q}, D)$ the numeraire pair $(\mathbb{Q}^M, P^{(O)}(\cdot, M)$ is unique. The Radon-Nykodym derivative between measure $\mathbb{Q}$ and $\mathbb{Q}^M$ is given by:

$$\frac{\partial\mathbb{Q}}{\partial\mathbb{Q}^M}(t) = \frac{D_T P(t, M)}{D_t P(T, M)}. \tag{2.5}$$

The forward measure and risk-neutral measure are the martingale measures corresponding to the forward rate and the futures rate, after assuming futures marking to market happens continuously instead of daily, see 2.6 for more details.

2.3 Yield curves

Under the most simple market model with a fixed risk free interest rate $r_t = r$ as described by Black [5], the corresponding time t discount curve has a very simple expression:

$$T \mapsto P(t, T) = \exp(-r(T - t)). \tag{2.6}$$

Which is equivalent to assuming a constant short rate equal to r. Due to using the overnight rate as the proxy for the r_t, the rate is time-dependent.

As has been mentioned in Section 1.2, bank issued fully collateralised derivatives are discounted using the overnight rate. This leads to the time t overnight curve:

Definition 2.3.1 (Overnight curve)**.**

$$T \mapsto P^{(O)}(t, T). \tag{2.7}$$

Unsecured funding curves of banks are represented by the Libor and before the mortgage crisis of 2007, the spread between overnight and Libor rates was negligible, but increased significantly in August 2007[10]:

[10] After the freezing of the assets of PNB Paribas, the biggest bank of France at the time.

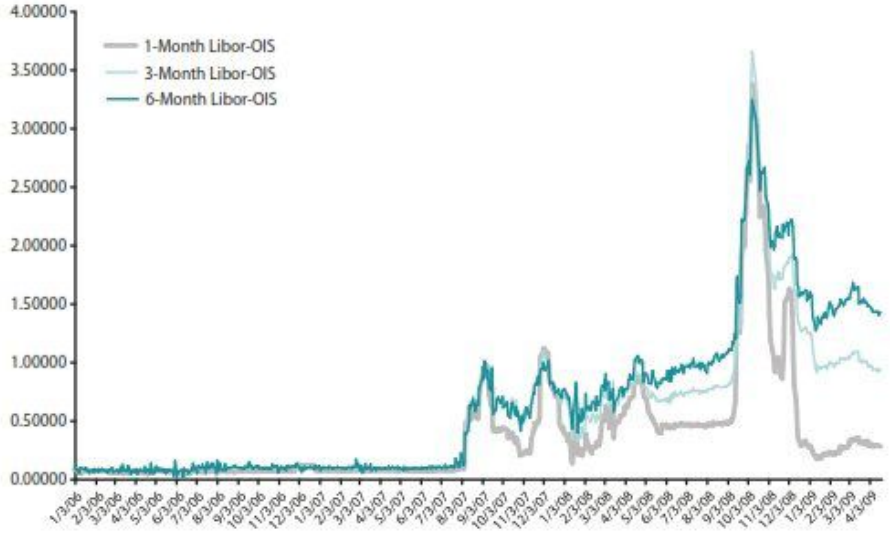

Figure 2.1: Development of the spread between overnight index. Source: Federal Reserve Bank of St. Louis.

In Figure 2.1 the 1-month, 3-month and 6-month Libor forward and overnight forward rates are compared, see 2.4 for forward rate definitions.

Therefore, before 2007 a single-curve framework was used for both pricing, forecasting forward rates and discounting, that assumed no difference between Libor and overnight curves. After 2007 the Libor has lost its interpretation as the correct rate for discounting of collateralised bank issued derivatives but is still used to price Libor indexed derivatives, which will be specified in Section 2.5. Furthermore, Libor rate derivatives are traded indexing Libor rates for one tenor, with the exception of basis-swaps or other more exotic instruments. Therefore, for modelling convenience the Libor curves are seperated per tenor as will be specified in Section 2.4.

This leads to multiple Libor τ-curves:

Definition 2.3.2 (Libor discount curve)**.**

$$T \mapsto P^{(\tau)}(t,T) = \exp(-y^{(\tau)}_{T-t}(T-t)). \tag{2.8}$$

With the corresponding time t yield curve:

Definition 2.3.3 (Libor yield curve)**.**

$$T \mapsto P^{(\tau)}(t,T) = \exp(-y^{(\tau)}_{T-t}(T-t)), \tag{2.9}$$

the corresponding time t yield curve. One way to visualize the τ-Libor curve is as the funding curve of an average Libor bank, that approximately loans for the spot Libor rate in τ time increments[11]. Whenever we will use $P(\cdot,\cdot)$ or y without a superscript we will be referring to the τ-Libor (yield) curve, with the value of τ clear from the context. If not so we will explicitly state this. See [1], [7] or [2] for more details on the multi-curve framework.

[11]There are several fallacies to this assumption like the fact that any Libor bank runs the risk of leaving the Libor panel when its credit-quality deteriorates or that banks tend to provide artificial quotes to the panel in times of illiquid Deposit markets, see [35] for more details.

2.4 Forward rates

We will now introduce Libor and overnight forward rates, which unlike current spot Libor rates, reflects market expectations for future spot Libor rates. Libor discount factors can be derived by a replication argument from forward rates in the single-curve framework. After which this relationship is inherited in the multi-curve framework, which will be further explained in Section 2.5.2. Given any derivative with payoff V_M at time M and some time t funding curve $T \mapsto P^{(O)}(t,T)$. Its forward value of V_t^F is defined such that:

$$\begin{aligned} V_t^F P^{(O)}(t,M) &= \mathbb{E}^{\mathbb{Q}}\left[\frac{D_t}{D_M} V_M | \mathscr{F}_t\right] \\ &= P^{(O)}(t,M)\mathbb{E}^M\left[V_M|\mathscr{F}_t\right], \end{aligned}$$

Which implies:

$$V_t^F = \mathbb{E}^M\left[V_M|\mathscr{F}_t\right]. \tag{2.10}$$

Knowing the forward value is useful for 2 reasons: It is the fair to agree fixed value to be exchanged for the payoff V_M at time M. Doing this type of deal is a way to fix the payment for the receival of a future asset. The present value can be computed requiring only one discount factor.

Choosing the spot Libor L_T as the underlying payoff[12] results in the forward rate L_t. In order to understand how a curve can be inferred from calibration instruments we need to link forward rates to discount factors of that funding curve. We can link the spot Libor rate L_T at time T with *tenor* τ to the time T Libor curve by the relationship:

$$\frac{1}{1+\tau L_T} = P(T,M),$$

which rewrites to:

$$L_T = \frac{1}{\tau}\Big(\frac{1}{P(T,M)} - 1\Big). \tag{2.11}$$

The forward rate is given by $L_t = \mathbb{E}^M\left[L_T|\mathscr{F}_t\right]$. This expression is not directly known, but can be connected to Libor discount factors using a replication argument in the single-curve framework[13]. Borrow $P(t,M)$ to pay back 1 at time M. Simultaneously lend $P(t,T)$ to receive back 1 at time T and reinvest again to receive back $1+\tau L_T$ at time M.

This strategy is visualized in the below diagram:

Figure 2.2: Libor forward rate defining payment structure.

Costs for entering this strategy are $P(t,M) - P(t,T)$, and replicate the payout $L_T\tau$ at time M. By no-arbitrage pricing this implies:

$$P(t,M) - P(t,T) = \tau\mathbb{E}^{\mathbb{Q}}\left[\frac{D_t}{D_M} L_T|\mathscr{F}_t\right]$$

[12] Fixed at an earlier time $T < M$.

[13] We assume the Libor curve equals the overnight curve.

$$= P(t,M)\tau\mathbb{E}^M\left[L_T|\mathscr{F}_t\right] \tag{2.12}$$

Combining Equation (2.12) and the forward rate L_t given by Equation (2.10) gives the following closed form expression of the Libor forward rate in terms of Libor discount factors:

Definition 2.4.1 (Libor forward rate)**.**

$$L_t = \frac{1}{\tau}\Big(\frac{P^{(\tau)}(t,T)}{P^{(\tau)}(t,M)} - 1\Big).$$

This replication argument works in the multi-curve framework because the strategy given by 2.12 is uncollateralised and represents loaning for the spot Libor in τ-increments to fund both strategies. We will leave out the superscript (τ) due to working in the single-curve framework for the rest of the thesis.

Equivalently the overnight forward rate with start T and maturity M at time t can be defined by:

Definition 2.4.2 (Overnight forward rate)**.**

$$F_t = \frac{1}{\tau}\Big(\frac{P^{(O)}(t,T)}{P^{(O)}(t,M)} - 1\Big)$$

2.5 Calibration instruments

We will focus on the Libor curve calibration instruments here, after which we will specify the calibration procedure in Chapter 3. Libor rate indexed instruments used for calibration are the following:

1. Cash deposits.
   The rates charged in the Libor market for unsecured interbank loans, to which only high-credit quality banks have access, see [35] for more details. Closely linked to spot Libor rates due to being the actual rates charged in unsecured loans. Deposits are uncollateralised and represent unsecured interbank loans in their purest form. Traded for maturities ranging between 1 day and 12 months and quoted via the corresponding *deposit rate*, as will be specified in Section 2.5.1.

2. Forward rate agreements.
   Agreement for the exchanges of a prespecified fixed rate for the receival of the spot Libor L_T at start T, with L_T fixed usually 2 business days before the starting date, discounted by the Libor to maturity, see Section 2.5.2. FRAs are fully collateralised, therefore discounted using the overnight curve. When referring to the 3-month spot Libor, FRAs are traded for maturities between 3 months[14] and 10 years and quoted via the corresponding *FRA rate*, as will be specified in Section 2.5.2.

3. Fixed-for-floating swaps.
   Agreement for a stream of fixed rate payments (fixed leg) for a stream of spot Libor rate payments (floating leg). Fully collateralised, therefore discounted using the overnight curve. When referring to the 3-month spot Libor, swaps are traded for maturities between 1 year (with a 2 business day settlement-start lag) and 60 years and quoted via the corresponding *swap rate*, as will be specified in Section 2.5.3.

These instruments are also called *linear* instruments because these instruments are vanilla derivatives with payoffs depending linearly on the underlying spot Libor rates. Deposits are uncollateralised, while FRAs and swaps are collateralised and therefore discounted using the overnight curve.

[14]With a 2 business day spot lag, with the corresponding FRA rate starting in 2 business days and maturing 3 months later. See [24].

2.5.1 Cash deposits

Figure 2.3 is an example of a strip of deposit quotes with different underlying Euro Libor[15] rates:

Instrument	Quote (ask, %)	Underlying	Start Date	Maturity Date	Settlement rule	Business Day Convention	End of Month Convention
Depo ON	0.040	Euribor1D	Tue 11 Dec 2012	Wed 12 Dec 2012	Today	Following	False
Depo TN	0.040	Euribor1D	Wed 12 Dec 2012	Thu 13 Dec 2012	Tomorrow	Following	False
Depo SN	0.040	Euribor1D	Thu 13 Dec 2012	Fri 14 Dec 2012	Spot	Following	False
Depo 1W	0.070	Euribor1W	Thu 13 Dec 2012	Thu 20 Dec 2012	Spot	Following	False
Depo 2W	0.080	Euribor2W	Thu 13 Dec 2012	Thu 27 Dec 2012	Spot	Following	False
Depo 3W	0.110	Euribor3W	Thu 13 Dec 2012	Thu 03 Jan 2013	Spot	Following	False
Depo 1M	0.110	Euribor1M	Thu 13 Dec 2012	Mon 14 Jan 2013	Spot	Mod. Following	True
Depo 2M	0.140	Euribor2M	Thu 13 Dec 2012	Wed 13 Feb 2013	Spot	Mod. Following	True
Depo 3M	0.180	Euribor3M	Thu 13 Dec 2012	Wed 13 Mar 2013	Spot	Mod. Following	True
Depo 4M	0.220	Euribor4M	Thu 13 Dec 2012	Mon 15 Apr 2013	Spot	Mod. Following	True
Depo 5M	0.270	Euribor5M	Thu 13 Dec 2012	Mon 13 May 2013	Spot	Mod. Following	True
Depo 6M	0.320	Euribor6M	Thu 13 Dec 2012	Thu 13 Jun 2013	Spot	Mod. Following	True
Depo 7M	0.350	Euribor7M	Thu 13 Dec 2012	Mon 15 Jul 2013	Spot	Mod. Following	True
Depo 8M	0.390	Euribor8M	Thu 13 Dec 2012	Tue 13 Aug 2013	Spot	Mod. Following	True
Depo 9M	0.420	Euribor9M	Thu 13 Dec 2012	Fri 13 Sep 2013	Spot	Mod. Following	True
Depo 10M	0.460	Euribor10M	Thu 13 Dec 2012	Mon 14 Oct 2013	Spot	Mod. Following	True
Depo 11M	0.500	Euribor11M	Thu 13 Dec 2012	Wed 13 Nov 2013	Spot	Mod. Following	True
Depo 12M	0.540	Euribor12M	Thu 13 Dec 2012	Fri 13 Dec 2013	Spot	Mod. Following	True

Figure 2.3: Euro Libor deposit rate quotes, 11 of December 2012, source: Reuters.

Here the quote represents the asked Libor rate for entering a loan with the corresponding starting and maturity dates. There are several things to consider:

- Time is counted in business days (in the U.S. usually 252).
  Let T_1 be the maturity of the deposit, let T_0 be the settlement date of the start given in days, time is quoted under the following convention:

  $$\tau(T_0, T_1) = \frac{T_1 - T_0}{ACT}.$$

  ACT is usually 252 or 256 in case only business days are counted. Similarly 360 or 365 in case all days are counted.

- The underlying is the Spot Libor rate

- The quote is given in percentages per year under some compounding convention (usually simple).

- The settlement rule column stands for whether the settlement is made directly or in the future, with spot standing for future which is usually 2 business days from now. We will denote this date by T_0.

- Business day convention is given in Following or Modified following.
  Following means that any payment made in the weekend is considered to happen on the next business day. Mod. Following means the same only if that next business day is in the next month the payment is considered to have been made on the previous business day.

These conventions hold across all Libor linked calibration instruments. For more specific details on quoting and payment structure conventions see [24], [32] or [44].

Libor rate cash deposits represent uncollateralised loan/borrowing rates for which interbank funds are provided. When a notional N deposit is agreed between a borrower and a lender the lender agrees to lend N now[16] and receive $N(1 + \tau L(0, M))$ back at time M, which holds inversely for the borrower.

[15] Euro Libor instruments are traded in the European market.

[16] As visible in Figure 2.3 the actual day of start will be 2 days after fixing, we will ignore this payment delay for the rest of the thesis but incorporate in when working with real data.

Given the deposit rate $L(0,M)$ with maturity M the value of the deposit for the lender is given by:

$$V_{deposit}^{lender}(0) = N(P(0,M)(1+\tau L(0,M)) - 1). \tag{2.13}$$

The loan is uncollateralised, therefore determines the corresponding Libor discount factor. Similarly for the borrower:

$$V_{deposit}^{borrower}(0) = N(1 - P(0,M)(1+\tau L(0,M))). \tag{2.14}$$

The lender and borrower agree on a rate such that neither pays a premium to the other. Therefore the quoted rate is the rate such that the deposit (for both lender and borrower) has value starting value 0, leading to the equation:

$$P(0,M)(1+\tau L(0,M)) - 1 = 0. \tag{2.15}$$

Deposit rates are quoted in the market as is visible in Figure 2.3. Which gives the Libor discount factor directly. As was mentioned at the start of this Section spot Libor rates and deposit rates are closely linked due to the fact that in general banks that are part of the Libor panel are also part of the Libor deposit market, when this market is illiquid banks part of the Libor panel provide artificial rate quotes, see [35] for more details. Therefore, dependent on liquidity of the Libor deposit market, for calibration of the corresponding Libor curve either the spot rate or the deposit rate should be used. After the deposit is entered the present value of the interest payback is given by:

$$P(t,M)(1+\tau K). \tag{2.16}$$

With strike K equalling the time 0 agreed deposit rate $L(0,M)$.

2.5.2 Forward rate agreements

Given a spot Libor rate L_T with start T and maturity M. A fixed value is agreed today to be exchanged for the Libor[17] at start, discounted towards maturity. Below is a diagram of the payoff:

Figure 2.4: FRA contract payoff diagram.

A FRA is fully collateralised, therefore discounted using the overnight curve. Let $(\mathbb{Q}, D)$ and $(\mathbb{Q}^T, P^{(O)}(\cdot,T))$ be respectively the risk neutral and the T-forward measure numeraire pairs as specified in Section 2.2.
In the single-curve framework where the overnight and Libor curves are assumed to be equal, this translates into the spot Libor rate L_T being a proxy for the risk free money market account between T and M:

$$1 + \tau L_T = \frac{D_M}{D_T}.$$

Resulting in a payoff with equivalent present value to the payoff given by Figure 2.4:

Figure 2.5: FRA contract, single-curve equivalent payoff diagram.

[17] The maturity can range between 2 days to 10 years or more.

The present value of a payer-FRA can be determined to be:

$$\begin{aligned} V_{FRA}^{payer}(t) &= N\tau\mathbb{E}^{\mathbb{Q}}\left[\frac{D_t}{D_T}\frac{L_T-K}{1+\tau L_T}|\mathscr{F}_t\right] \\ &= N\tau P^{(O)}(t,T)\mathbb{E}^{T}\left[\frac{L_T-K}{1+\tau L_T}|\mathscr{F}_t\right] \\ &= N\tau P^{(O)}(t,T)\mathbb{E}^{T}\left[\frac{L_T-K}{1+\tau L_T}|\mathscr{F}_t\right] \\ &= N\tau P^{(O)}(t,T) - P^{O}(t,T)\mathbb{E}^{T}\left[\frac{1+\tau K}{1+\tau L_T}|\mathscr{F}_t\right]. \end{aligned} \tag{2.17}$$

τ without reference stands for $\tau(T,M)$. Note that the spot Libor L_T is observed and fixed 2 business days before the accruing period starts, similarly to deposit rates. Analogously for the receiver:

$$V_{FRA}^{receiver}(t) = N\tau P^{(O)}(t,T)\mathbb{E}^{T}\left[\frac{K-L_T}{1+\tau L_T}|\mathscr{F}_t\right]. \tag{2.18}$$

In the single-curve framework the receiver FRA reduces to:

$$V_{FRA}^{receiver}(t) = N\left(P(t,M)(1+\tau K) - P(t,T)\right), \tag{2.19}$$

which is equivalent to giving out a loan at time T for fixed interest rate K until time M, in the multi-curve framework the present value is given by Equatin (2.22).

If a FRA is entered at time t, one pays no premium to enter it. Therefore the FRA has 0 present value and K equals the FRA rate L_t. This leads to the following equation:

$$P^{(O)}(t,T)\mathbb{E}^{T}\left[\frac{1+\tau L_t}{1+\tau L_T}|\mathscr{F}_t\right] = P^{(O)}(t,T). \tag{2.20}$$

Let F_T be the overnight rate with start T and M specified by the equation:

$$\frac{1}{1+\tau F_T} = \frac{D_T}{D_M}.$$

We define B, the *Libor-OIS basis-spread* the following way:

Definition 2.5.1 (Multiplicative Libor-OIS-basis-spread)**.** Given $t \in [0,T]$, the multiplicative Libor-OIS basis-spread is given by B, such that:

$$1+\tau B_t = \frac{1+\tau L_t}{1+\tau F_t}.$$

For any $t \in [0,T]$.

By measure change, theorem 2.2.1 we can change to the M-forward measure:

$$\begin{aligned} P^{(O)}(t,T) &= P^{(O)}(t,M)\mathbb{E}^{M}\left[\frac{1+\tau L_t}{P^{(O)}(T,M)(1+\tau L_T)}|\mathscr{F}_t\right] \\ &= P^{(O)}(t,M)\mathbb{E}^{M}\left[\frac{(1+\tau L_t)(1+\tau F_T)}{1+\tau L_T}|\mathscr{F}_t\right] \\ &= P^{(O)}(t,M)(1+\tau L_t)\mathbb{E}^{M}\left[\frac{1+\tau F_T}{1+\tau L_T}|\mathscr{F}_t\right]. \end{aligned} \tag{2.21}$$

Consequently, in the multi-curve framework the present value of a receiver-fra is given by:

$$V_{FRA}^{receiver}(t) = N\left(P^{(O)}(t,M)(1+\tau K)\mathbb{E}^{M}\left[\frac{1+\tau F_T}{1+\tau L_T}|\mathscr{F}_t\right] - P^{(O)}(t,T)\right), \tag{2.22}$$

Giving the following definition for the Libor FRA rate:

Definition 2.5.2 (Libor FRA rate)**.**

$$L_t = \frac{1}{\tau}\Big(\frac{P^{(O)}(t,T)}{P^{(O)}(t,M)}\frac{1}{\mathbb{E}^M\left[\frac{1+\tau F_T}{1+\tau L_T}|\mathscr{F}_t\right]} - 1\Big) \tag{2.23}$$

It can be directly denoted that definitions 2.4.1 and 2.5.2 are equivalent in the single-curve framework. In the multi-curve framework basis specification is necessary for $\mathbb{E}^M\left[\frac{1+\tau F_T}{1+\tau L_T}|\mathscr{F}_t\right]$, after which for convenience purposes the Libor curve is again defined by equating the definitions 2.4.1 and 2.5.2. FRA rates and forward rates are theoretically equivalent, in practice depending on the liquidity of the FRA market[18] the offered FRA rate may be different than the forward rate implied by a curve calibrated from more liquid instruments like Futures or low maturity swaps, therefore we will define FRA rates to be the rates visible in the FRA market and forward rates the implied FRA rates by a Libor curve.

2.5.3 Fixed-for-floating swaps

The fixed-for-floating swaps exchange multiple spot Libor rate payments[19] for fixed rate payments [20]. Again these instruments are fully collateralised.
The floating leg[21] structure is given by: $t < T_0 < ... < T_n = T$, tenor $\tau_i = T_{i+1} - T_i, i \in \{0, ..., n-1\}$.
Fixed leg structure is given by: $t < T'_0 < ... < T'_m = T$, tenor $\tau'_i = T'_{j+1} - T'_j, j \in \{0, ..., m-1\}$.
L_{T_i} is usually fixed at T_i^F, 2 business days before T_i. A payer-swap[22] with strike K and notional N has present value:

$$V_{swap}^{payer}(t) = N(\sum_{i=0}^{n-1}\tau_i P^{(O)}(t,T_{i+1})L_t^{(i)} - K\sum_{i=0}^{m-1}\tau'_j P^{(O)}(t,T'_{j+1})). \tag{2.24}$$

Analogously for the receiver swap:

$$V_{swap}^{receiver}(t) = N(K\sum_{i=0}^{m-1}\tau'_j P^{(O)}(t,T'_{j+1}) - \sum_{i=0}^{n-1}\tau_i P^{(O)}(t,T_{i+1})L_t^{(i)}). \tag{2.25}$$

Below a payoff diagram is visible for a swap:

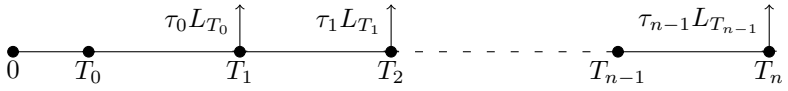

Figure 2.6: Floating leg.

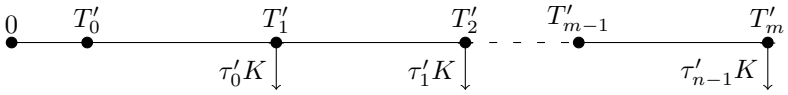

Figure 2.7: Fixed leg.

When issued, the strike is chosen equal to the swap rate, giving this contract 0 value, which implies:

$$N\Big(\sum_{i=0}^{n-1}\tau_i P^{(O)}(t,T_i)L_t^{(i)} - S_t\sum_{j=0}^{m-1}\tau'_j P^{(O)}(t,T'_{j+1})\Big) = 0. \tag{2.26}$$

[18]The higher the maturity the lower the liquidity
[19]The floating leg payments.
[20]The fixedleg payments.
[21]Given spot Libor $L(T_{i-1}, T_i)$, the loan accrues over the period $[T_{i-1}, T_i]$.
[22]Standing for a swap where the holder pays the fixed rate.

Which gives swap rate S_t:

$$S_t = \frac{\sum_{i=0}^{n-1} \tau_i P^{(O)}(t, T_i) L_t^{(i)}}{\sum_{j=0}^{m-1} \tau'_j P^{(O)}(t, T'_{j+1})}. \tag{2.27}$$

In the single-curve framework given no payment or reset delays the floating leg of the swap rate simplifies to:

$$S_t = \frac{P(0, T_0) - P(0, T_m)}{\sum_{j=0}^{m-1} \tau'_j P(t, T'_{j+1})}. \tag{2.28}$$

Which can again be used to directly solve for the Libor discount factors, using the following Equation:

$$P(0, T_0) - P(0, T_m) - S_t \sum_{j=0}^{m-1} \tau'_j P(t, T'_{j+1}) = 0. \tag{2.29}$$

In the multi-curve framework one can combine Equation (2.29) with Definition 2.4.1 and the overnight curve to determine higher maturity Libor discount factors.

2.6 Futures

Deposits, FRAs and swaps are *forward contracts* that agree on the delivery of an underlying[23] at some future time for a predetermined price, *futures contracts* are their exchange traded alternatives with the following characteristics:

1. Forward contracts are traded over the counter based on personally agreed terms between the 2 counter-parties. Exchange traded contracts are standardized and any exchange participant, with a sufficient margin-account balance, can trade them.

2. They have a daily margining mechanism.
   A futures contract holder deposits an *initial margin*, proportional to the value of the agreed deliverable. Daily movements in the value of the futures contract are either added to or subtracted from the contract holder's account.[24]. This daily payment mechanism reduces counter-party credit risk by settling the exposures counter-parties on both the long and short side have towards each other daily. The counter-parties do not know who they are exposed to and in case one of the parties defaults, the exchange finds another counter-party to sell the short or long side contract to, without any effect on the non-defaulting counter-party.

3. They allow leverage.
   The initial margin required to be deposited for purchase of the futures contract is never as large as the agreed exposure to the underlying. Around 1/10th as is visible for crude oil futures or 1/20th as visible for the E-mini S&P 500 index.[25]. Forward contracts allow for leverage too, depending on collateral agreements.

Eurodollar futures are futures contracts on the Libor rate and are standardized with a 3 month tenor with start/payment dates on the third Wednesday of every third month of the year[26].

[23] Could be any asset or a derivative.

[24] This depends on variation and maintanance margin agreements. No rebalancing is necessary in case of underlying movements lower than the variation margin and no deposits are necessary if the margin account balance is above a maintanance margin.

[25] For more examples visit cmegroup.com, barchart, ICE or literature like Hull [26].

[26] March,June,September,December. There are also 1 month, 6 month and 1 year Futures, visit CME group, barchart of ICE for more examples.

An *Eurodollar futures* contract with the spot Libor L_T with start T and maturity M the underlying, is structured to have a payoff of $N\alpha(1 - L_T)$. N is called the *notional* and α is a constant dependent on payment convention, also called the *accruing factor*. The following conventions hold for 3M USD futures[27]:

1. The contract is quoted as $100(1 - Fut_0)$, where Fut_0 is the underlying futures rate.
2. The accruing factor α is $\frac{1}{4}$.
   The accruing factor reweighs the futures rate by the tenor of the corresponding 3-month spot Libor rate, which is approximately $\frac{1}{4}$ under usual time-unit conventions like ACT/360, see Section 2.5.
3. The notional N is \$1.000.000. Consequently, increase of 1 basis point[28] of the futures rate leads to decrease of the underlying contract value by \$25.
4. The tick-size is 0.25 bp, which means that changes in the underlying futures rate are only registered in 0.25 basispoint increments, or equivalently for \$6.25 movements of the underlying contract.

We leave out details about maintanance and variation margins. For more details about Eurodollar futures see [1] or [24]. No premium is paid to enter an Eurodollar Futures contract, and the daily remargining happens the following way, let $0 = t_0 < ... < t_n = T$. For every $i \neq 0$ at t_i the payment $N\alpha(1 - Fut_{t_i}) - N\alpha(1 - Fut_{t_{i-1}}) = N\alpha(Fut_{t_{i-1}} - Fut_{t_i})$ is made. At final time T the payout is $N\alpha(Fut_{t_{n-1}} - Fut_{t_n}) = N\alpha(Fut_{t_{n-1}} - L_T)$.
Consequently, a long futures contract gives the holder an exposure of

$$N\alpha(1 - Fut_{t_i}), \tag{2.30}$$

therefore if the futures rate moves by 1 basis point the holder of the contract loses $N\alpha$ basis points of the corresponding currency. We define the futures rate the following way:

Definition 2.6.1. Let $0 = t_0 < ... < t_n = T$ be the n days of payment before starting time T. Let $(\mathbb{Q}, D)$ be the risk-neutral numeraire pair as given in (2.1.2). We define the *discretely marked-to-market futures rate* as the unique price process such that for every $t \in [t_{i-1}, t_i]$ satisfies the equation:

$$\mathbb{E}^{\mathbb{Q}}\Big[\sum_{j=i}^{n} \frac{D_t}{D_{t_j}}(Fut^{(d)}(t \vee t_{j-1}) - Fut^{(d)}(t \vee t_j))|\mathscr{F}_t\Big] = 0. \tag{2.31}$$

Such that

$$Fut^{(d)}(t_n) = L_T.$$

Below is a payoff diagram of the Eurodollar futures contract:

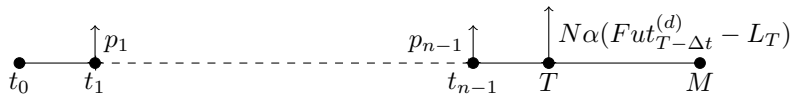

Figure 2.8: Eurodollar futures contract payoff diagram.

With $p_i = N\alpha(Fut^{(d)}_{t_{i-1}} - Fut^{(d)}_{t_i})$.
This definition makes sense because no premium is paid to enter a futures contract with the daily marking-to-market and the delivery of $N\alpha(1 - L_T)$ at time T, therefore by the fundamental pricing formula, Theorem 2.1.7, the net value of all the future payments should be 0. In practice

[27] Source: CME.
[28] One hundredth of a percent.

receiving/paying the margin resettlements daily or even in 3 month increments[29] differs little from receiving it continuously. Therefore for computational convenience we can model the futures rate under continuous marking-to-market, which gives the following definition for the futures rate:

Definition 2.6.2. Given the conditions used in definition 2.6.1, for any $t \in [0, T]$ we define the *continuously marked-to-market futures rate* as the unique process Fut_t that satisfies the equation:

$$\mathbb{E}^{\mathbb{Q}}\left[\int_t^T \frac{B_t}{B_u} dFut_u | \mathscr{F}_t\right] = 0, \tag{2.32}$$

with $(\mathbb{Q}, D)$ the risk neutral numeraire pair, as given by 2.1.2 and $Fut_{t_n} = L_T$.

Equation (2.32) has solution

$$Fut_t = \mathbb{E}^{\mathbb{Q}}[L_T | \mathscr{F}_t]. \tag{2.33}$$

See [40] or [12] for a proof or [2] for an informal proof. For the rest of the thesis we will assume continuous marking-to-market. We could convert futures rates to their implied forward rates by substracting a *convexity adjustment* given by:

$$C_t = Fut_t - L_t = \mathbb{E}^{\mathbb{Q}}\left[L_T | \mathscr{F}_t\right] - \mathbb{E}^{M}\left[L_T | \mathscr{F}_t\right]. \tag{2.34}$$

Using the convexity adjustment to price a Receiver-FRA, see (2.19), now gives the analogous equation:

$$V_{FRA}^{receiver}(0) = N\left(P(0,M)(1 + \tau(Fut_0 - C_0)) - P(0,T)\right), \tag{2.35}$$

Which links the Eurodollar futures rate, with a convexity adjustment to the underlying Libor curve in the single-curve framework.

2.6.1 Convexity

Convexity is described in various ways throughout literature. Assuming parallel yield shifts, Hull [26] describes it as error for hedging bond yield risk using only the first order derivative of the bond to the yield[30]. Pelsser describes it as the currency or payment timing induced mismatch when the forward value as given in Equation (2.10) is paid out in a different currency or at a different time [37]. For Eurodollar futures and similarly for CMS[31]-derivatives, the convexity adjustment is seen as the induced drift from measure change. With the change from the forward-measure to the risk-neutral measure in the former and change from the annuity measure to the forward measure in the latter.

Let $(\mathbb{Q}, D)$ and $(\mathbb{Q}^M, P(\cdot, M))$ be the risk neutral and M-forward numeraire pairs, given by respectively 2.1.2 and 2.2.2, the following expression for the futures rate is useful:

$$\begin{aligned} Fut_0 = \mathbb{E}^{\mathbb{Q}}[L_T] &= \mathbb{E}^{\mathbb{Q}}\left[\frac{D_0}{D_M}\frac{D_M}{D_0}L_T\right] \\ &= P^{(O)}(0,M)\mathbb{E}^{M}\left[\frac{D_M}{D_0}L_T\right] \end{aligned} \tag{2.36}$$

Final equation follows from $1 = \mathbb{E}^{\mathbb{Q}}\left[\frac{D_M}{D_0}\frac{D_0}{D_M}\right] = P^{(O)}(0,M)\mathbb{E}^{M}\left[\frac{D_M}{D_0}\right]$. Similarly the Libor forward rate can be written as:

$$L_0 = \mathbb{E}^{M}[L_T] = \frac{P^{(O)}(0,M)}{P^{(O)}(0,M)}\mathbb{E}^{M}\left[L_T\right]$$

[29] See [39], [29] or [28].
[30] Also called duration.
[31] Constant maturity swaps.

$$= P^{(O)}(0,M)\mathbb{E}^M\left[\frac{D_M}{D_0}\right]\mathbb{E}^M[L_T] \tag{2.37}$$

This gives final expression for the futures rate convexity adjustment:

$$C_0 = \frac{\mathrm{Cov}^M\left(\frac{D_M}{D_0}, L_T\right)}{P^{(O)}(0,M)} \tag{2.38}$$

The covariance identity given by 2.38 is a well known identity in literature, see [28], [1] or [29]. The expression can be further decomposed into:

$$\begin{aligned}
C_0 &= \frac{\mathbb{E}^M\left[\frac{D_M}{D_T}\frac{D_T}{D_0}L_T\right] - \mathbb{E}^M\left[\frac{D_M}{D_T}\frac{D_T}{D_0}\right]\mathbb{E}^M[L_T]}{P^{(O)}(0,M)} \\
&= \frac{\mathbb{E}^M\left[\frac{D_M}{D_T}\frac{D_T}{D_0}L_T\right] - \mathbb{E}^M\left[\frac{D_M}{D_T}\frac{D_T}{D_0}\right]\mathbb{E}^M[L_T]}{P^{(O)}(0,M)} \\
&= \frac{\mathbb{E}^M\left[\mathbb{E}^M\left[\frac{D_M}{D_T}|\mathscr{F}_T\right]\frac{D_T}{D_0}L_T\right] - \mathbb{E}^M\left[\mathbb{E}^M\left[\frac{D_M}{D_T}|\mathscr{F}_T\right]\frac{D_T}{D_0}\right]\mathbb{E}^M[L_T]}{P^{(O)}(0,M)} \\
&= \frac{\mathbb{E}^M\left[(1+\tau F_T)\frac{D_T}{D_0}L_T\right] - \mathbb{E}^M\left[(1+\tau F_T)\frac{D_T}{D_0}\right]\mathbb{E}^M[L_T]}{P^{(O)}(0,M)} \\
&= \frac{\mathrm{Cov}^M\left(\frac{D_T}{D_0}(1+\tau F_T), L_T\right)}{P^{(O)}(0,M)}
\end{aligned} \tag{2.39}$$

Equation (2.39) is particularly useful because it reveals the dependency of the futures rate convexity adjustment on the joint distributions of L_T, F_T and D_T under the M-forward measure. Caplet volatility surfaces, as will be explained in Section 2.7 provide information about the underlying distribution of L_T in the forward measure[32], which leads to expressions for the convexity adjustment after modelling correlations and variances of F_T and D_T. Due to working in the single-curve framework we can limit our attention to the joint distribution of L_T and D_T. We will finish the prerequisites by summarizing caplet volatility stripping.

2.7 Caplet volatility surface

Caplet volatilities are not known directly due to caplets not being traded individually, but in baskets called *caps*. Caplet volatility stripping is well known in literature, see [46] or [26], but requires knowing the Libor curve for construction of the surface. We include it in the thesis to show how the magnitude of convexity adjustments has little effect on the curve and consequently the caplet volatility surface, therefore it is 'safe' to assume a unique caplet volatility surface, which we will show in this section.

2.7.1 Caplet volatility stripping

Caplets are European call options on the Libor forward rate. In practice caplets are only traded in baskets, such a basket is called a *cap*. When looking at 3M Libor caps, they are traded with maturities ranging between 1 and 30 years, with a 3 month caplet frequency, meaning that given a 1 year cap it has 4 underlying caplets with maturities of 3, 6, 9 and 12 months, while caps are traded in general in 1 year frequencies[33]. As a result there are less caps traded than there are

[32] see [27] for more details about the link between the volatility smile and asset distributions.

[33] 3MEUR caps are traded for maturities $\{1, 1.5, 2, 3, 4, 5, 6, 7, 8, 9, 10, 12, 15, 20, 25, 30\}$, same for 3M USD caps with only the 1.5 year cap missing. This can be explained by market supply and demand for whole year maturity caps and.

underlying caplets. Let $0 \leq T'_0 < T'_1 < ... < T'_n$ be the corresponding caplet time structure, with $T'_1, ..., T'_n$ corresponding to caplet maturities[34]. Given numeraire pair $(\mathbb{Q}, D)$ the present value of a caplet with accruing period $[T'_i, T'_{i+1}]$ paid out at T_{i+1} is given below:

$$\begin{aligned} V_{caplet,i}(0) &= \tau'_i \mathbb{E}^{\mathbb{Q}}\Big[\frac{D_0}{D_{T_{i+1}}}(L^{(i)}_{T'_i} - K)^+\Big] \\ &= \tau'_i P(0, T_{i+1}) \mathbb{E}^{T'_{i+1}}[(L^{(i)}_{T'_i} - K)^+]. \end{aligned}$$

Here the spot Libor $L^{(i)}_{T'_i}$ is fixed at T^F_i usually 2 business days before T'_i, analogously to swaps. We define the corresponding Libor forward rate as $L^{(i)}_t$ for $t \leq T'_i$. Quotes of caps are provided for a subset of caplet maturities $T'_{I_1} < T'_{I_2} < ... < T'_n$, giving $n_2 < n$ different caps, via their implied flat volatilities: $(m, K) \mapsto \sigma^{(\theta_{flat})}_m(K)$ such that T'_{I_m} is the corresponding highest caplet maturity. his leads to the corresponding cap valuation, given a cap with maturity T'_{I_m}:

$$V_{cap_m}(0) = \sum_{i=0}^{I_m - 1} V_{caplet,i}(0) = \sum_{i=0}^{I_m - 1} P(0, T'_{i+1}) \tau'_i \mathbb{E}^{T'_{i+1}}[(L^{(i)}_{T'_i} - K)^+] \tag{2.40}$$

Note we can rewrite (2.40) with $\theta > 0$ being the *forward rate shift* parameter corresponding to caplets:

$$V_{cap_m}(0) = \sum_{i=0}^{I_m - 1} V_{caplet,i}(0) = \sum_{i=0}^{I_m - 1} P(0, T'_{i+1}) \tau'_i \mathbb{E}^{T'_{i+1}}[((L^{(i)}_{T'_i} + \theta) - (K + \theta))^+] \tag{2.41}$$

Computing the expectation $\mathbb{E}^{T'_{i+1}}[((L^{(i)}_{T'_i} + \theta) - (K + \theta))^+]$ depends on forward rate dynamics. Using lognormal dynamics leads to Black's formula, as specified by A.1, with $v = \sigma^{(\theta)}_{T'_i}(K)$ and $T - t = T'_i$ gives:

$$V_{cap_m}(0) = \sum_{i=0}^{I_m - 1} V_{caplet,i}(0) = \sum_{i=0}^{I_m - 1} \tau'_i P(0, T'_{i+1}) Black(L^{(i)}_0 + \theta, K + \theta, \sigma^{(\theta)}_{T'_i}(K), T'_i). \tag{2.42}$$

with $\sigma^{(\theta)}_{T'_i}(K)$ being the *caplet volatility*. Caplet flat volatilities are defined such that for every $I_m \in \{I_1, I_2, ..., n\}$:

$$V_{cap_m}(0) = \sum_{i=0}^{I_m - 1} \tau'_i P(0, T'_{i+1}) Black(L^{(i)}_0 + \theta_{flat}, K + \theta_{flat}, \sigma^{(\theta_{flat})}_m(K), T'_i). \tag{2.43}$$

With $\theta_{flat} > 0$ being the *forward rate shift* parameter corresponding to flat cap volatilities. In Figures 2.10 and 2.12 we show the difference between the flat volatility and caplet volatility term structure for 4 caps with strikes 0%, 5% and maturities 3 and 12 years, using the stripped caplet volatility surface given by Figure 2.15 and the flat volatility surface given by 2.13 for the Euro currency. Firstly the 3 year maturity :

[34] T'_0 is in 2 business days and $T'_{i+1} - T'_i$ is 3 months in the case of 3 month caplets, where T'_{i+1} is also corrected to be on a business day depending on the convention.

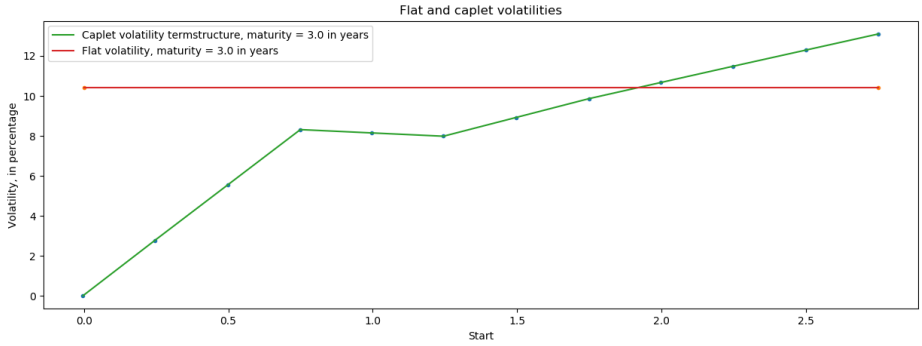

Figure 2.9: Flat volatility and caplet volatility term structure corresponding to a 3 year maturity caplet. $K = 0\%$.

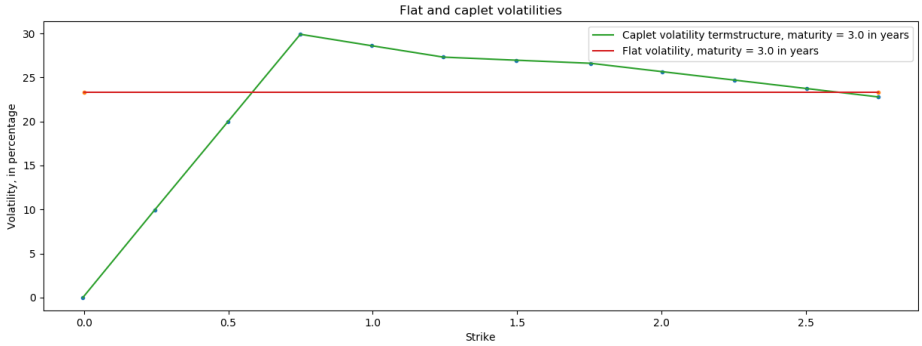

Figure 2.10: Flat volatility and caplet volatility term structure corresponding to a 3 year maturity caplet. $K = 5\%$.

Additionally for the 12 year maturity:

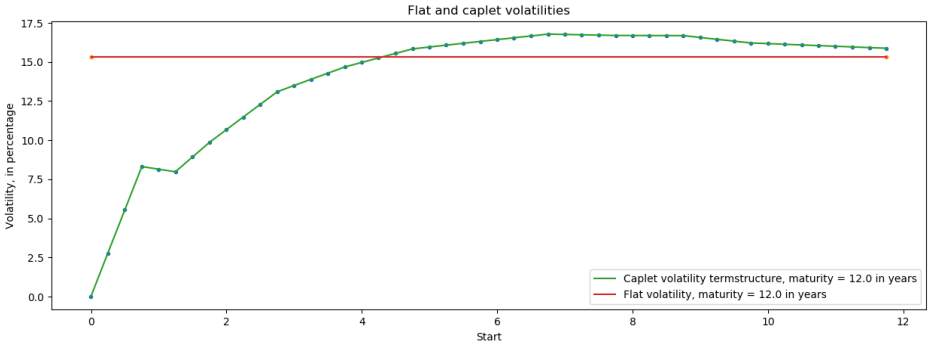

Figure 2.11: Flat volatility and caplet volatility term structure corresponding to a 12 year maturity caplet. $K = 0\%$.

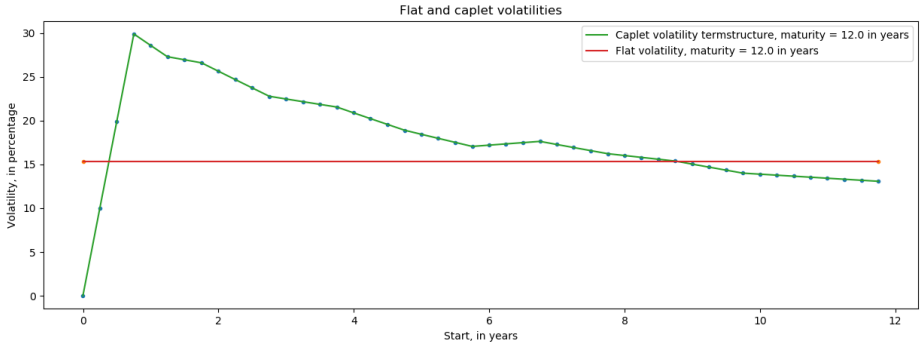

Figure 2.12: Flat volatility and caplet volatility term structure corresponding to a 12 year maturity caplet. $K = 5\%$.

Note that the 3 month caplet is deterministic, with underlying volatility 0. We have linearly extrapolated the caplet volatility termstructure up to the first cap maturity of 1 year, with the 3 month caplet volatility equal to 0.

2.7.2 Absolute strike stripping

It is directly visible from Equation (2.43) that a strike K cap contains information about the strike K caplet volatilities for all underlying caplets. Provided a shifting parameter θ and a Libor curve[35] allows, after collecting all caps that are traded for the same strike[36] K, to solve for the corresponding strike K caplet volatility term structure. Because there are more caplet volatilities than there are caps an interpolation procedure can be assumed to obtain a caplet volatility term structure that exactly prices back all caps. Doing this for every absolute strike and interpolating the corresponding term structure gives us back the caplet volatility surface.

Given one absolute strike K equations (2.43) and (2.42) lead to the following system:

$$\mathbf{G}_K = \hat{\mathbf{G}}_K(\sigma^{(\theta)}(K). \tag{2.44}$$

- $\mathbf{G}_K$ is the vector of strike K cap values derived from the quoted flat implied volatilities, see (2.43).
- $\sigma^{(\theta)}(K) = (\sigma^{(\theta)}_{T'_{I_1}}(K), ..., \sigma^{(\theta)}_{T'_n}(K))$ is the vector of the n_2 caplet volatilities.
- $\hat{\mathbf{G}}_K$ maps caplet volatilities to the corresponding vector of cap values with strike K, see (2.42) with shifting parameter vector θ_{caplet}.

Solving $\sigma^{(\theta)}(K)$ for every absolute strike K uniquely defines the caplet volatility surface after specifying an interpolation routine, given by the funtion f. We use linear term structure interpolation for the caplet volatility surface as detailed below with cubic spline interpolation of the volatility smile, this will be further addressed in chapter 4:

$$\sigma^{(\theta)}_T(K) = \begin{cases} \sigma^{(\theta)}_{T'_{I_{i+1}}}(K)\dfrac{T - T'_{I_i}}{T'_{I_{i+1}} - T'_{I_i}} + \sigma^{(\theta)}_{T'_{I_i}}(K)\dfrac{T'_{I_{i+1}} - T}{T'_{I_{i+1}} - T'_{I_i}} & \text{,if } T \in (T'_{I_i}, T'_{I_{i+1}}) \\ f(\sigma^{(\theta)}_T(K_i), \sigma^{(\theta)}_T(K_{i+1}), \sigma^{(\theta)}_T(K_{i-1}), K, T) & \text{,if } K \in (K_i, K_{i+1}). \end{cases} \tag{2.45}$$

Solving Equation (2.44) can again be done using any rootfinding algorithm like Newton-Rhapson, but during implementation it becomes apparent that the Jacobian of $\hat{\mathbf{G}}_K$ J_{G_K} is ill-conditioned. Therefore, we use the Levenberg-Marquardt algorithm, see [14] for more details.

[35] Assuming we know the Libor curve, from which the corresponding Libor forward rates $L_0^{(i)}$ are inferred.
[36] Absolute strike.

In Figure 2.13 we show the 3MEUR and 3MUSD flat volatility surfaces using datasets B.3 and B.4:

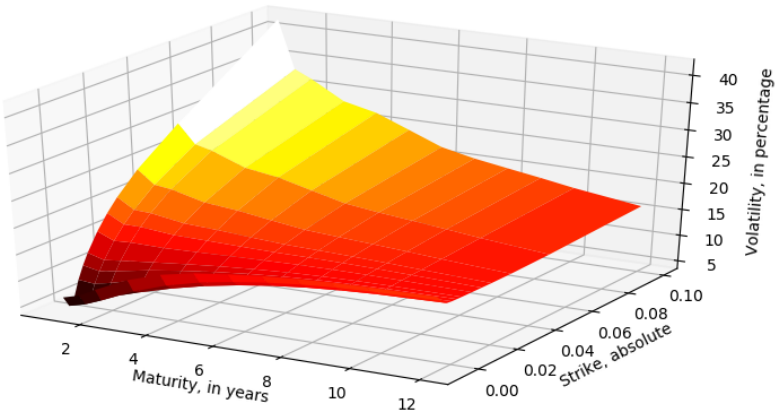

(a) 25th January 2018 3MEUR flat cap volatility surface, $\theta_{flat} = 0.03$.

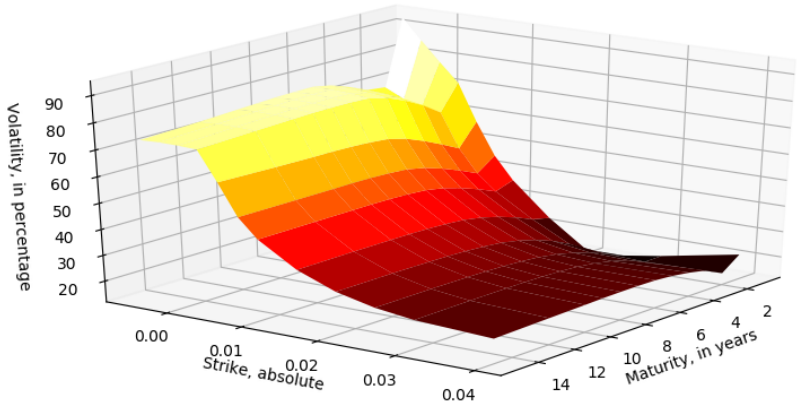

(b) 25th January 2018 3MUSD flat cap volatility surface, $\theta_{flat} = 0$.

Figure 2.13: 25th January 2018 3MEUR and 3MUSD flat cap volatility surfaces, for absolute strikes, bilinearly interpolated.

We use historical flat cap volatility data provided by a broker, see B.3 and B.4. The data provided gives the flat cap volatilities for both the 3M Euro Libor and the 3M USD Libor on the 25th of January 2018, provided by the options broker ICAP. Solving for the corresponding caplet volatility surfaces[37] results in:

[37] Given by the corresponding Libor curves from Chapter 3.

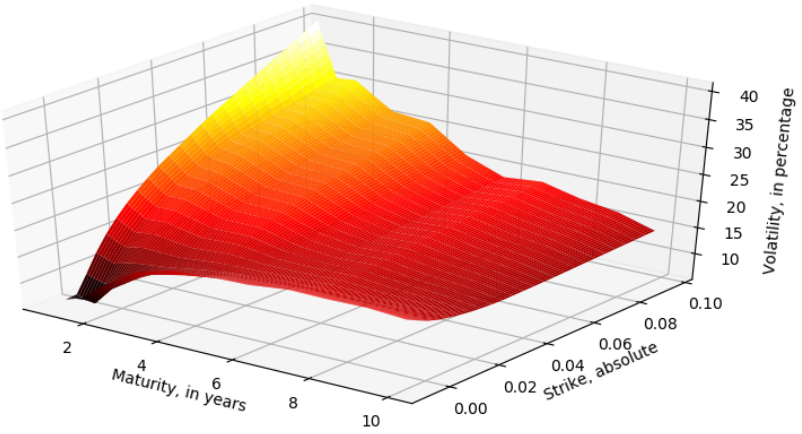

(a) 25th January 2018 3MEUR stripped caplet volatility surface, $\theta = 0.03$.

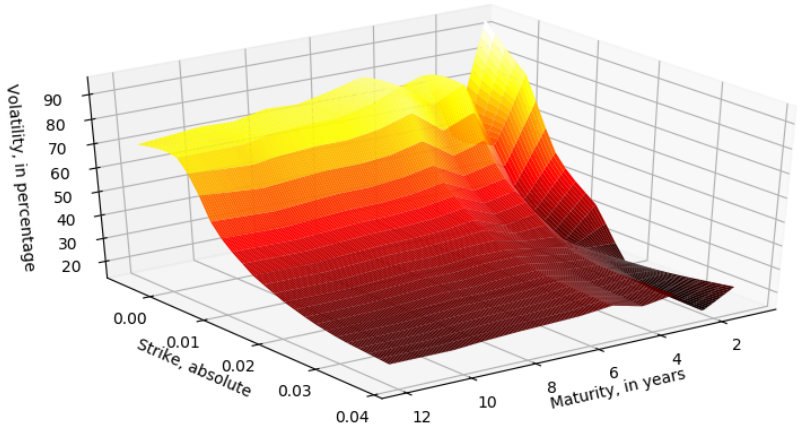

(b) 25th January 2018 3MUSD stripped caplet volatility surface, $\theta = 0.01$.

Figure 2.14: 25th January 2018 3MEUR and 3MUSD caplet volatility surfaces stripped using absolute strikes.

These caplet volatility surfaces reprice all caps up to 1/100th of a basispoint. It can be denoted that for both surfaces there is a visible oscillating behavior in the maturity direction. By rewriting (2.44) into an optimization problem and adding a smoothness and weighing penalty we obtain the following optimization problem:

$$\underset{\sigma^{(\theta)}(K)}{\operatorname{argmin}}(\mathbf{G}_K - \hat{\mathbf{G}}_K(\sigma^{(\theta)}(K)))^\top(\mathbf{G}_K - \hat{\mathbf{G}}_K(\sigma^{(\theta)}(K))) + \lambda\sigma^{(\theta)}(K)^\top P\sigma^{(\theta)}(K). \tag{2.46}$$

With λ a weighting constant and P the penalty matrix, see A.4. Solving for the corresponding caplet volatility surfaces results in:

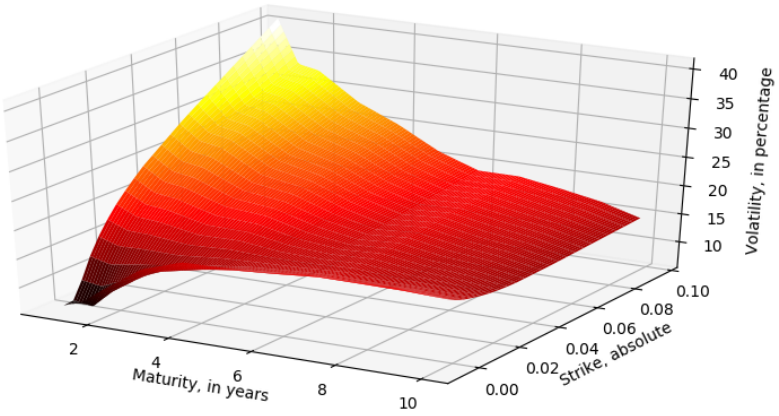

(a) 25th January 2018 3MEUR stripped caplet volatility surface, $\theta = 0.03$.

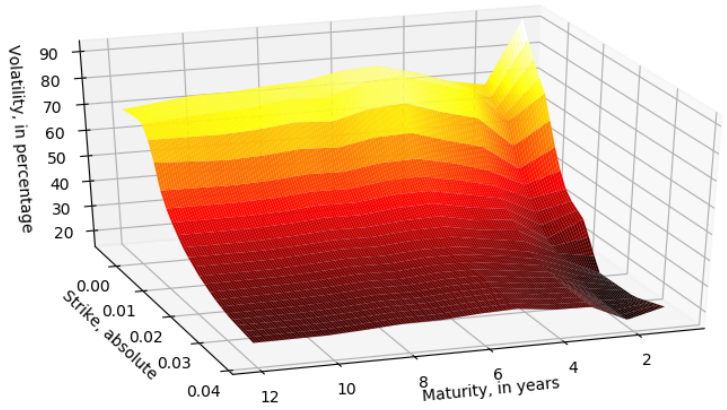

(b) 25th January 2018 3MUSD stripped caplet volatility surface, $\theta = 0.01$.

Figure 2.15: 25th January 2018 3MEUR and 3MUSD caplet volatility surfaces stripped using absolute strikes with smoothness penalty. $\lambda = 0.0003$ and both surfaces reprice the caps within an error of 1 basispoint. Curves used given in Figure 3.2.

We will use the surfaces given by Figure 2.15 in Chapter 4 when using short-rate model implied convexity adjustments.

We have stripped the surface assuming that the Libor curve is known. The Libor curve is unknown, but the at the money strikes (or equivalently the swap rates) are provided up to a basispoint. Therefore we will test our proprietarily calibrated Libor curve, see Figure 3.2 without convexity adjustments and compare the implied swap rates to the at the money strikes, in case the difference is small enough we will proceed to use the corresponding implied forward rates.

2.7.3 Hagan's formula

As will be noticed in Section 4.4.3 using linear or even cubic spline interpolation of the caplet volatility smile leads to unfeasible probability density functions of the underlying forward rates. Alternatively we can use Hagan's formula to parametrise the surface given in Figure 2.14. Let $\hat{L}_0^{(i)} = L_0^{(i)} + \theta$ and $\hat{K} = K + \theta$ be the θ-shifted strike and forward rate with accruing period $[T_i, T_{i+1}]$. Hagan's formula is given by:

$$\sigma^{\text{SABR},(\theta)}(L_0^{(i)}, K) = \frac{\alpha_{T_i}}{(\hat{L}_0^{(i)}\hat{K})^{(1-\beta_{T_i})/2}\left(1 + \frac{(1-\beta_{T_i})^2}{24}\log^2\left(\frac{\hat{L}_0^{(i)}}{\hat{K}}\right) + \frac{(1-\beta_{T_i})^4}{1920}\log^4\left(\frac{\hat{L}_0^{(i)}}{\hat{K}}\right) + \dots\right)} \cdot \frac{z}{x(z)}$$
$$\cdot \left[1 + \left(\frac{(1-\beta_{T_i})^2}{24}\frac{\alpha_{T_i}^2}{(\hat{L}_0^{(i)}\hat{K})^{1-\beta_{T_i}}} + \frac{1}{4}\frac{\rho_{T_i}\beta_{T_i}\nu_{T_i}\alpha_{T_i}}{(\hat{L}_0^{(i)}\hat{K})^{(1-\beta_{T_i})/2}} + \frac{2-3\rho_{T_i}^2}{24}\nu_{T_i}^2\right)T + \dots\right], \tag{2.47}$$

with:

$$z = \frac{\nu_{T_i}}{\alpha_{T_i}}(\hat{L}_0^{(i)}\hat{K})^{(1-\beta_{T_i})/2}\log\left(\frac{\hat{L}_0^{(i)}}{\hat{K}}\right), \tag{2.48}$$

and

$$x(z) = \log\left(\frac{\sqrt{1 - 2\rho_{T_i}z + z^2} + z - \rho_{T_i}}{1 - \rho_{T_i}}\right). \tag{2.49}$$

Hagan's formula is an approximation of the volatility smile given that the underlying shifted forward rate $L_t^{(i)} + \theta$ moves under SABR dynamics, see [19]. We will use the formula for both interpolation and extrapolation of the underlying volatility smile, calibrated using Figure 2.15. We calibrate Hagan's formula by fixing $\beta_{T_i} = 0.5$ and using an optimizer to solve for $\alpha_{T_i}, \beta_{T_i}, \rho_{T_i}$ such that the difference between the corresponding caplet volatility smile given by 2.15 and Hagan's formula implied smile is at most 2%, we do this for every cap maturity, resulting in n parameter sets for n cap maturities. The termstructure is interpolated using linear SABR parameter interpolation. Giving:

$$\alpha_T = \frac{T_{i+1} - T}{h_i}\alpha_{T_i} + \frac{T - T_i}{h_i}\alpha_{T_{i+1}},$$

for $T \in [T_i, T_{i+1}]$ and $h_i = T_{i+1} - T_i$, with analogous equations for parameters β_T, ρ_T and ν_T.

In case of the European caplet volatility surface given in Figure 2.15 Hagan's formua implied smile reprices all caps used in the absolute strike calibration used to strip the caplet volatility surface within 1 basis-point. Better calibration is in general not possible to a smile with 12 spine points due to the limitted degrees of freedom of the SABR model having only 4 parameters.

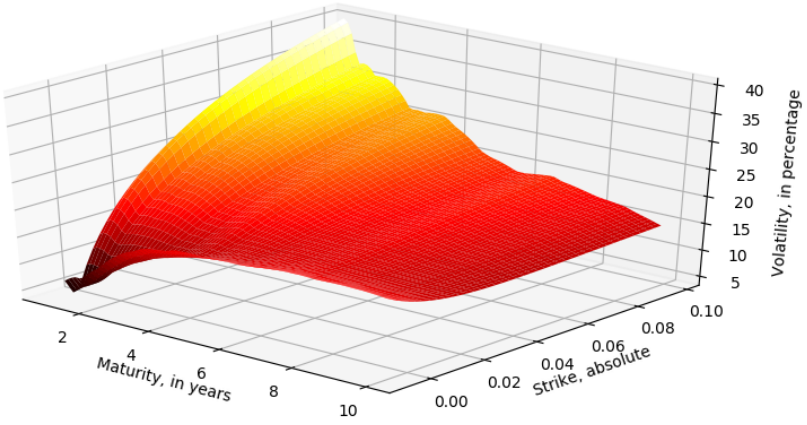

Figure 2.16: SABR surface calibrated to the 3MEUR caplet volatility surface with penalty in Figure 2.15.

When using the replication method to value convexity adjustments we will be required to extrapolate the caplet volatility surface for strikes near the lower boundary $-\theta$, see Section 4.4.3. Extending the strike boundaries of the caplet volatility surface it becomes visible that the surface becomes unfeasible for low strikes near the lower boundary $-\theta = -0.03$:

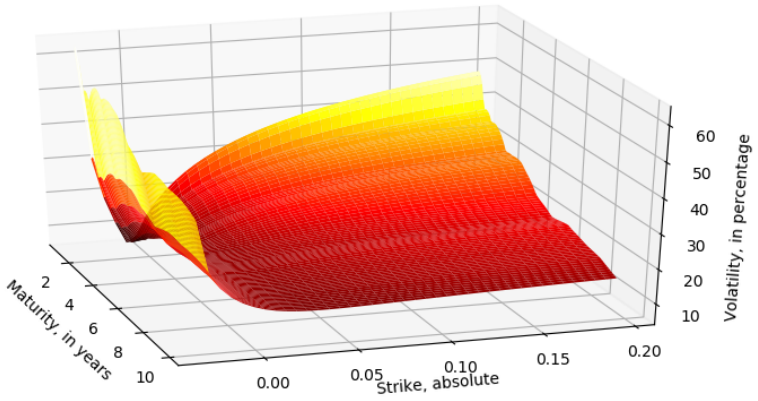

Figure 2.17: Surface given by Figure 2.16, extrapolated between $-\theta + 0.001$ and $b' + 0.1$.

This is a well-known shortcoming of Hagan's formula, see [18]. This problem can be solved by increasing the underlying shifting parameter. In Figure 2.18 we display the underlying absolute-strike stripped European volatility surfaces using θs of 6% and 10% respectively after stripping the caplet volatility surface analogously to those in Figure 2.15:

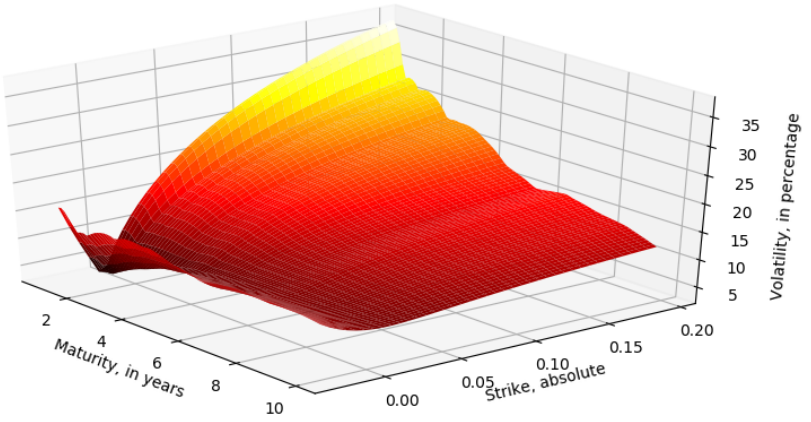

(a) 25th January 2018 3MEUR stripped caplet volatility surface, $\theta = 6\%$.

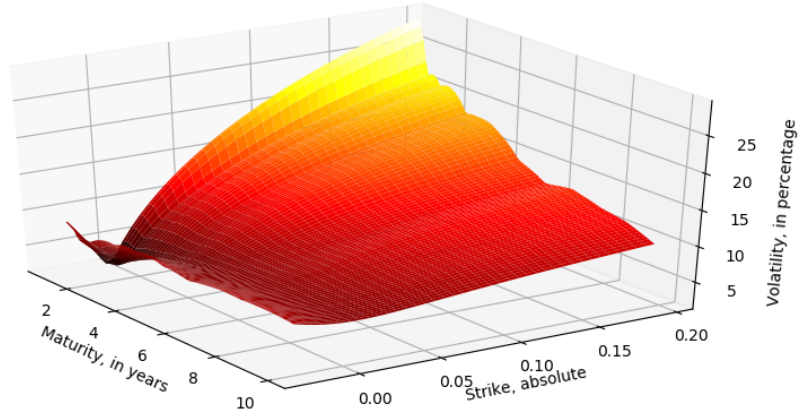

(b) 25th January 2018 3MEUR stripped caplet volatility surface, $\theta = 10\%$.

Figure 2.18: SABR surfaces calibrated to the 3MEUR caplet volatility surface with penalty in Figure 2.15. $\theta = 6\%$ and 10% respectively. Extrapolated between -0.029 and $b' + 0.1$, which is the same for Figure 2.17.

What can also directly be denoted is that the volatility surfaces decrease when the shifting parameter increases, this makes sense from the perspective that the volatility surfaces in Figures 2.18 corresponds to the implied volatilities using shifted Libor forward rates following the stochastic differential equation:

$$dL_t^{(\theta)} = (L_t^{(\theta)} + \theta)\sigma^{(\theta)} dW_t^M.$$

Given $\theta_2 >> \theta_1$ and given that implied volatilities are derived by calibrating the dynamics to the same option prices it makes sense that $L_T^{(\theta_1)}$ and $L_T^{(\theta_2)}$ should be approximately equal in distribution due to both being governed by lognormal dynamics. From this follows $\sigma^{(\theta_1)} > \sigma^{(\theta_2)}$ in order to compensate for $L_t^{(\theta_1)} + \theta_1 < L_t^{(\theta_2)} + \theta_2$. We will use the 10% shifted caplet volatility surface for in the replication method in Section 4.4 and 2.15 when using short-rate models in

Section 4.3.

2.7.4 Curve dependence of the volatility surface

Given the curves implied by dataset B.1, without convexity adjustments and dataset B.2, with quoted convexity adjustments, computed using Algorithm 1 and cubic spline interpolation of intermediate discount factors, see Chapter 3, we compare the implied swap rates to the at the money strikes below:

Maturity in years	ATM strikes	Implied swap rates
1	-0.003	-0.0031
1.5	-0.0025	-0.0026
2	-0.0016	-0.0018
3	0.0003	0.0000
4	0.0022	0.0019
5	0.0038	0.0035
6	0.0051	0.0050
7	0.0063	0.0062
8	0.0074	0.0073
9	0.0084	0.0084
10	0.0094	0.0093
12	0.0109	0.0110

Table 2.1: 3MEUR, 25-1-2018

Maturity in years	ATM strikes	Implied swap rates
1	0.0211	0.0205
2	0.0231	0.0227
3	0.0242	0.0241
4	0.0248	0.0247
5	0.0252	0.0252
6	0.0255	0.0256
7	0.0258	0.026
8	0.0261	0.0263
9	0.0263	0.0265
10	0.0266	0.0268
12	0.0269	0.0272
15	0.0272	0.0276

Table 2.2: 3MUSD, 25-1-2018

Strikes and swap rates only deviate by a few basispoints, therefore we will perform the stripping using the fixed convexity adjustment curve. Because the effect of convexity adjustments on forward rates is in the order of basispoints, as will be show in chapters 4, we will use the stripped caplet volatility surfaces using curves calibrated with fixed convexity adjustments for the rest of the thesis[38]. The surface is given by given by Figure 2.18 when using dataset B.1.

[38]Fixed convexity adjustments are provided in datasets B.1 and B.2.

Chapter 3

Yield curve calibration basics

Having introduced the Libor curve intuitively in chapter 2 we will show how the curve is calibrated from deposits, FRAs and swaps and analogously from futures with fixed convexity adjustments. We will work in the single-curve framework where the Libor curve is assumed to be equal to the overnight curve and argue the extension into the multi-curve framework in Chapter 5.

3.1 Curve calibration in the single-curve framework

Combining Equations (2.24), (2.19) and (2.13) for a set of N instruments of all 3 categories provides us with a system of N equations, which defines a subspace for the possible values of N_2 possible Libor discount factors used in the various equations. Let $0 < T_0 < ... < T_N$ be the corresponding time structure of maturities[1], let $\mathbf{Q}$ be the corresponding set of instrument rates.

In case $N_2 = N$ we can solve system uniquely obtaining the vector of discount factors $\mathbf{P} = (P(0,T_0),...,P(0,T_N))$. The Libor curve can be further inferred by assuming an interpolation procedure for $P(0,T)$ for $T \in (T_i, T_{i+1})$, we will consider linear discount curve and cubic-spline interpolation in this Section given by:

$$P(0,T) = \frac{T_{i+1} - T}{h_i} P(0,T_i) + \frac{T - T_i}{h_i} P(0,T_{i+1}). \tag{3.1}$$

With $h_i = T_{i+1} - T_i$. We will consider alternative interpolation routines in Section 3.3. It makes intuitive sense that a discount factor for some intermediate year should be a weighted average of the discount factors at spine points dates, given by T_i and T_{i+1}. In case the maturities, starting dates and fixed leg payment dates of Libor rates underlying the FRAs and swaps do not align, then $N_2 > N$, in which case our Libor discount factors are not unique.

By pre-specifying the interpolation procedure our Libor curve is uniquely determined (for maturities up to the largest calibration instrument maturity) by the N discount factors at spine point dates T_i. This leads to a system of N equations with N unknowns with an interpolation dependent unique solution:

$$NPV_1(\mathbf{P}, Q_1) = 0 \tag{3.2}$$

$$\vdots \tag{3.3}$$

$$NPV_n(\mathbf{P}, Q_n) = 0. \tag{3.4}$$

[1] Working with a strip of FRA-rates or futures rates with maturity range $T_1 < ... < T_n$ with $n < N$ it is usual to use a deposit/spot rate as your very first instrument with maturity T_0. We will stick to this convention in later chapters.

Such that:

$$NPV_i(\mathbf{P}, Q_i) = \begin{cases} P(0,T_i)(1+\tau_{i-1}Q_i) - 1 = 0 & Q_i \text{ is a deposit rate.} \\ P(0,T_i)(1+\tau_{i-1}Q_i) - P(0,T_i-\tau_{i-1}) = 0 & Q_i \text{ is a FRA-rate.} \\ \sum_{j=0}^{i-1} \tau_j L_0^{(j)} P(0,T_{j+1}) - Q_i \sum_{j=0}^{I_i-1} \tau'_j P(0,T'_{j+1}) = 0 & Q_i \text{ is a swap-rate.} \end{cases} \tag{3.5}$$

Given floating-leg tenor structure $0 < T_1 < ... < T_i$, the corresponding fixed leg payments are made on $0 < T'_1 < ... < T'_{I_i}$ with $\tau'_j = T'_{j+1} - T'_j$. All n equations then give:

$$\mathbf{NPV}(\mathbf{P}, \mathbf{Q}) = 0. \tag{3.6}$$

Here $\mathbf{P} = (P(0,T_1), ..., P(0,T_N))$ is the solution vector of Libor discount factor *spine points* with $\mathbf{Q}$ the length N vector of calibration instrument rates. Equivalently when calibrating using futures rates instead of FRA rates, with fixed convexity adjustments $\mathbf{C}$, using Equation (2.35) leads analogously to:

$$\mathbf{NPV}(\mathbf{P}, \mathbf{C}, \mathbf{Q}) = 0. \tag{3.7}$$

Equations (3.6) and (3.7) can be solved by any multivariate root finding algorithm. We will be using the Newton-Rhapson algorithm:

Algorithm 1: Newton-Rhapson algorithm for solving equation (3.6).

Data: $\mathbf{Q}$,$\mathbf{C}$
$\mathbf{P}_{(0)} = \mathbf{1}$;
$\epsilon = 10^{-14}$;
while $||\mathbf{P}_{(n)} - \mathbf{P}_{(n-1)}|| > \epsilon$ **do**
  $\mathbf{P}_{(n)} = \mathbf{P}_{(n)} - \mathbf{J_{NPV}}^{-1}(\mathbf{P}_{(n-1)})\mathbf{NPV}(\mathbf{P}_{(n-1)})$;
end

With $\epsilon = 10^{-15}$, $\mathbf{P}_{(0)} = \mathbf{1}$ and $\mathbf{NPV}(\cdot) = \mathbf{NPV}(\mathbf{Q}, \mathbf{C}, \cdot)$ when using futures rates or $\mathbf{NPV}(\cdot) = \mathbf{NPV}(\mathbf{Q}, \cdot)$ when using FRA rates and $\mathbf{J_{NPV}}$ the corresponding discount factor Jacobian, given by:

$$\mathbf{J_{NPV}}(\mathbf{P}) = \begin{pmatrix} \frac{NPV_1(\mathbf{P})}{\partial P(0,T_1)} & \cdots & \frac{NPV_1(\mathbf{P})}{\partial P(0,T_N)} \\ \vdots & & \vdots \\ \frac{NPV_N(\mathbf{P})}{\partial P(0,T_1)} & \cdots & \frac{NPV_N(\mathbf{P})}{\partial P(0,T_N)} \end{pmatrix}$$

Finally we will use short the hand notation:

$$\mathbf{P_{solve}}(\mathbf{P^{(0)}}, \mathbf{C}), \tag{3.8}$$

For the calibrated discount factor vector $\mathbf{P}$ resulting from Algorithm 1, with starting vector $\mathbf{P^{(0)}} = \mathbf{1}$, linear discount factor interpolation[2] and fixed convexity adjustments[3]. What can be quickly denoted is that using linear discount factor interpolation the system 3.7 reduces to a matrix equation given by:

$$\mathbf{NPV}(\mathbf{Q}, \mathbf{C}, \mathbf{P}) = \mathbf{A}(\mathbf{C}, \mathbf{Q})\mathbf{P} - \mathbf{b} = 0.$$

Consequently the system can be solved using any linear equation solver. The Newton-Rhapson algorithm converges after one iteration using initial spine point vector $\mathbf{P^{(0)}} = \mathbf{1}$:

$$\mathbf{P^{(1)}} = \mathbf{P^{(0)}} - \mathbf{A}(\mathbf{C}, \mathbf{Q})^{-\mathbf{1}}(\mathbf{A}(\mathbf{C}, \mathbf{Q})\mathbf{P^{(0)}} - \mathbf{b})$$

From which follows:

$$\mathbf{P^{(1)}} = \mathbf{A}(\mathbf{C}, \mathbf{Q})^{-\mathbf{1}}\mathbf{b}, \tag{3.9}$$

[2]Unless explicitly stated otherwise.
[3]$\mathbf{C} = \mathbf{0}$ unless explicitly stated otherwise.

which is the solution of $\mathbf{A}(\mathbf{C}, \mathbf{Q})\mathbf{P} = \mathbf{b}$.

Using alternative interpolation routines introduces non-linearity into the system (3.7), consequently the Newton-Rhapson algorithm will take more iterations to converge, as we will see in Section 3.3. We will construct 2 curves using datasets B.1 and B.2, from the 25th of January 2018 for deposit, forward rate agreements and swaps under the following conventions, as have been mentioned in 2.5.1: Quotes are given in percentages. Time unit is given under the ACT/360 modified following convention. Floating swap legs have 3 month frequency. Fixed swap legs have 1y frequency. Linear interpolation is used over the discount curve between the spine points.
We will calibrate using the implied FRA rates, which is equivalent to using the futures rates with fixed convexity adjustments. Below we display both discount curves:

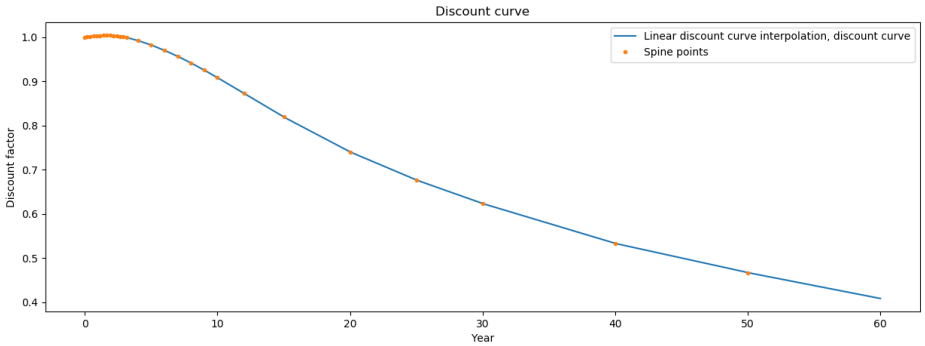

Figure 3.1: 25th of January 2018, 3MEUR discount curve. 1 iterations.

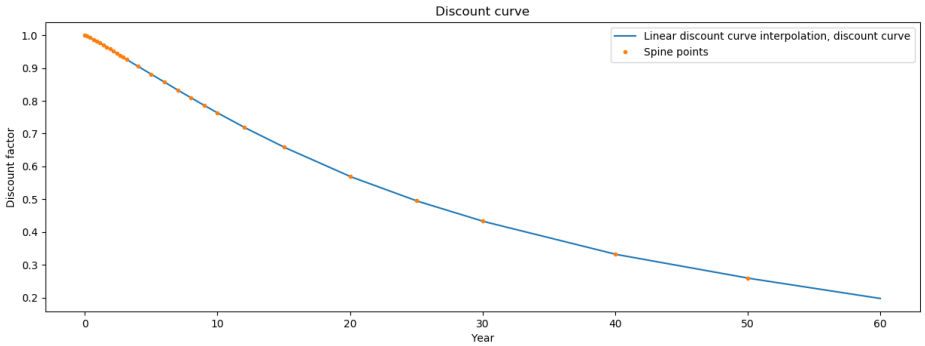

Figure 3.2: 25th of January 2018, 3MUSD discount curve. 1 iterations.

The curves are defined between maturities of 0 and 60 years and are constructed within 1 Newton-Rhapson iteration.

3.2 Calibration in the multi-curve framework

In the multi-curve-framework in general the overnight curve and higher tenor Libor curves are solved in order, specified by the systems:

$$\mathbf{NPV^{(O)}}(\mathbf{P^{(O)}}, \mathbf{Q^{(O)}}) = \mathbf{0}.$$

and the conditional system:

$$\mathbf{NPV}^{(\tau)}(\mathbf{P}^{(\tau)}, \mathbf{P^{(O)}}, \mathbf{Q}^{(\tau)}, \mathbf{C}) = \mathbf{0}.$$

This is done using both Libor and overnight rate instruments. Given the addition of spread instruments like basis-swaps, structured similarly to the fixed-for-floating swap introduced in Section 2.3, introduce dependencies between the 2 curves and the overnight curve can not be solved on its own. This leads to a system where the overnight and Libor curves are solved globally, analogously to (3.7):

$$\mathbf{NPV}(\mathbf{P^{(O)}}, \mathbf{P}^{(\tau_1)}, ..., \mathbf{P}^{(\tau_n)}, \mathbf{C}, \mathbf{Q}) = 0. \tag{3.10}$$

Considering a multi-curve framework with only the overnight and 3-month curve gives the system:

$$\mathbf{NPV}(\mathbf{P^{(O)}}, \mathbf{P^{(3m)}}, \mathbf{C}, \mathbf{Q}) = 0, \tag{3.11}$$

Overnight curves are calibrated using deposits, OIS or basis-swaps, see [1]. Analogously to Equation (3.5) we can derive:

$$NPV_i(\mathbf{P^{(O)}}, \mathbf{P^{(3m)}}, C_i, Q_i) =$$
$$\begin{cases} P^{(\tau)}(0,T_i)(1+\tau_{i-1}Q_i) - 1 = 0 & Q_i \text{ is a 3m deposit rate.} \\ P^{(\tau)}(0,T_i)(1+\tau_{i-1}(Q_i - C_i)) - P^{(\tau)}(0,T_i - \tau_{i-1}) = 0 & Q_i \text{ is a 3m futures rate.} \\ \sum_{j=0}^{i-1} \tau_j L_0^{(j)} P^{(O)}(0,T_{j+1}) - Q_i \sum_{j=0}^{I_i-1} \tau'_j P^{(O)}(0,T'_{j+1}) = 0 & Q_i \text{ is a 3m swap-rate.} \\ \sum_{j=0}^{i-1} \tau_j F_0^{(j)} P^{(O)}(0,T_{j+1}) - Q_i \sum_{j=0}^{I_i-1} \tau'_j P^{(O)}(0,T'_{j+1}) = 0 & Q_i \text{ is a OIS-swap rate.} \\ \sum_{j=0}^{i-1} \tau_j L_0^{(j)} P^{(O)}(0,T_{j+1}) - \sum_{j=0}^{i-1} \tau_j (F_0^{(j)} + Q_i) P^{(O)}(0,T_{j+1}) = 0 & Q_i \text{ is a basis-swap rate.} \end{cases} \tag{3.12}$$

With $L_0^{(j)}$ and $F_0^{(j)}$ given by Definitions 2.4.1 and 2.4.2 with accuing period $[T_j, T_{j+1}]$. Details about OIS (overnight indexed swaps) and basis-swaps can be found in [1]. We will ignore the multi-curve framework for the rest of the thesis and mention it again in Further Research 5.

3.3 Alternative interpolation routines

In this section we will look at hidden assumptions behind using linear discount factor interpolation. Below are the forward Libor rate curves[4] corresponding to Figure 3.2:

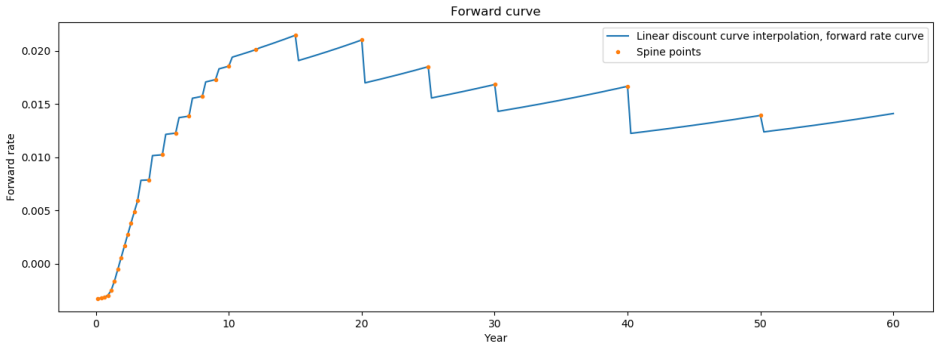

Figure 3.3: 25th of January 2018, 3MEUR forward curve.

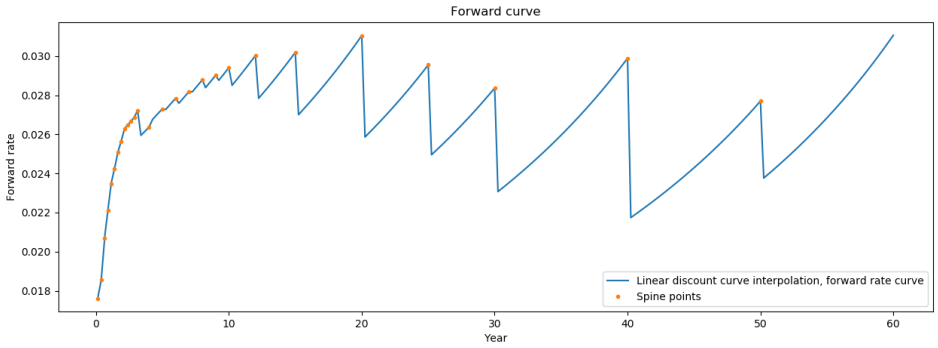

Figure 3.4: 25th of January 2018, 3MUSD forward curve.

Oscillating forward rates are a well known consequence of linear discount curve interpolation, see [2] for more details. Which can be solved by imposing alternative interpolation schemes. We use cubic splines, which rests on imposing continuous second order derivatives of yield curve spine points, see Appendix A.6 for details. Using the defining equation for the yield:

$$\exp(-y(T)T) = P(0,T),$$

which can be rewritten to:

$$y(T) = -\frac{\log(P(0,T))}{T},$$

our yield curve is fully determined on $[0, T_N]$ given $\mathbf{y} = (y(0), y(T_0), ..., y(T_N)) = (y_{-1}, y_0, ..., y_N)$ using Equation (A.19) after imposing values for y_{-1}, y''_{-1} and y''_N. We using 'natural cubic splines' specified by $y''_{-1} = y''_N = 0$.

y_{-1} is further specified by Equation (A.21) we get the following forward curves with smooth corresponding discount curves:

[4] Given by the mapping $T \mapsto \frac{1}{\tau}\left(\frac{P(0,T-\tau)}{P(0,T)} - 1\right)$ ising Equation (2.4.1) with $t = 0$ and $T > \tau$.

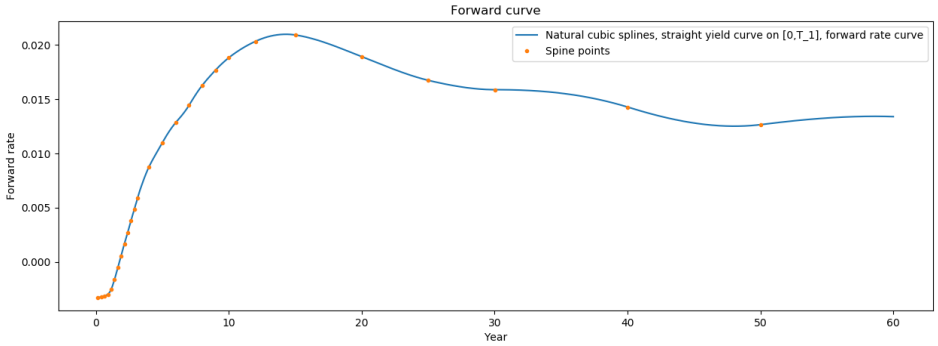

Figure 3.5: 25th of January 2018, 3MEUR forward curve.

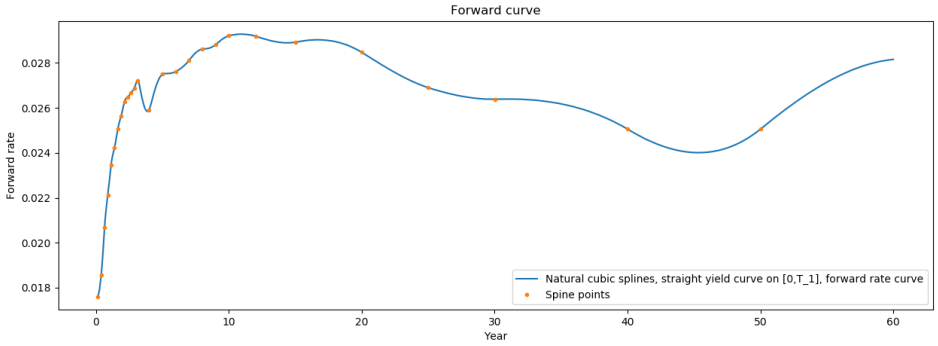

Figure 3.6: 25th of January 2018, 3MUSD forward curve.

Both curves converge after 10 iterations, which is when $|\mathbf{P^{(n)}} - \mathbf{P^{(n-1)}}| < 10^{-15}$. Cubic spline interpolation results in smooth discount and forward rate curves, but is computationally more expensive for calibration than using linear discount curve interpolation. What can be noted is that in Figures 3.4 the forward curves do not oscillate in the maturity strip calibrated from futures and deposits[5]. When forecasting high maturity forward rates it therefore becomes important to use a non-oscillating interpolation routine like cubic-splines, but on the flipside curve calibration is significantly slower[6]. We will analyze convexity adjustments and implied forward rates within the maturity strip calibrated from futures rates. Therefore for computational convenience we will use linear discount factor interpolation the rest of the thesis.

[5]For maturities up to 3 years.
[6]For both the EUR and USD curves calibration took 25 seconds and 10 iterations, implemented in Python.

Chapter 4

Convexity in the single-curve framework

Having done basic yield curve calibration in Chapter 3 we can now start with modelling the Libor futures rate convexity adjustment and extend the calibration algorithm 1. We will derive a model-dependent mapping from the Libor curve and caplet volatility surface to the vector of convexity adjustments corresponding to futures rates used in calibration. This will allow us to solve for the convexity adjustments and the curve simultaneously. We will look at the resulting convexity adjustments using data-sets B.1 and B.2 for the 3-month Euro Libor and USD Libor curves after which we will stress test our curve calibration routine and convexity adjustments under high rate and high volatility scenarios. We start calibrating convexity adjustments to their corresponding at the money caplet volatilities using one factor short-rate models, after which we will combine a mapping function[1] approach with the replication method in order to calibrate convexity adjustments to arbitrary caplet volatility surfaces. We will use the corresponding volatility surfaces 2.15 and 2.18. We will finish by looking at the significance of the implied vega-profiles of linear Libor derivatives in hedging.

4.1 Criteria for the convexity adjustment model

Having established a curve calibration algorithm where Eurodollar futures can be used given known convexity adjustments in Chapter 3, the algorithm can naturally be extended to include modelled convexity adjustments, that are dependent on the underlying curve and a volatility surface. Let L_T be a spot Libor rate with accruing period $[T, M]$. In the single-curve framework the Libor and the overnight curve are not distinguished and consequently the convexity adjustment can be written the following way after rewriting Equation (2.39):

$$C_0 = \frac{\mathrm{Cov}^M\left(D_T, (1+\tau L_T)L_T\right)}{P(0,M)}, \tag{4.1}$$

In the single-curve framework we can limit our attention to the joint distribution of L_T and D_T.

4.1.1 Literature about convexity in the single-curve framework

The simplest models for the convexity adjustment are Gaussian one factor short-rate models, see [2] like Ho-Lee and Hull-White, see [30] or [17]. They provide us with direct closed form expressions for the convexity adjustment, after calibrating the constant parameters to the corresponding at the money caplet volatility. These simple models fix underlying assumptions about the correlation between L_T and D_T in the M-forward measure. In [40] it has been shown empirically that

[1] This will be explained in detail in 4.4.

even though a condition that guarantees positive convexity adjustments in Gaussian one factor short-rate models hold in practice, negative convexity adjustments were still observed for 3 month futures rates during the period between the year 2000 and 2004, using data collected from the British Banker's Association.

More complex expressions have been derived in the Libor market model, decomposing discretely[2] marked to market futures rates into their underlying variances and correlations. Piterbarg and Renedo [39] derive a closed form Taylor-based expression of the Libor forward rates in terms of futures rates with the same accruing periods and the underlying covariance matrix between the Libor forward rates. After decomposing covariances into correlations and standard deviations of Libor forward rates the standard deviation parameters are estimated using a seperate stochastic volatility model per forward rate and the correlation parameters are calibrated from a Libor market model. The replication method is avoided for the comptutation of the standard deviations. Jaeckel [29] similarly derives an expansion based expression of futures rates in terms of forward rates, but is not calibrated using stochastic volatility models.

Because we use futures rate convexity adjustments for curve calibration we are not interested in complex Libor market model based models that require joint calibration of volatility and correlation parameters. We are interested in simple models that do not give unfeasible convexity adjustments under stressed market scenarios but are rich enough to be calibrated to the entire corresponding caplet volatility smile. We will consider convexity adjustments implied by one factor short-rate models and the replication method in Section 4.3 and 4.4.

4.2 Calibration algorithm

The vector $\mathbf{C}$ used to solve Equation (3.7) exists of a vector of fixed convexity adjustments. In Sections 4.3 and 4.4 we will derive functional expressions for convexity adjustments in terms of the underlying Libor curve and the caplet volatility surface, given by:

$$\mathbf{C}(\mathbf{P}, \sigma_{\mathbf{P}}^{(\theta)}), \tag{4.2}$$

when using solely the at the money caplet volatilities term-structure, where the curve determines the corresponding at the money strikes and

$$\mathbf{C}(\mathbf{P}, \sigma^{(\theta)}), \tag{4.3}$$

when using the caplet volatility surface surface. We use stripped caplet volatility surfaces, as has been explained in Section 2.7.

To simplify we introduce short hand notation

$$\mathbf{C}(\mathbf{P}), \tag{4.4}$$

for both expressions (4.2) and (4.3). Combining this with Equation (3.7) allows us to define a new system from which to solve for Libor discount factors:

$$\mathbf{NPV}(\mathbf{Q}, \mathbf{C}(\mathbf{P}), \mathbf{P}) = \mathbf{0}, \tag{4.5}$$

with $\mathbf{NPV}$ is given by Equation (3.7). $\mathbf{Q}$ is the vector of deposit, futures and swap rates used in calibration. $\mathbf{P}$ is the vector of Libor discount factor spine points. $\mathbf{C}(\mathbf{P})$ converts the curve and caplet volatility surface to the vector of convexity adjustments corresponding to the futures rates used in Equation (3.7). Note that our calibrated curve $\mathbf{P}$ from Equation (4.4) now depends on either the term-structure of at the money caplet volatilities or the entire volatility surface, which

[2] In 3 month increments when pricing 3 month futures, as has been mentioned in Section 2.6.

will be further specified in Section 4.6 where we look at the implied vegas of Linear Libor curve instruments.

Equation (4.5) can again be solved using the Newton-Rhapson algorithm, Implementing it directly is however quite tedious due to the underlying Jacobian of $\mathbf{NPV}(\mathbf{Q}, \mathbf{C}(\mathbf{P}), \mathbf{P})$ to discount factor spine points depending on partial derivatives of the valuation function **NPV** and **C**, changing **C** would require additional implementation of $\nabla\mathbf{C}$. Since we will only be modelling **C** a much simpler approach is using a Picard style iteration of the form:

$$\begin{aligned} \mathbf{NPV}(\mathbf{Q}, \mathbf{C^{(0)}}, \mathbf{P^{(1)}}) &= \mathbf{0} \\ \mathbf{NPV}(\mathbf{Q}, \mathbf{C}(\mathbf{P^{(1)}}), \mathbf{P^{(2)}}) &= \mathbf{0} \\ &\vdots \\ \mathbf{NPV}(\mathbf{Q}, \mathbf{C}(\mathbf{P^{(n-1)}}), \mathbf{P^{(n)}}) &= \mathbf{0} \end{aligned} \tag{4.6}$$

Starting with $\mathbf{C^0} = \mathbf{0}$. This leads to an alternative calibration algorithm where in every step the curve is calibrated using Algorithm 1 and the convexity adjustments are adjusted accordingly after which the curve is calibrated again until the difference between subsequent convexity adjustments are below some error bound ϵ_2:

Algorithm 2: Nested calibration algorithm for solving equation (4.5).

Data: $\mathbf{Q}$,$\mathbf{C}$,$\sigma_{\mathbf{P}}^{(\theta)}$
$\mathbf{C^{(0)}} = \mathbf{0}$;
$\mathbf{P^{(0)}} = \mathbf{1}$;
$\epsilon_2 = 10^{-12}$;
while $||\mathbf{C^{(n)}} - \mathbf{C^{(n-1)}}|| > \epsilon_2$ **do**
  $\mathbf{P^{(n)}} = \mathbf{P_{solve}}(\mathbf{P^{(n-1)}}, \mathbf{C^{(n-1)}})$;
  $\mathbf{C^{(n)}} = \mathbf{C}(\mathbf{P^{(n)}})$;
end

$\mathbf{P_{solve}}$ is given by Equation (3.8). We will use the short-hand notation for the spine point vector resulting from algorithm 2 by:

$$\mathbf{P_{solve,nested}}(\mathbf{P^{(0)}}, \sigma^{(\theta)}) \tag{4.7}$$

The model used to relate convexity adjustments to the caplet volatility surface $\sigma_{\mathbf{P}}^{(\theta)}$, are made clear from the context.

Finally due to using linear discount factor interpolation we can derive conditions on the function **C** that guarantees convergence and uniqueness of the curve resulting from algorithm 2. Unicity is non-trivial due to the dependence of the function **C** on the underlying curve introduce non-linearity into the system (4.5). In A.7 we provide the conditions using the Banach fixed point theorem.

4.3 The one factor short-rate model

Let $(\mathbb{Q}, D)$ be the risk neutral measure numeraire pair as specified by (2.1.2). Given a time t Libor curve, we define the *instantaneous forward rate* such that:

$$f(t,T) = -\frac{\partial}{\partial T}\ln(P(t,T)), \tag{4.8}$$

which can be rewritten to:

$$P(t,T) = \exp\Big(-\int_t^T f(t,u)du\Big). \tag{4.9}$$

As explained in section 4.4 of Piterbarg [2] the Gaussian model is given by the following assumption on the dynamics of the instantaneous forward rate:

$$df(t,T) = \alpha_t dt + \sigma_f(t,T) dW_t^{\mathbb{Q}}. \tag{4.10}$$

Note that the starting curve given by $T \mapsto f(0,T)$ is determined by the initial yield curve due to equation (4.8). Because $P(t,T)$ is a tradeable strictly positive asset (buying a collateralised contract that pays out 1 at time T), the following martingale property holds for $t < s < T$:

$$P(t,T) = \mathbb{E}^{\mathbb{Q}}\left[\frac{D_t}{D_s} P(s,T) | \mathscr{F}_t\right].$$

Using the martingale property Heath, Jarrow and Morton have linked the instantaneous forward rate and short rate by the definition $r_t = f(t,t)$, giving the following dynamics:

$$dr_t = \theta_t dt + \sigma_f(t,t) dW_t^{\mathbb{Q}}. \tag{4.11}$$

such that the discount factor $P(t,T)$ for $t < T$ is given by $\mathbb{E}^{\mathbb{Q}}[\exp(-\int_t^T r_u du)|\mathscr{F}_t]$. Where α_t is dependent on σ_f and $T \mapsto f(0,T)$ due to the martingale property:

$$\alpha_t = \sigma_f(t,T)\sigma_P(t,T). \tag{4.12}$$

Furthermore, $\sigma_f(t,T) = \dfrac{\partial}{\partial T}\sigma_P(t,T)$ and σ_P is some deterministic function of t and T. θ_t is a function dependent on the short rate r_t, the initial instantaneous forward curve $T \mapsto f(0,T)$ and σ_f, see [7] for more details.

Note that instantaneous forward rate dynamics imply discount curve dynamics, which can be derived by using (4.9):

$$\begin{aligned} dP(t,T) &= d\Big(\exp(-\int_t^T f(t,u)du)\Big) \\ &= P(t,T) d\Big(-\int_t^T f(t,u)du\Big) \\ &= P(t,T)[r_t dt - \int_t^T \sigma_f(t,u) du dW_u^{\mathbb{Q}}]. \end{aligned}$$

The third equation follows after applying the Leibniz rule and because the dimensions of change for $f(t,u)$ are t and $W_t^{\mathbb{Q}}$ for any $u \geq t$. After imposing $\sigma_P(t,t) = 0$ we get:

$$dP(t,T)/P(t,T) = r_t dt - \sigma_P(t,T) dW_t^{\mathbb{Q}}. \tag{4.13}$$

Therefore σ_P can be defined as the *discount curve volatility function*. The discount curve dynamics allow us to derive forward bond rate dynamics by using Ito's formula: $G_t = \dfrac{1}{P(t,T,M)} = \dfrac{P(t,T)}{P(t,M)}$,

$$\begin{aligned} dG_t &= d\frac{P(t,T)}{P(t,M)} \\ &= \Big[\frac{dP(t,T)}{P(t,M)} - \frac{dP(t,M)P(t,T)}{P(t,M)^2} + \frac{d\langle P(t,M)\rangle P(t,T)}{P(t,M)^3} - \frac{dP(t,T)dP(t,M)}{P(t,M)^2}\Big] \\ &= \frac{P(t,T)}{P(t,M)}\Big[\frac{dP(t,T)}{P(t,T)} - \frac{dP(t,M)}{P(t,M)} + \frac{d\langle P(t,M)\rangle}{P(t,M)^2} - \frac{dP(t,T)dP(t,M)}{P(t,T)P(t,M)}\Big] \\ &= G_t\Big[[\sigma_P(t,M) - \sigma_P(t,T)]dW_t^{\mathbb{Q}} + [\sigma_P^2(t,M) - \sigma_P(t,M)\sigma_P(t,T)]dt\Big]. \end{aligned}$$

The final equality follows from (4.13), which gives:

$$dG_t/G_t = (\sigma_P(t,M) - \sigma_P(t,T))\sigma_P(t,M)dt + (\sigma_P(t,M) - \sigma_P(t,T))dW_t^{\mathbb{Q}} \tag{4.14}$$

We can note now for the Libor forward rate:

$$L_t = \frac{1}{\tau}\Big(G_t - 1\Big). \tag{4.15}$$

Because the Libor forward rate is a martingale under the M-forward measure so is G_t which implies by Girsanov's theorem, with

$$dW_t^{\mathbb{Q}} + \sigma_P(t,M)dt = dW_t^M, \tag{4.16}$$

see Equation (4.34) in [2]:

$$dG_t/G_t = (\sigma_P(t,M) - \sigma_P(t,T))dW_t^M. \tag{4.17}$$

Which combined with (4.15) determines the dynamics of the *shifted Libor forward rate*[3]:

$$L_t + \frac{1}{\tau} = \frac{1}{\tau}G_t = \frac{1}{\tau}\frac{P(t,T)}{P(t,M)},$$

.

$$d\Big(L_t + \frac{1}{\tau}\Big)/\Big(L_t + \frac{1}{\tau}\Big) = (\sigma_P(t,M) - \sigma_P(t,T))dW_t^M. \tag{4.18}$$

This allows us to get the following expression using Ito:

$$\begin{aligned} L_T + 1/\tau = (L_0 + 1/\tau) \\ \exp\Big(\int_0^T [\sigma_P(u,M) - \sigma_P(u,T)]dW_u^M - \frac{1}{2}\int_0^T [\sigma_P(t,M) - \sigma_P(t,T)]^2 dt\Big) \end{aligned} \tag{4.19}$$

and

$$\sigma_T = \sqrt{\frac{1}{T}\int_0^T |\sigma_P(u,M) - \sigma_P(u,T)|^2 du}. \tag{4.20}$$

σ_T is the corresponding the implied volatility with shifting parameter $1/\tau$. This allows us to derive the present value of a $1/\tau$-shifted Libor caplet with start T, strike K and tenor τ using Black's formula, see A.1:

$$\begin{aligned} V_{caplet,1/\tau}(0) &= \tau P(0,M)\mathbb{E}^M[(L_T - K)^+] \\ &= \tau P(0,M)\mathbb{E}^M[([L_T + 1/\tau] - [K + 1/\tau])^+] \\ &= \tau P(0,M)Black(L_0 + 1/\tau, K + 1/\tau, \sigma_T, T) \end{aligned} \tag{4.21}$$

Equation (4.20) now allows us to calibrate model parameters, depending on the choice of σ_P, to a $1/\tau$-shifted caplet volatility. In general at the money caplet volatility is used. This choice is not motivated by liquidity, due to caplets not being directly traded, as has been shown in Section 2.7, but provided that we have a θ-shifted caplet volatility surface we need a way to transform θ-shifted caplet volatility surfaces to the specific $\frac{1}{\tau}$.

The implied volatility represents the option price implied forward looking volatility of returns of the underlying forward rate L_t for $t \in [0,T]$, with T the starting date underlying the spot Libor L_T. Because of the observation of negative forward rates in the market, θ is generally chosen high

[3]We look at the shifted Libor forward rate because unlike the Libor rate it cannot be negative because that would imply one of the implied discount factors is negative, which makes no sense.

enough to ensure that $L_0 + \theta$ and expected shifted forward rates are positive, but low enough to retain the transparent relationship to the implied volatility of forward rate returns as much as possible. For the 3-month USD Libor and Euro Libor curves we will use the volatility surfaces given in Figures 2.15 with shifting parameters of 1% and 3% respectively.

Let L_0 be the forward Libor rate with accruing period $[T, M]$ and tenor τ, let $P(0, M)$ be the time M Libor discount factor. As will shown in Equation (4.20) one factor short-rate model parameters are related to caplet volatilities with a particular shifting parameter $1/\tau$. Therefore given a caplet volatility surface with an arbitrary shifting parameter θ we want to obtain the $1/\tau$-shifted caplet volatility given that we know the θ-shifted caplet volatility. Let $\sigma_T^{(\theta)}(L_0)$ be the at the money caplet volatility with shifting paremeter θ corresponding to a caplet with underlying the spot Libor rate with start T and maturity M, let σ be the $1/\tau$-shifted at the money caplet volatility with expiry T. The following approximation holds for σ:

$$\sigma = \frac{L_0 + \theta}{L_0 + \frac{1}{\tau}} \sigma_T^{(\theta)}(L_0) \tag{4.22}$$

Proof. See A.5. □

The approximation is $O(\sigma^3)$ accurate and can be validated by adding an extra Taylor term in the proof of approximation (4.22) given by:

$$(\hat{\sigma} - \frac{1}{6}\hat{\sigma}^3) = \frac{L_0 + \theta}{L_0 + \frac{1}{\tau}} (\sigma_T^{(\theta)}(L_0) - \frac{1}{6}\sigma_T^{(\theta)}(L_0)^3). \tag{4.23}$$

Here $\hat{\sigma}$ is solved from (4.23) and σ is solved from (4.22). Using Equations (4.23) and (4.22) now results in:

$$\hat{\sigma} - \frac{1}{6}\hat{\sigma}^3 = \sigma - \frac{1}{6}\left(\frac{L_0 + 1/\tau}{L_0 + \theta}\right)^2 \sigma^3.$$

Defining $f(x) = x - \frac{1}{6}x^3 - \left[\sigma - \frac{1}{6}\left(\frac{L_0+1/\tau}{L_0+\theta}\right)^2 \sigma^3\right]$ From which follows:

$$f(\hat{\sigma}) - f(\sigma) = -\frac{1}{6}\left(1 - \left(\frac{L_0 + 1/\tau}{L_0 + \theta}\right)^2\right)\sigma^3$$

We can find an upper bound for $|\hat{\sigma} - \sigma|$ using the mean value theorem:

$$\hat{\sigma} - \sigma = \frac{f(\hat{\sigma}) - f(\sigma)}{f'(y)},$$

with y between σ and $\hat{\sigma}$.

From the magnitudes of θ, τ, L_0 and $\sigma_T^{(\theta)}(L_0)$ we can find an upper bound for $|\hat{\sigma} - \sigma|$. As a test case we will look at the 10% shifted 3MEUR caplet volatility surface in Figure 2.18 and the curve given in Figure 3.6 we can see: $L_0 + 3\% \leq 0.05$, $\theta = 0.1$, $\frac{1}{\tau} = 4$ and $\sigma_T^{(\theta)}(L_0) + 10\% \approx 0.45$. This gives following from Equation (4.23):

$$\sigma = \frac{0.15}{4.05} 0.45 \approx 0.016.$$

We increase the forward rates by 3% and the volatilities by 10% to compute $|\sigma - \hat{\sigma}|$ under a stressed market scenario, given that the difference is small clearly under the base scenario the difference is small. Which gives, ignoring the $O((f(\hat{\sigma}) - f(\sigma))^2)$ term:

$$f(\sigma) - f(\hat{\sigma}) = -\frac{1}{6}\left(1 - \left(\frac{4.05}{0.15}\right)^2\right)(0.016)^3 \approx 5 \cdot 10^{-4}.$$

This finally gives:

$$|\hat{\sigma} - \sigma| < \frac{5 \cdot 10^{-4}}{1 - \frac{1}{2}y^2} \approx 5 \cdot 10^{-4}.$$

Because $y \approx 0.016$. Finally, given that $\frac{partialBlack}{\partial \sigma}(\hat{\sigma} - \sigma)$
Using more Taylor terms in (4.23) gives analogous results. Therefore, Equation (4.22) allows one to accurately relate the θ-shifted at the money caplet volatility to the $1/\tau$-shifted at the money caplet volatility of the same strike. How a different strike θ-shifted caplet volatility could be used is unclear. The present value of a futures rate with start T and tenor τ can be derived to be:

$$Fut_0 = \mathbb{E}^{\mathbb{Q}}[L_T] = \frac{1}{\tau}(\mathbb{E}^{\mathbb{Q}}[G_T] - 1) = \frac{1}{\tau}\Big(\frac{P(0,T)}{P(0,M)}e^{\Omega(0,T)} - 1\Big) \tag{4.24}$$

using the risk neutral dynamics of G_t (4.14), with

$$\Omega(0,T) = \int_0^T (\sigma_P(u,M) - \sigma_P(u,T))\sigma_P(u,M)du. \tag{4.25}$$

Which gives the following formula for the convexity adjustment:

$$C_0 = Fut_0 - L_0 = \frac{1}{\tau}\frac{P(0,T)}{P(0,M)}(e^{\Omega(0,T)} - 1). \tag{4.26}$$

Using Taylor we can derive a lower bound for the convexity adjustment given by:

$$C_0 \geq \frac{1}{\tau}\frac{P(0,T)}{P(0,M)}\Omega(0,T).$$

Using a simple Ho-Lee short-rate model it can be shown that the underlying correlation between L_T and D_T is positive, see A.10.

Given a positive correlation of L_T and D_T positive convexity adjustments make sense intuitively due to a positive correlation implying that one tends to expect in case of a change of expectations of the underlying spot Libor rate the pre-settlement interest rates changes too, therefore the margin paid out by the futures contract can be invested for a higher rate, or funded for a lower rate. Negative convexity adjustments are a result of negative correlation between pre-settlement interest rates and the spot Libor rate.

Given tenorstructure $0 < T_0 < ... < T_n$ corresponding to futures rates $\{Fut_0^{(0)}, ..., Fut_0^{(n-1)}\}$, we define $C_0^{(i)}$ by Equation (4.36) using $T = T_i$ and $M = T_{i+1}$. Therefore, Equations (4.22), (4.20) and (4.26) are the defining links between the convexity adjustments and at the money caplet volatilities of arbitrary shift when assuming a one factor Gaussian short-rate model. Evaluation of $\mathbf{C}(\mathbf{P})$ in Equation 2 now happens in 2 steps:

1. $\mathbf{\Theta_{model}}(\mathbf{P}, \sigma_{\mathbf{P}}^{(\theta)})$ converts θ-shifted at the money caplet volatility vector and curve implied forward rates to $1/\tau$-shifted at the money caplet volatilities using Equation (4.22) and subsequently Equation (4.20) to calibrate a model parameter vector directly to the $1/\tau$-shifted at the money caplet volatilities.

2. Finally $\mathbf{C}(\mathbf{P})$ is given by $\mathbf{C_{SR}}(\mathbf{P}, \mathbf{\Theta_{model}}(\mathbf{P}, \sigma_{\mathbf{P}}^{(\theta)})) = (C_0^{(0)}, .., C_0^{(n-1)})$, which calibrates the curve and model parameter vector to the vector of convexity adjustments using Equations (4.25) and (4.26).

Using simple constant parameter short-rate models like Ho-Lee or Hull-White calibrates n seperate short-rate models to the corresponding n at the money caplet volatilities, resulting in dependence between the convexity adjustment to only its corresponding at the money. One may argue that

a better approach would be to use a time-dependent short-rate model where one calibrates the convexity adjustment to the term-structure of at the money caplet volatilities instead of solely individual, see for any example [33] or [7].

We will not do this because calibrating a time-dependent more advanced short-rate model to the term structure of volatilities is done for simulation or the pricing of exotic interest rate derivatives, this is not important for curve calibration.
Performing the calibration using algorithm 2 for the 3-month EUR an USD Libor curves, using datasets B.1 and B.2 with the corresponding caplet volatility surfaces given in Figure 2.15. In Figures 4.1 and 4.2 we show the corresponding forward rate curves with and without convexity adjustments, using the Ho-Lee model with constant parameters, see Equation (A.8), limitted between 0 and the highest futures rate maturity[4]:

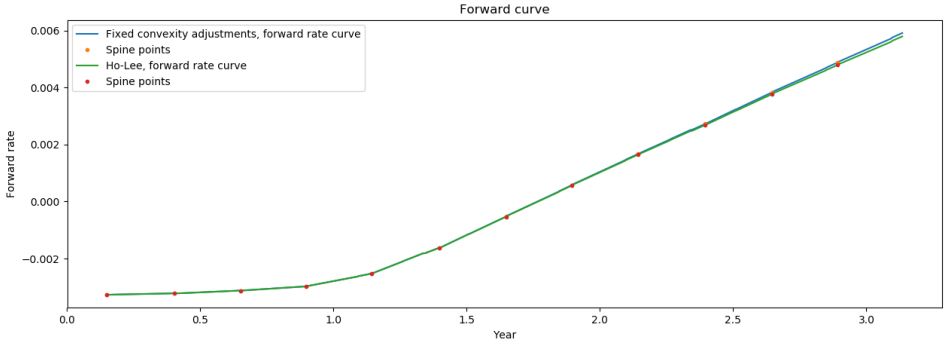

Figure 4.1: 25th of January 2018, 3MEUR forward rate curves. 4 iterations.

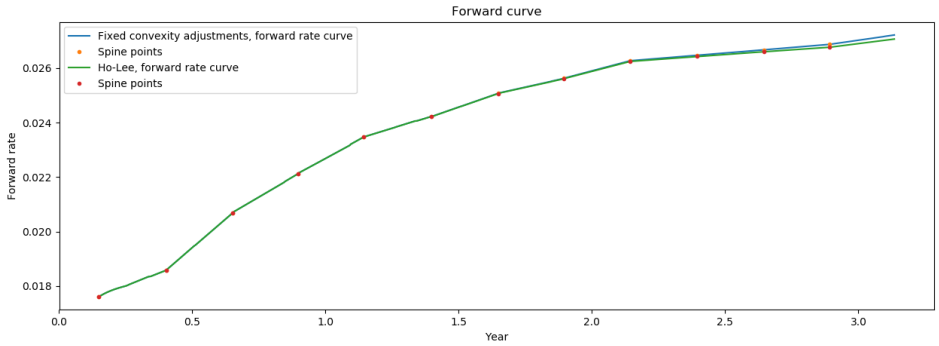

Figure 4.2: 25th of January 2018, 3MUSD forward rate curves. 5 iterations.

Differences beween the 2 curves are hardly visible, in Figure 4.4 we show the corresponding convexity adjustments:

[4]See 3.4 for the full forward rate curves without convexity adjustments.

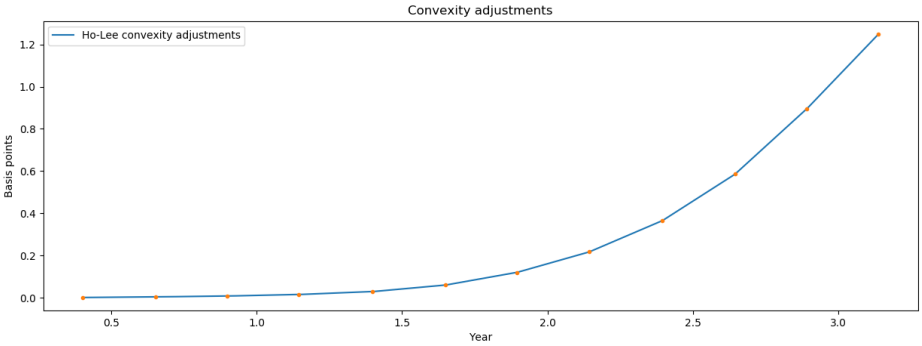

Figure 4.3: 25th of January 2018, 3MEUR convexity adjustments.

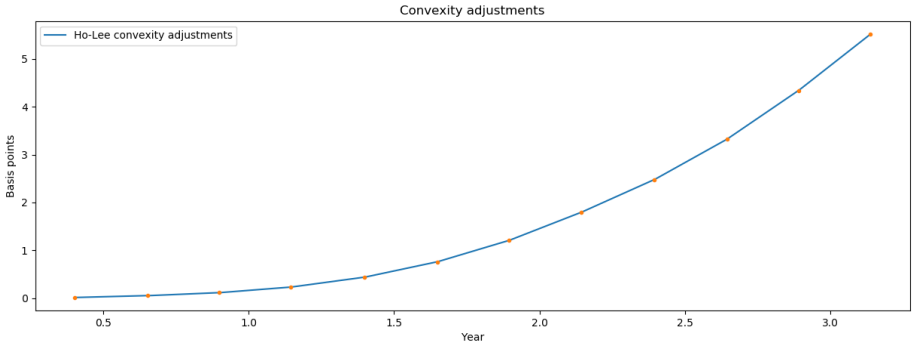

Figure 4.4: 25th of January 2018, 3MUSD convexity adjustments.

Note that USD futures rates range around 2.5% for maturities below 4 years while European futures rates range around 0%, see B.1 and B.2. This explaines the difference in magnitude of the convexity adjustments after comparing Equations (4.26) and (4.24).

We will not formally check curve uniqueness using the criterium A.25, but provide $\frac{\partial C_i}{\partial P(0,T_j)}$ for the convexity adjustments in Figure 4.4 for the starting flat curve $\mathbf{P} = 1$ and the calibrated curve using dataset B.1 with their corresponding caplet volatility surfaces given in Figure 2.15, which results in the following spine-point derivatives $\frac{\partial C_i}{\partial P(0,T_j)}$:

	1.144 years	2.144 years	3.138 years
0,402	0	0	0
0,652	0	0	0
0,898	-0,00485	0	0
1,144	0,004849	0	0
1,399	0	0	0
1,648	0	0	0
1,895	0	-0,00706	0
2,144	0	0,00706	0
2,396	0	0	0
2,645	0	0	0
2,891	0	0	0,000812
3,138	0	0	-0,00081

	1.144 years	2.144 years	3.138 years
0,402	0	0	0
0,652	0	0	0
0,898	-0,00246	0	0
1,144	0,002465	0	0
1,399	0	0	0
1,648	0	0	0
1,895	0	-0,0105	0
2,144	0	0,010496	0
2,396	0	0	0
2,645	0	0	0
2,891	0	0	-0,01407
3,138	0	0	0,014072

Table 4.1: 3MEUR $\frac{\partial C_i}{\partial P(0,T_j)}$ using the Ho-Lee model with respectively a calibrated and a flat 1 Libor curve. Columns are the 4th, 8th and 12th convexity adjustments with the last one being the largest used in calibration. Rows are curve spine-point maturities in years.

It can be clearly denoted that for the 2 choices of spinepoints the condition $\frac{\partial C_i}{\partial P(0,T_j)} < 4a^{n+2}q/n \approx 0.211$ is satisfied with $a = 0.975, q = 0.9$ and $n = 12$ for both a flat 1 and a calibrated spine-point vector $\mathbf{P}$. Due to crudeness of criterium (A.25) and the non-oscillating nature of the convexity adjustment expression (A.9), it makes sense to assume uniqueness of the curve resulting from (4.5) using (A.9).

There exists no objective reference to compare our resulting convexity adjustments to. We can nevertheless perform several tests to look at how different models and different market scenarios affect the convexity adjustments, we will start by comparing our convexity adjustment between using the Ho-Lee and the Hull-White model, the 2 models are equivalent except for the Hull-White model having an additional mean-reversion parameter λ, see A.15, we calibrate the volatility parameter and fix λ to 0,1 and 2. For $\lambda = 0$ the model is equivalent to the Ho-Lee model:

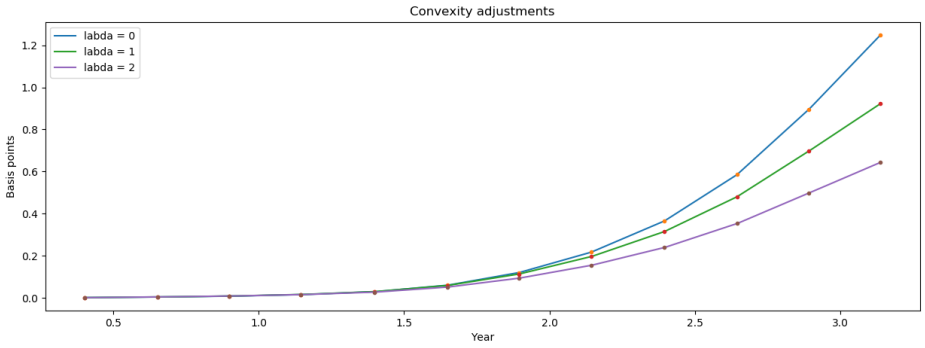

Figure 4.5: 25th January 2018, 3MEUR convexity adjustments using respectively the Ho-Lee model ($\lambda = 0$) and the Hull-White model with $\lambda = 1$ and $\lambda = 2$.

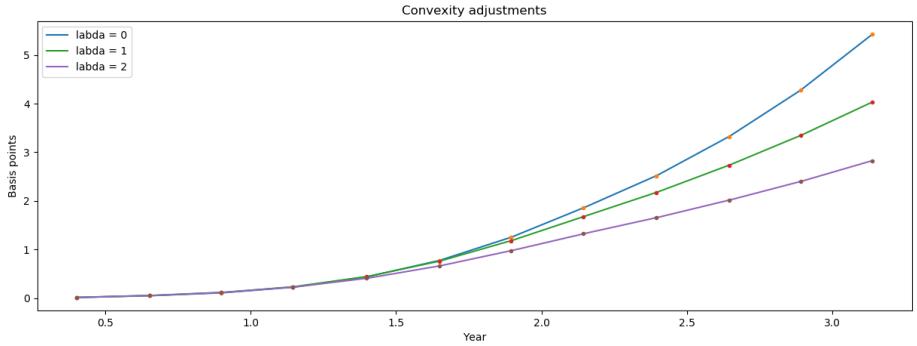

Figure 4.6: 25th January 2018, 3MUSD convexity adjustments using respectively the Ho-Lee model ($\lambda = 0$) and the Hull-White model with $\lambda = 1$ and $\lambda = 2$.

λ appears to have a decreasing effect on the convexity adjustments. Other short-rate models could be used, but it has been denoted in [29] that using for an example the Black-Karasinski or Black-Derman-Toy models continuously marked to market convexity adjustments can be shown to be positively infinite. We are interested in calibrating convexity adjustments to the volatility smile and will not spend more time on short-rate models.

4.4 Replication method

For this we will combine the Carr-Madan replication method with a mapping function approach, inspired by the TSR[5]-method used to model the annuity-forward measure Radon-Nykodym derivative, see Chapter 16 of [2] or [20]. Using any deterministic, twice differentiable function f allows us to express the expectation the following way:

$$\begin{aligned}\mathbb{E}^M[f(L_T)] &= \int_{-\infty}^{\infty} f(x)\psi^{L_0}(x)dx \\ &\approx \int_a^b f(x)\psi^{L_0}(x)dx \end{aligned} \tag{4.27}$$

The density $\psi^{L_0}(x)$ can be obtained from second partial derivatives of underlying European call or put payoffs to the strike, see A.8 for proof. In literature out of the money calls and puts are used, giving density function:

$$\psi^{L_0}(x) = \begin{cases} \frac{\partial^2}{\partial K^2}P(L_0,K)|_{K=x} & x > L_0 \\ \frac{\partial^2}{\partial K^2}C(L_0,K)|_{K=x} & x \leq L_0 \end{cases} \tag{4.28}$$

See A.9 for a justification. We use short hand notation

$$\begin{aligned} C(L_0,x) &= Black(L_0+\theta, x+\theta, \sigma_T^{(\theta)}(x), T) \\ P(L_0,x) &= Black_p(L_0+\theta, x+\theta, \sigma_T^{(\theta)}(x), T) \end{aligned}$$

With $Black$ and $Black_p$ Black's formulas corresponding to call and put payoffs, see A.1, with forward rate L_0, time to maturity T, strike K, caplet volatility $\sigma_T^{(\theta)}(K)$ and shifting parameter θ.

After partially integrating the right-hand-side of Equation (4.27) twice we obtain:

$$\begin{aligned}\mathbb{E}^M\left[f(L_T)\right] = f\left(L_0\right) &+ f(b)\frac{\partial}{\partial K}C(L_0,b) - f(a)\frac{\partial}{\partial K}P(L_0,a) \\ &+ f'(a)P(L_0,a) - f'(b)C(L_0,b) \\ &+ \int_a^{L_0} f''(x)P(L_0,x)dx + \int_{L_0}^b f''(x)C(L_0,x)dx. \end{aligned} \tag{4.29}$$

We do not consider the possibilities of $L_0 > b$ or $L_0 < a$, which is not necessary when choosing the boundaries wide enough.
We will use (4.29) after finding a mapping function f such that:

$$Fut_0 = \mathbb{E}^M[f(L_T)].$$

[5]Terminal swap rate

4.4.1 Mapping functions

Using the single-curve covariance identity (4.1) makes the following expression of the futures rate useful:

$$\begin{aligned} Fut_0 &= P(0,M)\mathbb{E}^M\left[\frac{D_T}{D_0}(L_T+\tau L_T^2)\right] \\ &= P(0,M)\mathbb{E}^M\left[\frac{D_T}{D_0}\right]\mathbb{E}^M\left[L_T+\tau L_T^2\right]+v_1 \\ &= P(0,T)\mathbb{E}^T\left[\frac{D_T}{D_0}P(T,M)\right]\mathbb{E}^M\left[L_T+\tau L_T^2\right]+v_1 \\ &= P(0,T)\mathbb{E}^T\left[\frac{D_T}{D_0}\right]\mathbb{E}^T\left[P(T,M)\right]\mathbb{E}^M\left[L_T+\tau L_T^2\right]+v_1+v_2 \\ &= \frac{P(0,M)}{P(0,T)}\mathbb{E}^M\left[L_T+\tau L_T^2\right]+v_1+v_2 \end{aligned} \tag{4.30}$$

v_1 depends on the T-forward correlation between D_T and $P(T,M)=\frac{1}{1+\tau L_T}$ and v_2 depends on the correlation between D_T and $L_T+\tau L_T^2$. The following mapping function results from assuming independence between L_T and D_T.

Definition 4.4.1 (Independence mapping function)**.** Assuming $v_1=v_2=0$ simplifies Equation (4.30), for time 0 to:

$$Fut_0 \approx \frac{1}{1+\tau L_0}\mathbb{E}^M\left[L_T+\tau L_T^2\right]=\mathbb{E}^M\left[f(L_T)L_T\right].$$

With $f(x)=\dfrac{1+\tau x}{1+\tau L_0}$, after noting $\dfrac{P(0,M)}{P(0,T)}=\dfrac{1}{1+\tau L_0}$, using Equation (2.4.1).

In more generality finding some function f such that:

$$\begin{aligned} Fut_0 &= \mathbb{E}^{\mathbb{Q}}[L_T] \\ &= \mathbb{E}^M\left[\frac{\partial\mathbb{Q}}{\partial\mathbb{Q}^M}L_T\right] \\ &\approx \mathbb{E}^M\left[f(L_T)L_T\right]. \end{aligned} \tag{4.31}$$

allows one to use the underlying caplet volatility smile to evaluate the futures rate. In the context of CMS-derivatives the mapping function approach is used to find an expression for the Radon-Nykodym derivative from the annuity[6] to the corresponding forward measure in terms of the underlying swap rate, which is a martingale under the annuity measure, see Chapter 16 of [2] for more details. Approximation (4.4.1) can be seen as the consequence of assuming independence between L_T and D_T and obviously does not capture the underlying correlation structure between L_T and D_T which is one of the determining factors of the futures convexity adjustment. An alternative model would be to use some parametric form for f and impose several conditions to derive the underlying parameters. One example is a polynomial model:

$$f(L_T)\approx(\beta_0+\beta_1 L_T+...+\beta_n L_T^n)(1+\tau L_T). \tag{4.32}$$

$f(L_T)$ represents the Radon-Nykodym derivative of the risk-neutral to M-forward measure change, given some constants $\{\beta_{T_i}\}$. The constants can be derived by imposing several feasibility conditions:

[6]The annuity measure is specified by numeraire $A(t)=\sum_{i=0}^{m-1}\tau_j' P(t,T_{j+1}')$, given some payment timestructure $0<T_0'<...<T_m'$ as given in Equation (2.24) with $t<T_0'$.

1. No arbitrage:
$$1 = \mathbb{E}^{\mathbb{Q}}[1],$$
which implies after measure change:
$$1 = \mathbb{E}^{M}[f(L_T)].$$

2. Reprice futures:
$$Fut_0 = \mathbb{E}^{\mathbb{Q}}[L_T], \tag{4.33}$$
which implies after measure change:
$$Fut_0 = \mathbb{E}^{M}[f(L_T)L_T].$$

3. Reprice futures options:
$$FutOption_{0,K} = \mathbb{E}^{\mathbb{Q}}[(L_T - K)^+],$$
which implies after measure change:
$$FutOption_{0,K} = \mathbb{E}^{M}[f(L_T)(L_T - K)^+].$$

4. Consistency:
$$\frac{1}{\tau}\big(P(t,T)\mathbb{E}^{M}[f(L_T)|\mathscr{F}_t] - 1\big) = L_t.$$
Which follows by combining the no arbitrage condition with equation (2.4.1).

Provided that we can calibrate to futures and their corresponding volatility smile at n points we have $n+1$ degrees of freedom. In turn allowing us to calibrate $\beta_0, .., \beta_n, L_0$ to $\{Fut_0, FutOption_0(K_1), ..., FutOption_0(K_n)\}$ using n strikes. Provided we use n futures rates $\{Fut_0^{(i)}\}$ in calibration over tenor structure $0 \leq T_0 < T_1 < ... < T_n$ one step further could be to use swaption volatilities, containing information about underlying correlations between the forward rates, see [39]. This may be something to look into in further research. Using high order polynomials means that we will use the replication method to price high order monomials:
$$\mathbb{E}^{M}[L_T^n].$$
It is clear that the higher n the more the underlying spot rate distribution depends on the underlying tails, therefore smile shapes for high/low strikes. In [21] a closed form solution is derived for quadratic CMS-caplets in the SABR model. This could analogously be used to price $\mathbb{E}^{M}[L_T^2]$ after the SABR model to the underlying caplet volatility smile and possibly be extended to price back higher order monomial expectations $\mathbb{E}^{M}[L_T^n]$. This is also something to look into in further research. There are several more feasibility conditions:

1. Realism:
f should be strictly positive on at least $[a, b]$.

2. Negative convexity adjustments:
$$\begin{aligned} C_0 &= \mathbb{E}^{\mathbb{Q}}[L_T] - \mathbb{E}^{M}[L_T] \\ &= \mathbb{E}^{M}[(f(L_T) - 1)L_T]. \end{aligned} \tag{4.34}$$
Should allow for negative values.

We will look at the simple independence mapping function given in (4.4.1).

4.4.2 Independence mapping function

Using mapping function (4.4.1), Equation (4.29) can be rewritten:

$$\begin{aligned} Fut_0 = L_0 &+ \frac{b+\tau b^2}{1+\tau L_0}\frac{\partial}{\partial K}C(L_0,b) - \frac{a+\tau a^2}{1+\tau L_0}\frac{\partial}{\partial K}P(L_0,a) \\ &+ \frac{1+2\tau a}{1+\tau L_0}P(L_0,a) - \frac{1+2\tau b}{1+\tau L_0}C(L_0,b) \\ &+ \frac{1}{1+\tau L_0}\int_a^{L_0} 2\tau x P(L_0,x)dx + \frac{1}{1+\tau L_0}\int_{L_0}^{b} 2\tau x C(L_0,x)dx \end{aligned} \tag{4.35}$$

This finally gives for the convexity adjustment:

$$\begin{aligned} C_0 = &\frac{b+\tau b^2}{1+\tau L_0}\frac{\partial}{\partial K}C(L_0,b) - \frac{a+\tau a^2}{1+\tau L_0}\frac{\partial}{\partial K}P(L_0,a) \\ &+ \frac{1+2\tau a}{1+\tau L_0}P(L_0,a) - \frac{1+2\tau b}{1+\tau L_0}C(L_0,b) \\ &+ \frac{1}{1+\tau L_0}\int_a^{L_0} 2\tau x P(L_0,x)dx + \frac{1}{1+\tau L_0}\int_{L_0}^{b} 2\tau x C(L_0,x)dx \end{aligned} \tag{4.36}$$

This again provides us, analogously to Equation (4.26), an expression for the convexity adjustment in terms of the corresponding θ-shifted caplet volatility smile $K \mapsto \sigma_T^{(\theta)}(K)$ and Libor curve.

4.4.3 Smile parametrisation

In Figure 4.7 we consider the caplet volatility smiles and implied forward rate densities, using the 3MEUR Libor caplet volatility surface, see 2.18, with shifting parameter $\theta = 0.1$. We use a Libor curve calibrated using with dataset B.1 and 0 convexity adjustments:

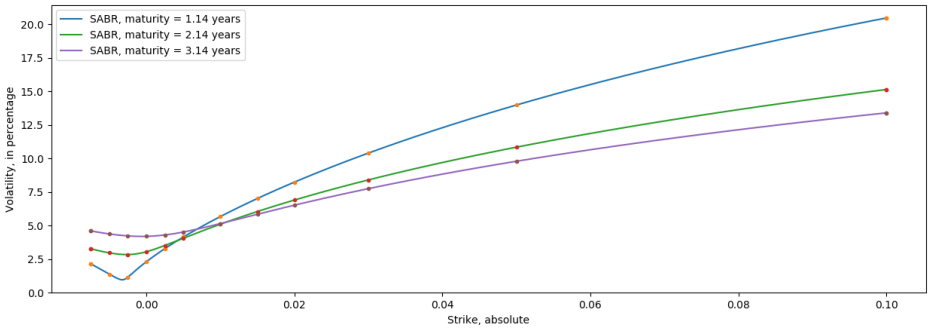

(a) Caplet volatility smiles.

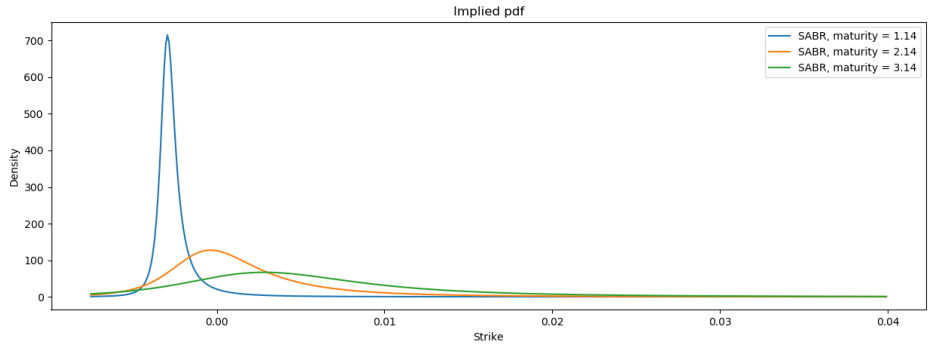

(b) Libor forward rate densities.

Figure 4.7: Libor forward rate densities over $[a', b']$.

In order for Equation (4.27) to be accurate a needs to be chosen smaller than $a' = -0.0075$, which is the lowest strike for the stripped 3MEUR caplet volatility surface given by Figure 2.15. b also needs to be chosen larger than b', which is not visible from Figure 4.7. Given that the caplet volatility smile $K \mapsto \sigma_T^{(\theta)}(K)$ is only known for $K \in [a', b']$, a' being the lowest absolute strike, -0.75% in case of the European surface, see Figure 2.15, we will need an extrapolation routine of the smile for $b \geq b'$ or $a \leq a'$. In Figures 2.15 and 2.16, we have respectively considered a penalized linear smile interpolation and fitting Hagan's formula on the underlying smile.

We will consider 3 smile extrapolation routines: Linear interpolation and constant extrapolation, where constant extrapolation means that for $K > b'$: $\sigma_T^{(\theta)}(K) = \sigma_T^{(\theta)}(b')$ and for $K < a'$: $\sigma_T^{(\theta)}(K) = \sigma_T^{(\theta)}(a')$. We will also consider cubic spline interpolation and sloped extrapolation, see A.6 for more details. And finally Hagan's formula, see Figure 2.16.

Details about cubic-spline interpolation in context of the volatility smile are provided in A.6. Below we show the underlyiing probability density functions and smiles when using linear interpolation, cubic-spline interpolation and Hagan parametrisation, The underlying is the Libor forward rate with maturity 3.14 years corresponding to the highest maturity futures rate used in calibration:

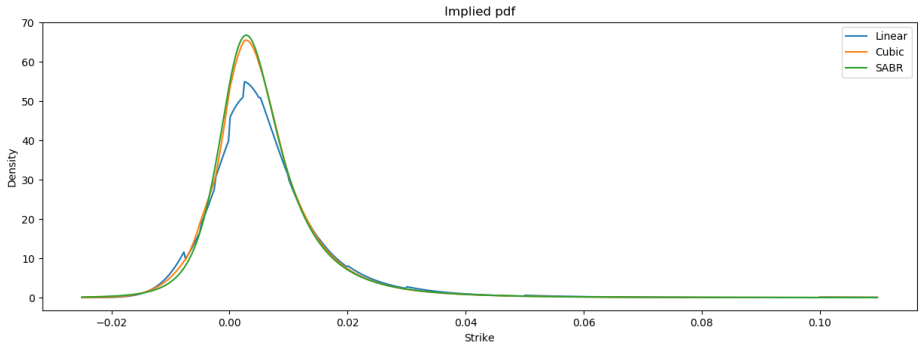

(a) Implied volatility densities.

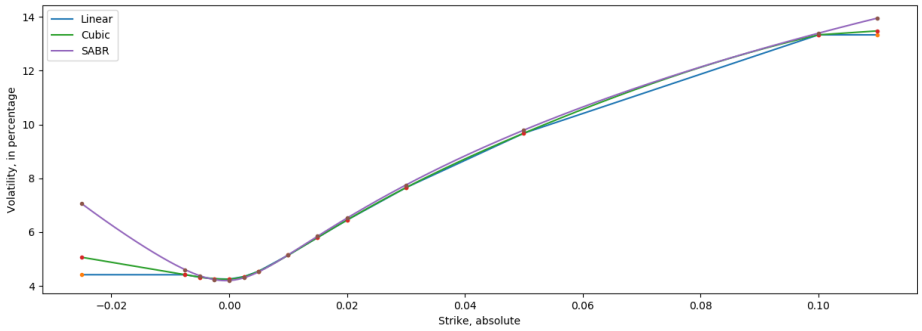

(b) Implied volatility smiles.

Figure 4.8: Probability density functions and smiles.

Figure 4.8 shows the probability densities under base market scenarios, see Figure 4.10. Plots are made after calibrating a Libor curve with 0 convexity adjustments and using a central difference estimator for the underlying probability densities. The biggest thing to notice here is that using both the linear and cubic-spline interpolation routines cause oscillations in the underlying density function. Even though the underlying smile is second order smooth when using cubic-spline interpolation. in Figure 4.9 we display the smiles and densities under stressed market scenarios, with elevated volatilities by 10%:

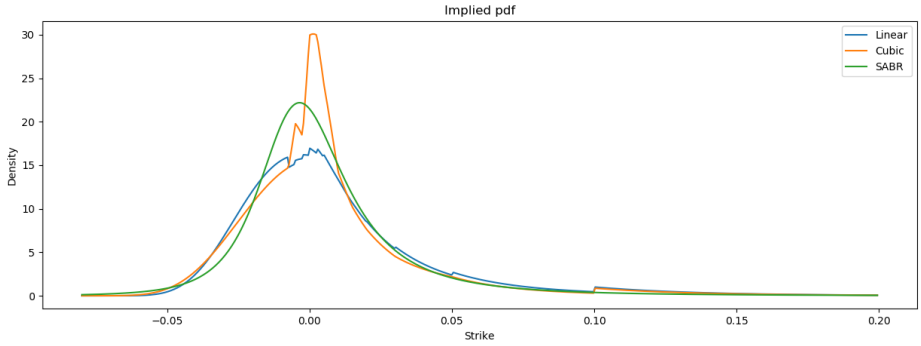

(a) Implied volatility densities.

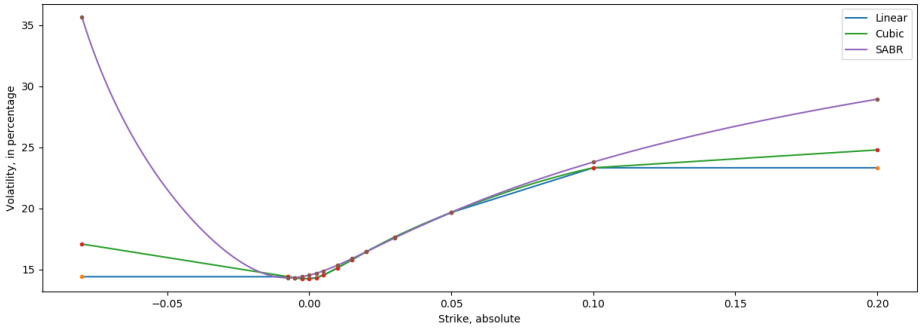

(b) Implied volatility smiles.

Figure 4.9: Probability density functions and smiles. Stressed market scenario, see 4.10.

The discontinuities and oscillations are worse. This shows that there is more to correct smile parametrisation than solely continuity or smoothness and choosing either linear or cubic-spline interpolation exposes one to arbitrage. Analogously the way linear discount curve interpolation leads to oscillations in the forward rate curve between swap maturities.

In order to have a more formal notion about what choice of $[a, b]$ is wide enough we will compute the probabilities $\mathbb{Q}^M(L_T \geq b)$ and $\mathbb{Q}^M(L_T \leq a)$ under stressed market scenarios. This will ensure that our boundaries are chosen wide enough under any feasible scenario for rates and volatilities. In Figure 4.10 we display our futures rates and volatility smiles under normal and stressed scenarios:

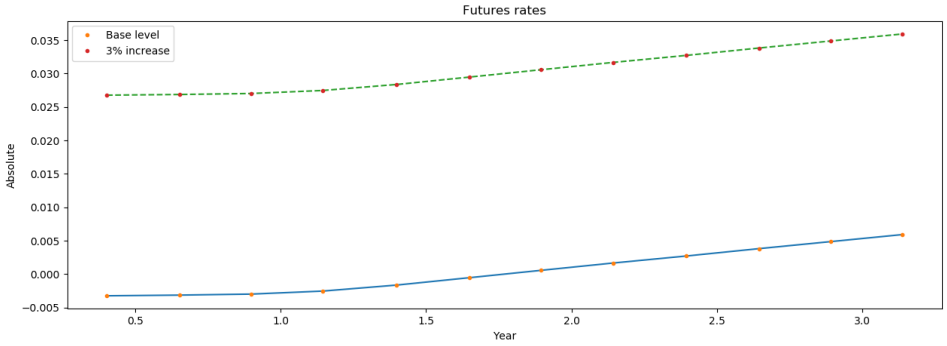

(a) Implied Libor futures rates.

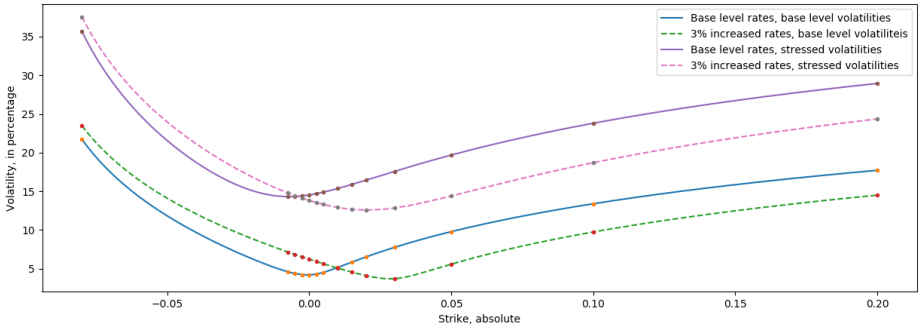

(b) Implied volatility smiles.

Figure 4.10: Stressed futures rates and volatility smiles.

We will select b using stressed volatilities and 3% increased rates, while using only stressed volatilities for the selection of a. Below are the results for a range of b and a values:

	$b = b'$	$b = b' + 0,15$	$b = b' + 0.4$	$b = b' + 0.65$	$b = b' + 0.9$	$b = b' + 1.4$
Base, $\mathbb{Q}^M(L_T > b)$	0.000062	$3 \cdot 10^{-6}$	0	0	0	0
Stressed, $\mathbb{Q}^M(L_T > b)$	0.32991	0.05667	0.00702	0.00129	0.00051	0.00005

Table 4.2: Cummulative distributions for varrying b.

	$a = a'$	$a = -0.03$	$a' = -0.06$	$a' = -0.09$	$a' = -0.099$	$a' = -0.09995$
Base, $\mathbb{Q}^M(L_T < a)$	0.02996	0.00044	$1.4 \cdot 10^{-5}$	$1 \cdot 10^{-6}$	0	0
Stressed, $\mathbb{Q}^M(L_T < a)$	0.32991	0.05667	0.007015	0.001287	0.000512	0.00005

Table 4.3: Cummulative distributions for varrying a.

We choose $a = -\theta + 0.00005 = -0.09995$ and $b = b' + 1.4 = .5$ such that $\mathbb{Q}^M(L_T > b)$ and $\mathbb{Q}^M(L_T < a)$ are under a basis-point under stressed market conditions, below we show convexity adjustment levels under the various values of a and b:

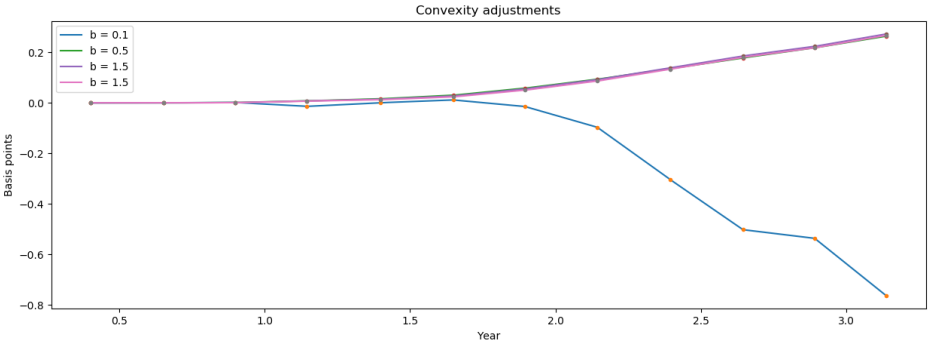

(a) Convexity adjustments for various values of b, $a = -\theta + 0.00005$.

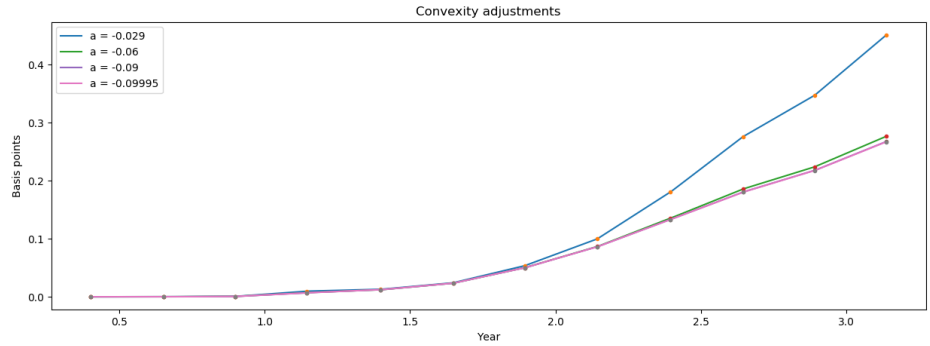

(b) Convexity adjustments for various values of a, $b = b' + 1.4$.

Figure 4.11: Effect on the convexity adjustments for using various boundaries, using the independence mapping function given by (4.36) and algorithm 2.

This shows the importance of choosing sufficiently wide boundaries a and b, also note that negative convexity adjustments are not possible due to (4.4.1) rewriting to:

$$\frac{\mathbb{E}^M[L_T^2\tau + L_T]}{1+\tau L_0} - L_0 = \frac{\mathbb{E}^M[L_T^2\tau + L_T] - (L_0^2\tau + L_0)}{1+\tau L_0} \geq 0,$$

due to Jensen's inequality. Showing the importance of smile parametrisation.

4.5 Convexity adjustments stress tests

In this section we will compare the convexity adjustments resulting from algorithm 2 using the Ho-Lee model (A.8) and the replication method using the independence mapping (4.36), boundaries $[a, b] = [-0.09995, 1.5]$, linear discount curve interpolation and the corresponding Hagan's formula parametrised caplet volatility surfaces given in 2.18 and the dataset B.1: below we show the base level convexity adjustments:

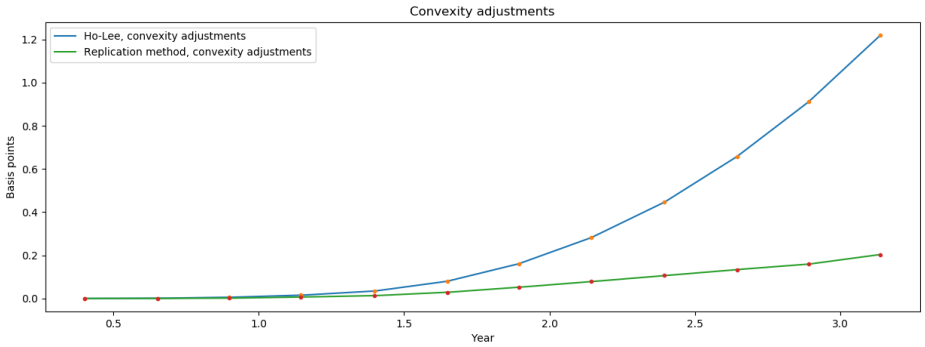

Figure 4.12: Convexity adjustments using Ho-Lee model and the replication method.

The replication method convexity adjustments are lower than those implied by the Ho-Lee model, which makes sense due to one assuming independence between pre-settlement Libor rates and the spot Libor rate and the other positive dependence, see A.10. In Figures 4.13 and 4.14 we display the corresponding discount and forward rate curves between 0 and the highest futures rate maturity:

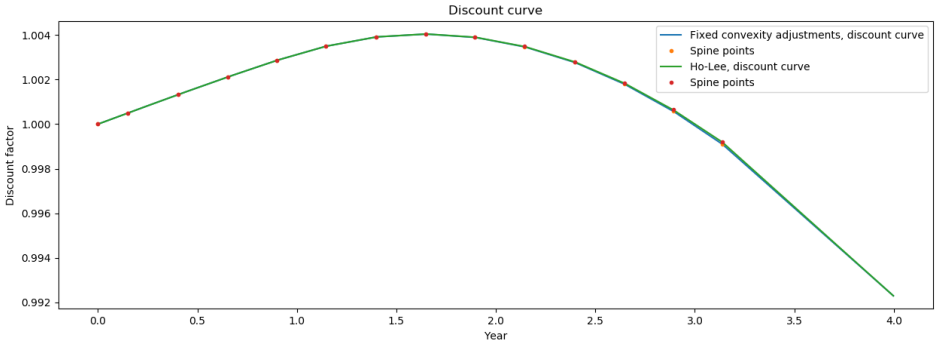

Figure 4.13: Discount curves using the Ho-Lee model and replication method.

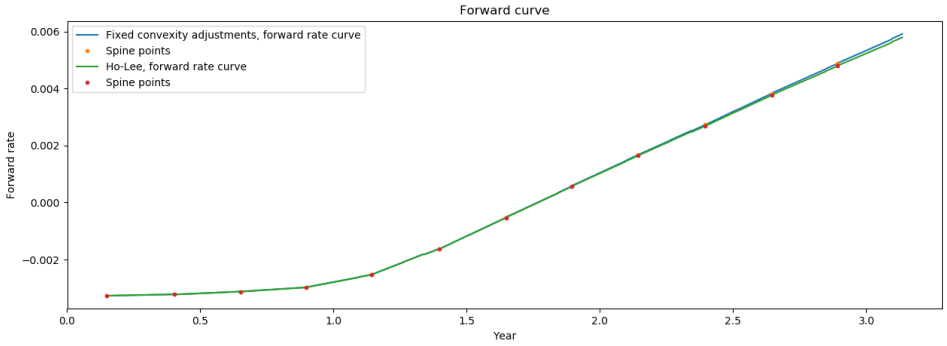

Figure 4.14: Forward rate curves using the Ho-Lee model and replication method.

Differences between forward or discount curves are hardly visible.
Checking curve uniqueness using (4.36) for is done analogously as was done in Table 4.1:

	1.144 years	2.144 years	3.138 years
0,402	0	0	0
0,652	0	0	0
0,898	0,001392	0	0
1,144	-0,00139	0	0
1,399	0	0	0
1,648	0	0	0
1,895	0	0,003397	0
2,144	0	-0,0034	0
2,396	0	0	0
2,645	0	0	0
2,891	0	0	0,004607
3,138	0	0	-0,00461

	1.144 years	2.144 years	3.138 years
0,402	0	0	0
0,652	0	0	0
0,898	0,000646	0	0
1,144	-0,00065	0	0
1,399	0	0	0
1,648	0	0	0
1,895	0	0,004075	0
2,144	0	-0,00408	0
2,396	0	0	0
2,645	0	0	0
2,891	0	0	0,007042
3,138	0	0	-0,00705

Table 4.4: 3MEUR $\frac{\partial C_i}{\partial P(0,T_j)}$ using the replication method with respectively a calibrated and a flat 1 Libor curve. Columns are the 4th, 8th and 12th convexity adjustments with the last one being the largest used in calibration. Rows are curve spine-point maturities in years.

Again the condition A.25 is satisfied pointwise when using the flat and calibrated curve.

4.5.1 Rate level

The following convexity adjustments are calibrated after increasing all the underlying rates in dataset B.1 by 3%. The difference between high and low futures rates is visible in Figure 4.10. This increases the corresponding convexity adjustments, which is similar to what we saw with the convexity adjustments in (4.4) using the USD dataset:

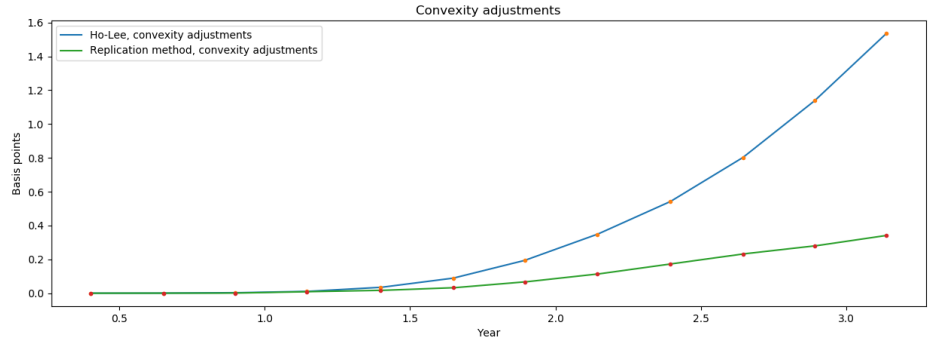

Figure 4.15: Convexity adjustments using Ho-Lee model and replication method. Futures rates increased by 3%.

In Figures 4.16 and 4.17 we display the corresponding discount and forward rate curves between 0 and the highest futures rate maturity:

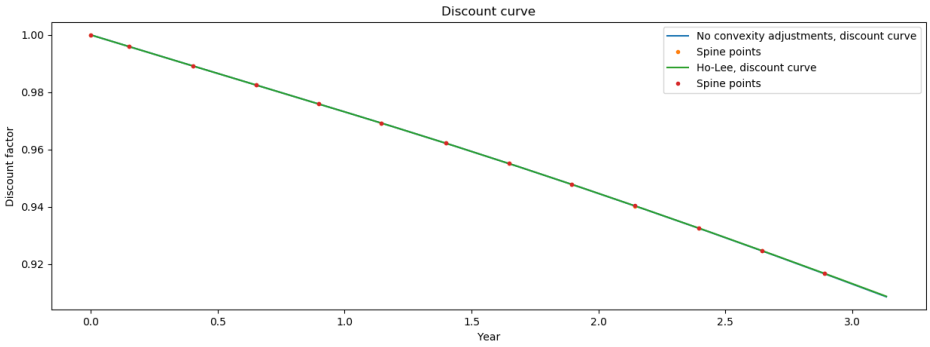

Figure 4.16: Discount curves using Ho-Lee model and replication method. Futures rates increased by 3%.

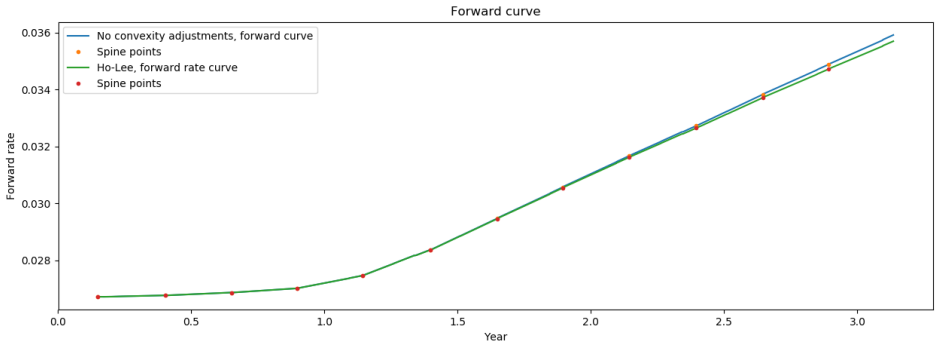

Figure 4.17: Forward rate curves using Ho-Lee model and replication method. Futures rates increased by 3%.

The difference between the forward or discount curves are more visible compared to Figures 4.14 and 4.13.

4.5.2 Smile level

Here we show the effects of increasing the caplet volatility surface by 10%, see Figure 4.10. The smile is a consequence of recalibrating Hagan's formula to smiles higher by 10%.

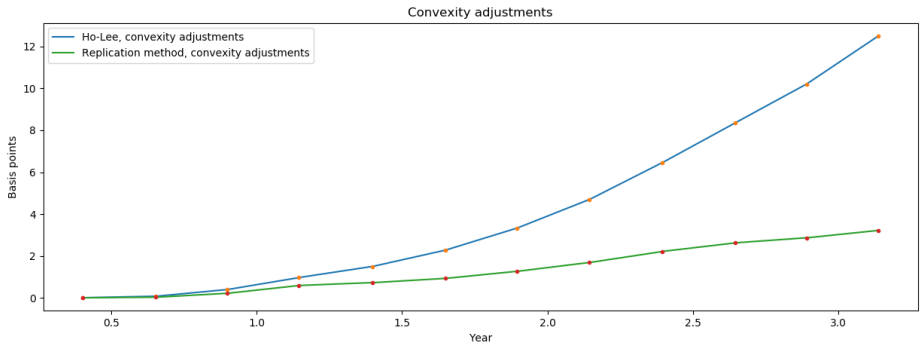

Figure 4.18: Convexity adjustments using Ho-Lee model and replication method. Volatility level increase.

In Figures 4.19 and 4.20 we display the corresponding discount and forward rate curves between 0 and the highest futures rate maturity:

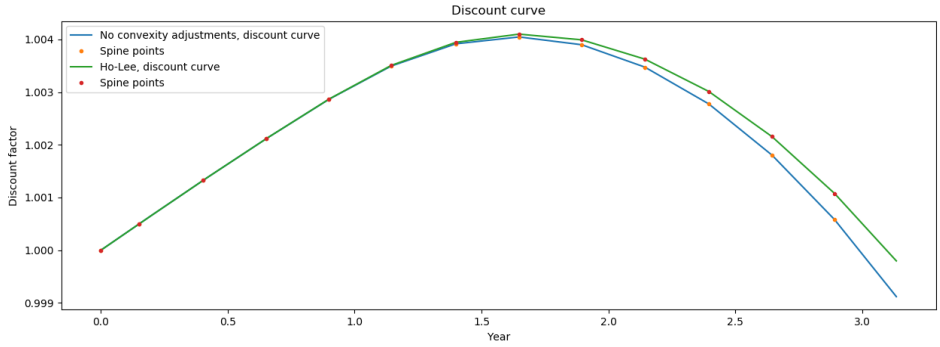

Figure 4.19: Discount curves using Ho-Lee model and replication method. Caplet volatilities increased by 10%.

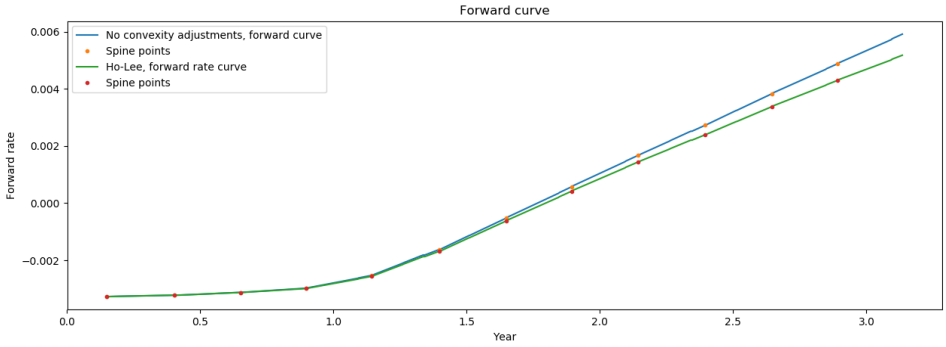

Figure 4.20: Forward rate curves using Ho-Lee model and replication method. Caplet volatilities increased by 10%.

Importance of the convexity adjustment becomes apperent in Figures 4.20 and 4.19.

4.5.3 Smile and rate level

Here we show the compounded effects of increasing futures rate by 3% and the caplet volatility surface by 10%, see 4.10:

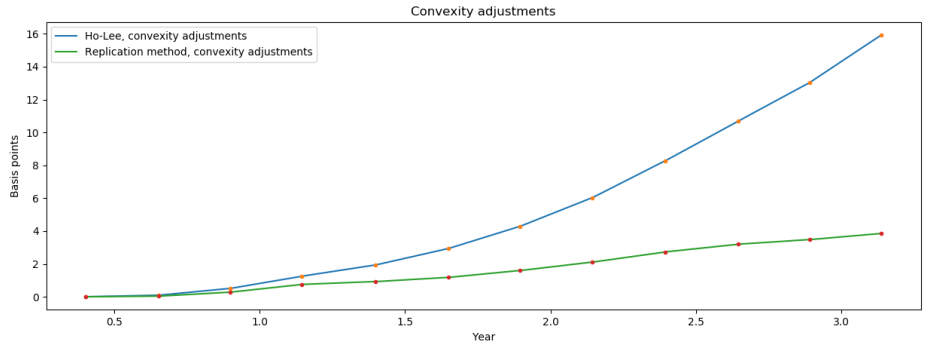

Figure 4.21: Convexity adjustments using Ho-Lee model and replication method. Rate and volatility level increase.

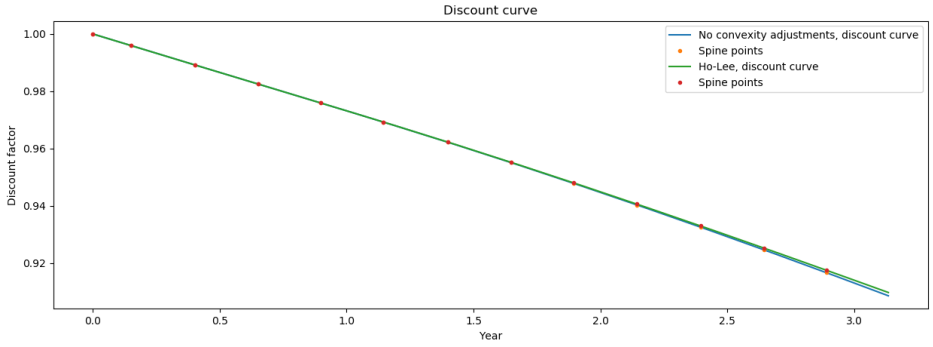

Figure 4.22: Discount curves using Ho-Lee model and replication method. Futures rates increased by 3% and caplet volatilities increased by 10%.

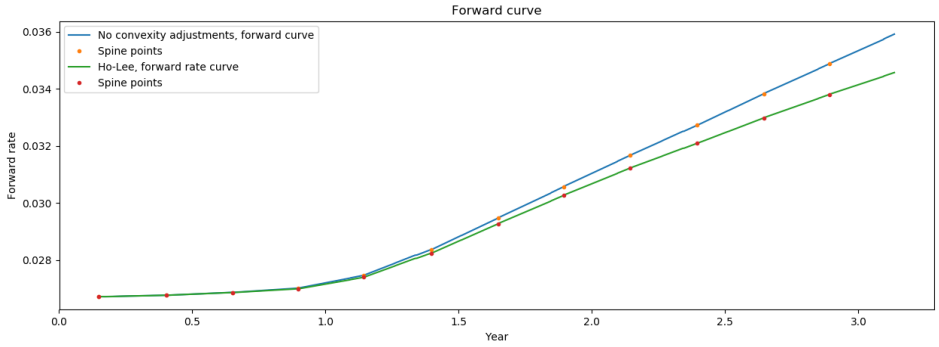

Figure 4.23: Forward rate curves using Ho-Lee model and replication method. Futures rates increased by 3% and caplet volatilities increased by 10%.

We can conclude that taking into account the convexity adjustments becomes more important under stressed market scenarios.

4.6 Vega profiles

Solving a Libor curve using volatility-dependent convexity adjustments in algorithm 2 introduces volatility dependence into the Libor curve. Consequently, the prices of all Libor curve derivatives become volatility-dependent. We are curious how large these vegas can become in stressed market scenarios. We will use the caplet volatility surface 2.16 for the replication method model and volatility surface 2.15 for the Ho-Lee model with dataset B.1 and look at the vega profiles of deposits, FRAs and swaps, with the following specifications:

Notional set at 10.000. We will consider the Lender-Deposit with value given by (2.13), maturity set at 3 months. We will consider Lender-FRAs and Payer-swaps given by (2.19) and (2.24), maturities set at 2 years. For the short-rate model algorithm we will use the Ho-Lee model with the corresponding convexity adjustment expression given by Equation (A.8). For the replication method we will use the independence model with convexity adjustment given by (4.36), constant surface extrapolation, $[a, b] = [-0.029, 2]$.

Since we are using a caplet volatility surface parametrised using Hagan's formula, see Figure 2.18, the sensitivities to individual strike and maturity volatilities can be computed analytically by using an inverse derivative and chain rule combination after denoting that every instrument's value is a function of the yield curve and the yield curve is a function of the underlying SABR parameters, the procedure goes the following way, let I be an instrument[7] present value dependent on spine point vector $\mathbf{P}$, the corresponding vega to the caplet volatility with strike K and fixing date T_i is given by:

$$\frac{\partial I(\mathbf{P})}{\partial \sigma^{\text{SABR},(\theta)}(L_0^{(i)}, K)} = \nabla I(\mathbf{P}) \cdot \left[\frac{\partial \mathbf{P}}{\partial \alpha_{T_i}} \left(\frac{\partial \sigma^{\text{SABR},(\theta)}(L_0^{(i)}, K)}{\partial \alpha_{T_i}} \right)^{-1} + \frac{\partial \mathbf{P}}{\partial \beta_{T_i}} \left(\frac{\partial \sigma^{\text{SABR},(\theta)}(L_0^{(i)}, K)}{\partial \beta_{T_i}} \right)^{-1} + ... \right] \tag{4.37}$$

We compute $\dfrac{\partial \mathbf{P}}{\partial \alpha_{T_i}}$ for α_{T_i} using a central difference estimator by using Equation (4.7), giving:

$$\frac{\partial \mathbf{P}}{\partial \alpha_{T_i}} = \frac{1}{h} \mathbf{1} \cdot (\mathbf{P}_{\mathbf{solve,nested}}(\mathbf{P^{(0)}}, \sigma_+^{(\theta)}) - \mathbf{P}_{\mathbf{solve,nested}}(\mathbf{P^{(0)}}, \sigma_-^{(\theta)})),$$

with $h = 10^{-4}$ and $\sigma_+^{(\theta)}$ is equal to the caplet volatility surface implied by parameter vectors $\{\alpha_{T_j}\}$, $\{\beta_{T_j}\}$, $\{\rho_{T_j}\}$, $\{\nu_{T_j}\}$ and curve $\mathbf{P}$, where α_{T_i} is increased by h. Analogously $\sigma_-^{(\theta)}$ is equal to the caplet volatility surface implied by parameter vectors $\{\alpha_{T_j}\}$, $\{\beta_{T_j}\}$, $\{\rho_{T_j}\}$, $\{\nu_{T_j}\}$ and curve $\mathbf{P}$, where α_{T_i} is decreased by h. Analougously partial derivatives $\dfrac{\partial \mathbf{P}}{\partial \beta_{T_i}}$, $\dfrac{\partial \mathbf{P}}{\partial \rho_{T_i}}$ and $\dfrac{\partial \mathbf{P}}{\partial \nu_{T_i}}$ are computed. Furthermore, $\dfrac{\partial \alpha_{T_i}}{\partial \sigma^{\text{SABR},(\theta)}(L_0^{(i)}, K)}$ is not known, but $\dfrac{\partial \sigma^{\text{SABR},(\theta)}(L_0^{(i)}, K)}{\partial \alpha_{T_i}}$ is, so we use the inverse derivative theorem that states that on some invertible neighbourhood of $\sigma^{SABR,(i)}$ to its parameters the partial derivative of the inverse function is the multiplicative inverse of the partial derivative.

We will look at sensitivities of Libor curve derivatives to movements in caplet volatilities corresponding to the first 12 fixing dates (3 months up to 3 years). We will look at sensitivities to

[7] For an example a fixed-for-floating swap given by Equation (2.29).

caplet volatilities of every absolute[8] strike when using the replication method and only to at the money strike caplet volatilities when using the Ho-Lee model.
Consequently, we will display the vega profile of a Libor curve derivative where the Libor curve is calibrated using Ho-Lee model-dependent convexity adjustments by a barchart and a Table of sensitivities to the term-structure of at the money caplet volatility with cap maturities. The vega profile of a Libor curve derivative where the Libor curve is calibated using the replication method is a matrix, with the absolute strikes on one axis and the caplet maturities the other, we will again use cap maturities and display the profiles using a heatmap and a Table.

Finally the risk profiles will also computed under stressed market scenarios, with rates being higher by 3% and caplet volatilities higher by 10%, see A.11.

4.6.1 Cash deposits

We will consider the present value of 3 month lender deposits, see Equation (2.16). We start by plotting replication method implied vega profiles where we look at sensitivities to movements of volatilities per individual strike, sensitivities are calculated using Equation (4.37):

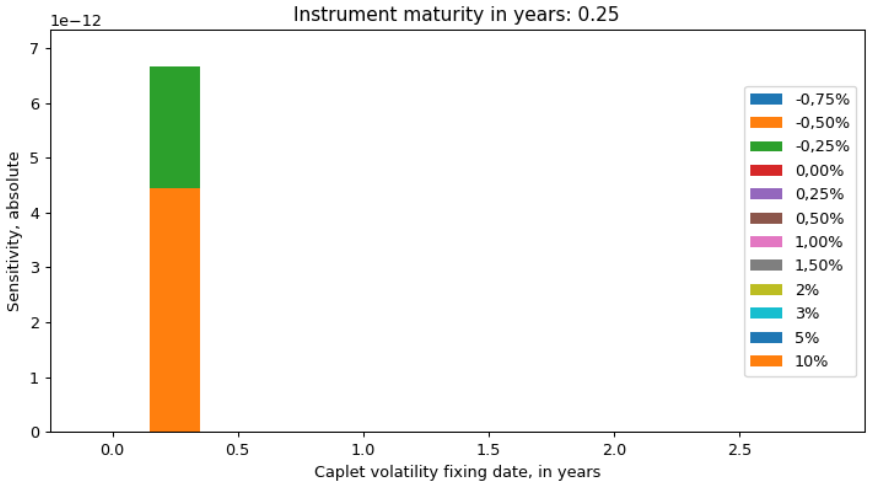

Figure 4.24: Individual vegas, replication method model.

	0.25	0.5	0.75	1.0	1.25	1.5	1.75	2.0	2.25	2.5	2.75	3.0
-0,75%	0	0	0	0	0	0	0	0	0	0	0	0
-0,50%	0	4,44E-12	0	0	0	0	0	0	0	0	0	0
-0,25%	0	2,22E-12	0	0	0	0	0	0	0	0	0	0
0,00%	0	0	0	0	0	0	0	0	0	0	0	0
0,25%	0	0	0	0	0	0	0	0	0	0	0	0
0,50%	0	0	0	0	0	0	0	0	0	0	0	0
1,00%	0	0	0	0	0	0	0	0	0	0	0	0
1,50%	0	0	0	0	0	0	0	0	0	0	0	0
2%	0	0	0	0	0	0	0	0	0	0	0	0
3%	0	0	0	0	0	0	0	0	0	0	0	0
5%	0	0	0	0	0	0	0	0	0	0	0	0
10%	0	0	0	0	0	0	0	0	0	0	0	0

Table 4.5: Individual vegas, replication method model. Table, $xE-y$ means $x \cdot 10^{-y}$

[8] Absolute strikes are given by $[-0.75\%, -0.5\%, -0.25\%, 0, 0.25\%, 0.5\%, 0.75\%, 1\%, 2\%, 3\%, 5\%, 10\%]$, see 2.7 for details about the absolute strikes.

Here we display the vega profiles implied by a constant parameter Ho-Lee model and the replication method model:

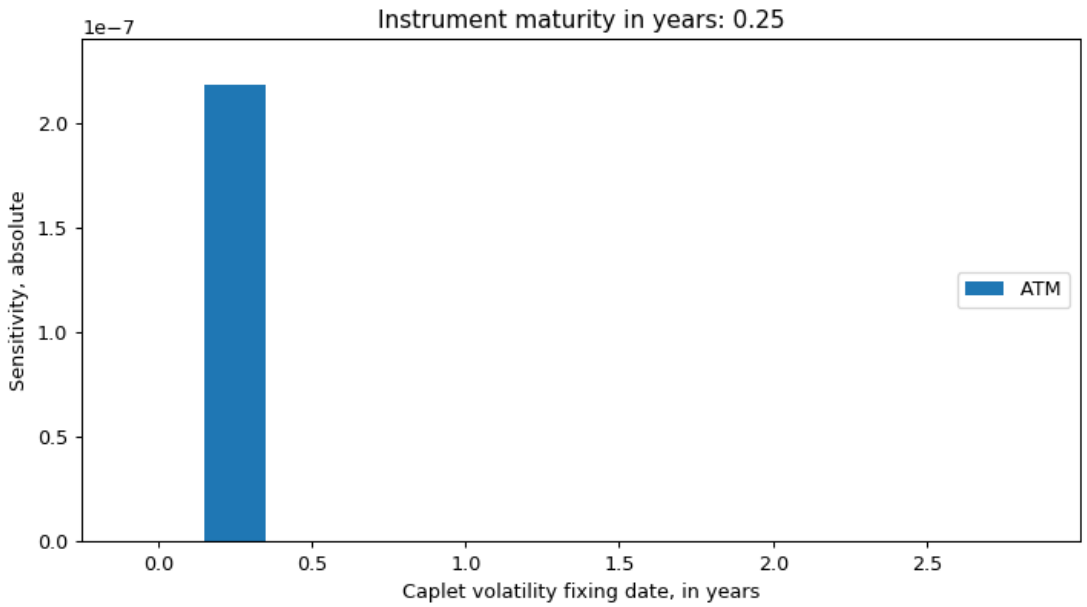

Figure 4.25: Parallel smile vegas, Ho-Lee model.

	0.25	0.5	0.75	1.0	1.25	1.5	1.75	2.0	2.25	2.5	2.75	3.0
ATM	0	2,18E-07	0	0	0	0	0	0	0	0	0	0

Table 4.6: Individual vegas, Ho-Lee model. Table

Note that in dataset B.1 the first futures rates has a start of approximately 2 months and a maturity of 5 months in the future (between March 2018 and June 2018). Consequently the convexity adjustment depends on the 2-month fixing caplet volatility. Which consequently explains the dependency on solely the 3-month fixing caplet volatility smiles. Furthermore, increasing the at the money caplet volatility in the Ho-Lee model seems to have a bigger effect on the underlying deposit than the sum of all the sensitivities in the replication method model. Other observations are mentioned in Section **??**.

4.6.2 FRAs

We will consider the present value of 2 year lender FRAs, see equation (3.6), sensitivities are calculated using Equation (4.37).

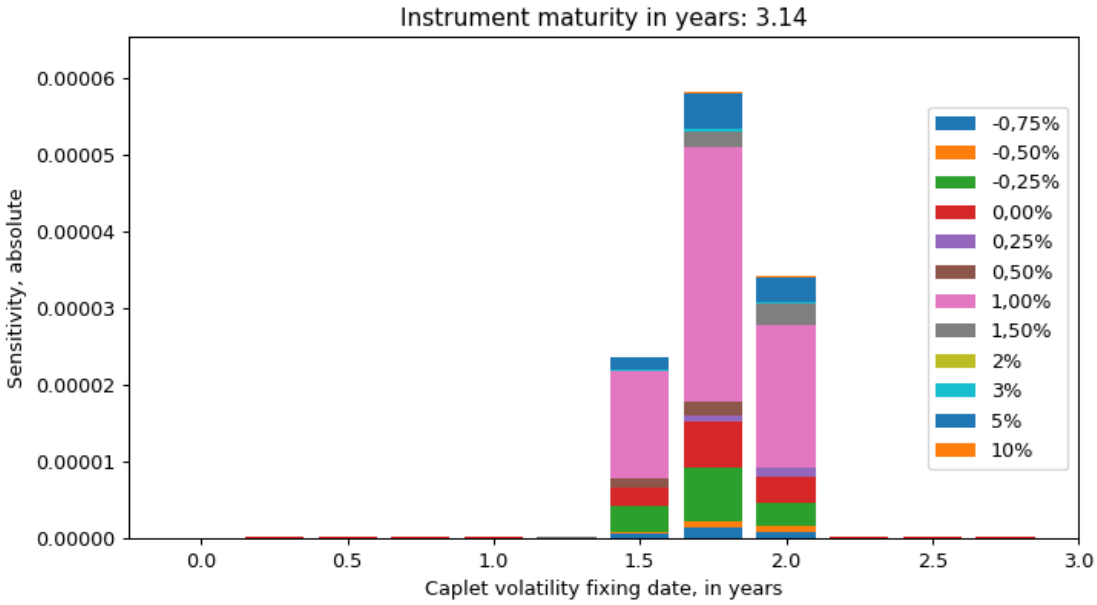

Figure 4.26: Individual vegas, replication method model.

	0.25	0.5	0.75	1.0	1.25	1.5	1.75	2.0	2.25	2.5	2.75	3.0
-0,75%	0	1,56E-08	1,57E-08	1,57E-08	1,55E-08	1,43E-08	5,43E-07	1,26E-06	6,99E-07	1,56E-08	1,57E-08	1,57E-08
-0,50%	0	1,56E-08	1,57E-08	1,57E-08	1,56E-08	5,99E-09	2,27E-07	9,86E-07	9,19E-07	1,56E-08	1,57E-08	1,57E-08
-0,25%	0	1,56E-08	1,57E-08	1,57E-08	1,57E-08	-5,9E-09	3,36E-06	6,88E-06	2,9E-06	1,56E-08	1,57E-08	1,57E-08
0,00%	0	1,56E-08	1,57E-08	1,57E-08	1,55E-08	3,04E-09	2,42E-06	5,94E-06	3,48E-06	1,56E-08	1,57E-08	1,57E-08
0,25%	0	1,56E-08	1,57E-08	1,57E-08	1,55E-08	1,56E-08	1,57E-08	8,57E-07	1,19E-06	1,56E-08	1,57E-08	1,57E-08
0,50%	0	1,56E-08	1,57E-08	1,57E-08	1,58E-08	-1,3E-08	1,27E-06	1,87E-06	1,56E-08	1,56E-08	1,57E-08	1,57E-08
1,00%	0	1,56E-08	1,57E-08	1,57E-08	1,57E-08	-5,2E-08	1,38E-05	3,3E-05	1,84E-05	1,56E-08	1,57E-08	1,57E-08
1,50%	0	1,56E-08	1,57E-08	1,57E-08	1,55E-08	1,56E-08	1,57E-08	2,03E-06	2,83E-06	1,56E-08	1,57E-08	1,57E-08
2%	0	1,56E-08	1,57E-08	1,57E-08	1,55E-08	1,56E-08	1,57E-08	1,57E-08	1,56E-08	1,56E-08	1,57E-08	1,57E-08
3%	0	1,56E-08	1,57E-08	1,57E-08	1,55E-08	1,45E-08	2,2E-07	4,74E-07	2,46E-07	1,56E-08	1,57E-08	1,57E-08
5%	0	1,56E-08	1,57E-08	1,57E-08	1,55E-08	1,03E-08	1,52E-06	4,47E-06	3,23E-06	1,56E-08	1,57E-08	1,57E-08
10%	0	1,56E-08	1,57E-08	1,57E-08	1,55E-08	1,54E-08	1,11E-07	3,34E-07	2,69E-07	1,56E-08	1,57E-08	1,57E-08

Table 4.7: Individual vegas, replication method model. Table

Here we display the vega profiles implied by a constant parameter Ho-Lee model and the replication method model:

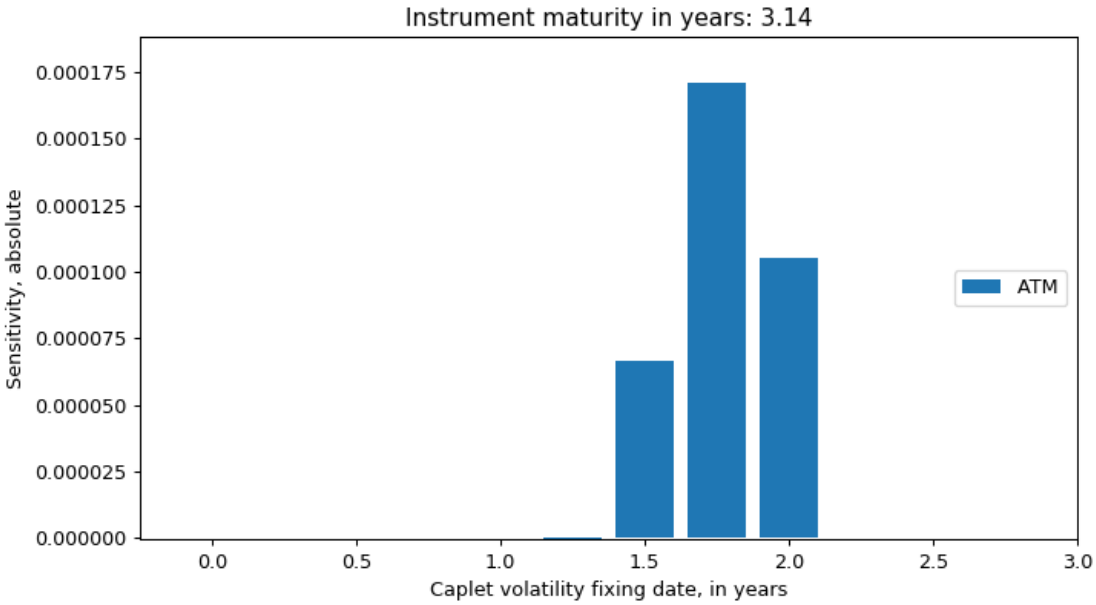

Figure 4.27: Parallel smile vegas, Ho-Lee model.

	0.25	0.5	0.75	1.0	1.25	1.5	1.75	2.0	2.25	2.5	2.75	3.0
ATM	0	-1,2E-09	-1,1E-09	-9,9E-10	1,41E-09	-4,1E-07	6,66E-05	0,000171	0,000105	-1,2E-09	-1,2E-09	-1,2E-09

Table 4.8: Individual vegas, Ho-Lee model. Table

The 2 year maturity FRA is a contract over the spot Libor with a start of 1 year and 9 months and a maturity of 2 years in the future. The strange dependency structure can be explained by a maturity mismatch between the underlying caplets and the futures:

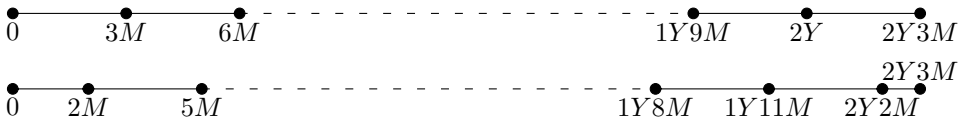

Figure 4.28: Tenor structures of respectively caplets and futures rates.

Increasing the 1Y9M maturity caplet volatility affects the interpolated caplet volatilities used to compute the convexity adjustments of the 1Y11M maturity futures rates and consequently the 2Y maturity implied forward rate. Similarly the 2Y3M maturity caplet volatility affects the interpolated caplet volatilities used to compute the convexity adjustments of the 2Y2M maturity futures rates and consequently the 2Y maturity implied forward rate.

4.6.3 Swaps

We will consider the present value of 2 year Payer swaps, see Equation (2.24), sensitivities are calculated using Equation (4.37)

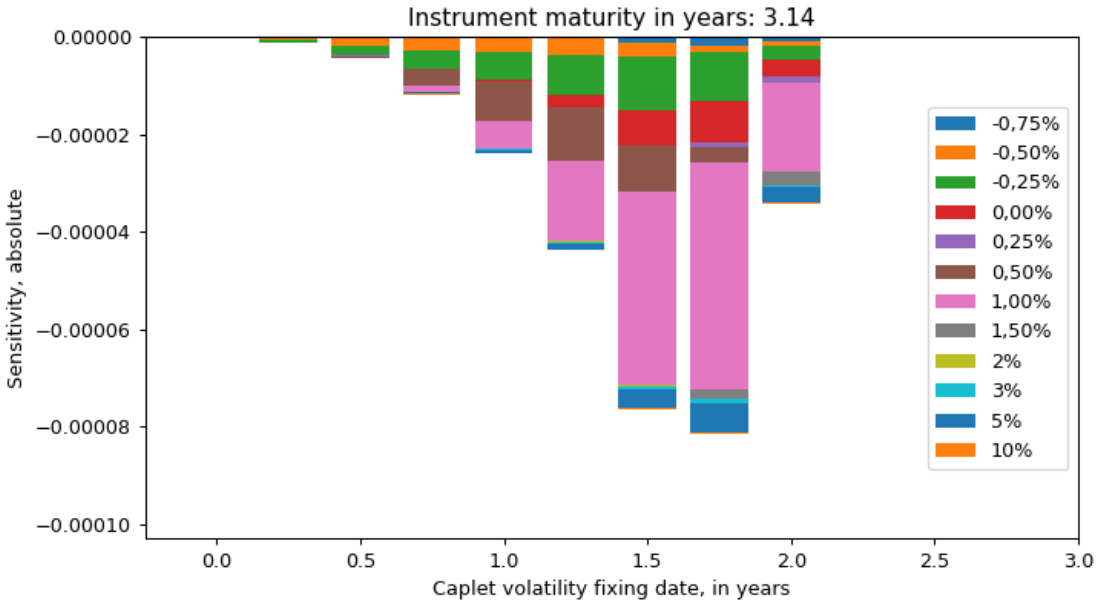

Figure 4.29: Individual vegas, replication method model.

	0.25	0.5	0.75	1.0	1.25	1.5	1.75	2.0	2.25	2.5	2.75	3.0
-0,75%	0	-2,2E-08	-4E-08	-1,7E-07	-2,1E-07	-2,5E-07	-1,2E-06	-1,8E-06	-7E-07	-2,2E-08	-2,2E-08	-2,2E-08
-0,50%	0	-4,9E-07	-1,7E-06	-2,4E-06	-2,7E-06	-3,5E-06	-2,8E-06	-1,2E-06	-9,2E-07	-2,2E-08	-2,2E-08	-2,2E-08
-0,25%	0	-5,2E-07	-2E-06	-3,8E-06	-5,8E-06	-8E-06	-1,1E-05	-1E-05	-2,9E-06	-2,2E-08	-2,2E-08	-2,2E-08
0,00%	0	-2,2E-08	-2,2E-08	-2,2E-08	-3,7E-07	-2,5E-06	-7,2E-06	-8,3E-06	-3,5E-06	-2,2E-08	-2,2E-08	-2,2E-08
0,25%	0	-2,2E-08	-2,2E-08	-2,2E-08	-2,2E-08	-2,2E-08	-2,2E-08	-8,6E-07	-1,2E-06	-2,2E-08	-2,2E-08	-2,2E-08
0,50%	0	-2,2E-08	-3,6E-07	-3,4E-06	-8,2E-06	-1,1E-05	-9,4E-06	-3,2E-06	-2,2E-08	-2,2E-08	-2,2E-08	-2,2E-08
1,00%	0	-2,2E-08	-1,1E-07	-1,4E-06	-5,5E-06	-1,7E-05	-4E-05	-4,7E-05	-1,8E-05	-2,2E-08	-2,2E-08	-2,2E-08
1,50%	0	-2,2E-08	-2,2E-08	-2,2E-08	-2,2E-08	-2,2E-08	-2,2E-08	-2E-06	-2,8E-06	-2,2E-08	-2,2E-08	-2,2E-08
2%	0	-2,2E-08	-2,2E-08	-2,2E-08	-2,2E-08	-2,2E-08	-2,2E-08	-2,2E-08	-2,2E-08	-2,2E-08	-2,2E-08	-2,2E-08
3%	0	-2,2E-08	-2,4E-08	-1,2E-07	-2,5E-07	-3,5E-07	-6,4E-07	-6,8E-07	-2,5E-07	-2,2E-08	-2,2E-08	-2,2E-08
5%	0	-2,2E-08	-2,6E-08	-2,8E-07	-7,1E-07	-1,4E-06	-3,9E-06	-6E-06	-3,2E-06	-2,2E-08	-2,2E-08	-2,2E-08
10%	0	-2,2E-08	-2,2E-08	-5,3E-08	-8,3E-08	-8,2E-08	-2,4E-07	-4,3E-07	-2,7E-07	-2,2E-08	-2,2E-08	-2,2E-08

Table 4.9: Individual vegas, replication method model. Table

Here we display the vega profiles implied by a constant parameter Ho-Lee model and the replication method model:

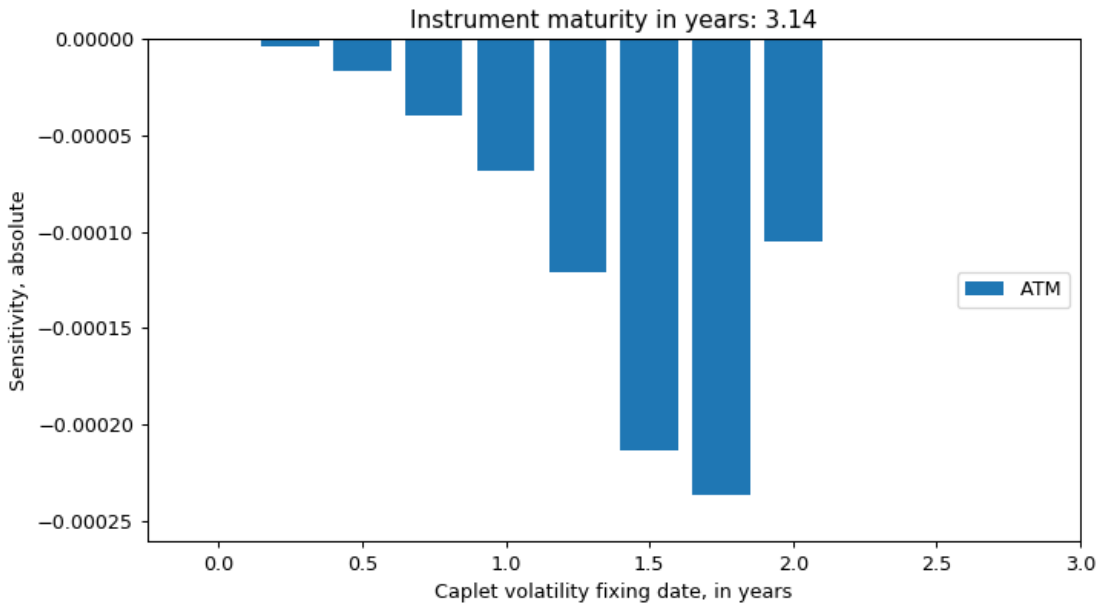

Figure 4.30: Parallel smile vegas, Ho-Lee model.

	0.25	0.5	0.75	1.0	1.25	1.5	1.75	2.0	2.25	2.5	2.75	3.0
ATM	0	-3,7E-06	-1,6E-05	-3,9E-05	-6,8E-05	-0,00012	-0,00021	-0,00024	-0,0001	1,49E-09	1,49E-09	1,49E-09

Table 4.10: Individual vegas, Ho-Lee model. Table

2 year swaps have 8 underlying floating Libor payments and 2 underlying fixed rate payments. Consequently, they depend on the caplet volatilities corresponding to the first 9 maturity caplet volatilities.

There are several general observations that can be made. In all cases the Ho-Lee sensitivities are higher than those implied by the replication method, even when bumping the entire corresponding volatility smile, which can again be explained due to the larger magnitude of Ho-Lee implied convexity adjustments compared to replication method convexity adjustments. Stressed market scenarios imply higher caplet sensitivities, see A.11, nevertheless sensitivities never exceed 10 basispoints, see Figure A.10. Conclusively, holding a 1 million Euro notional position in a linear Libor derivative even under stressed market scenarios one should not expect higher than a 1 Eurocent deviations for every basispoint move of the underlying caplet volatility, therefore the induced vega risks of linear instruments are negligible.

Chapter 5

Conclusions and further research

Our main goal was to derive a curve calibration algorithm that can simultaneously calibrate the Libor curve with volatility dependent convexity adjustments, which we have, given 2 combined with Equations (4.36) and (A.8). We have translated the convexity adjustment into the dependency of the underlying distributions of pre-settlement realised interest rates given by $\frac{D_T}{D_t}$ and the spot Libor rate L_T, we have further looked at how the convexity adjustment can be modelled using simple one-factor short-rate models, which assume positive correlation between $\frac{D_T}{D_t}$ and the spot Libor rate L_T, see (A.37). We have compared our resulting convexity adjustments to a replication method model that assumes independence between $\frac{D_T}{D_t}$ and the spot Libor rate L_T. Equation (4.30) implies a positive relationship between convexity adjustments and the underlying correlation between pre-settlement interest rates and the spot Libor rate. Ho-Lee shows higher convexity adjustments than the replication method model. Which makes sense due to the underlying assumptions about the covariance between pre-settlement interest rates and the spot Libor rate. The nested calibration algorithm 2 converges after 5-10 convexity adjustment iterations, with stopping criterium $|\mathbf{C^{(n)}} - \mathbf{C^{(n-1)}}| < 10^{-12}$ and 10^{-14} for $\mathbf{P_{solve}}$. Choice of a high enough boundary is important due to the unfeasible effects observed for the convexity adjustments in Figures 4.11b and 4.11a. Due to the maturity mismatch between futures and caplets, when using caplet volatilities to forecast the corresponding forward rate via the convexity adjustment in curve calibration it will have dependencies on the surrounding caplet volatilities too, as has been observed in Section 4.6.2. Finally due to small vegas observed in Sections 4.6 and A.11 we can conclude that modelling volatility dependent convexity adjustments introduces negligible vegas when pricing Libor rate derivatives.

There are 3 main topics of interest for further research. Firstly, an extension into the multi-curve framework of joint calibration of the overnight and 3-month Libor curves is possible. From Equation (3.12), provided an exact solution exists it becomes clear that the Libor curve on the interval $[T_0, T_n]$ is not dependent on the overnight curve. Therefore, Libor curve calibration using futures remains the same, the only difference being that the convexity adjustment now also dependent on both curves. Given that we can find functional forms of the convexity adjustment of the form: $\mathbf{C}(\mathbf{P^{(3m)}}, \mathbf{P^{(O)}}, \sigma_{\mathbf{P}}^{(\theta)})$. We can extend the nested calibration algorithm 2 into the multi-curve framework. Finally, Libor rate derivatives are still being issued in large volumes, even though banks in the Libor panel will no longer be encouraged to provide Libor sport rate quotes after 2021, []. Therefore an extension into a multi-curve framework with overnight, Libor and alternative reference rate curves is necessary, see for an example [34].

Bibliography

[1] F. M. Ametrano and M. Bianchetti. Everything you always wanted to know about multiple interest rate curve bootstrapping but were afraid to ask. 2013.

[2] L. B. Andersen and V. V. Piterbarg. *Interest Rate Modeling Volume I-III*. Atlantic Financial Press, 2010.

[3] W. Andong. Modern pricing of caps: Volatility transformation based on the multi-curve setting. Master's thesis, University of Amsterdam, 2013.

[4] M. Beinker and S. Georg. New volatility conventions in negative interest environment. *D-Fine*, 2012.

[5] F. Black. The pricing of commodity contracts. *Journal of financial economics*, 3(1-2):167–179, 1976.

[6] D. T. Breeden and R. H. Litzenberger. Prices of state-contingent claims implicit in option prices. *Journal of business*, pages 621–651, 1978.

[7] D. Brigo and F. Mercurio. *Interest rate models-theory and practice: with smile, inflation and credit*. Springer Science & Business Media, 2007.

[8] R. Burden and J. Faires. Numerical analysis 9th edn (boston: Brooks/cole—cengage learning). 2010.

[9] P. Carr and D. Madan. Towards a theory of volatility trading. *Volatility: New estimation techniques for pricing derivatives*, 29:417–427, 1998.

[10] A. Castagna. Pricing of derivatives contracts under collateral agreements: Liquidity and funding value adjustments. *Available at SSRN 1974479*, 2013.

[11] P. Collin-Dufresn, R. S. Goldstein, and J. S. Martin. The determinants of credit spread changes. *The Journal of Finance*, 56(6):2177–2207, 2001.

[12] J. C. Cox, J. E. Ingersoll Jr, and S. A. Ross. The relation between forward prices and futures prices. *Journal of Financial Economics*, 9(4):321–346, 1981.

[13] J. Gatheral. *The volatility surface: a practitioner's guide*, volume 357. John Wiley & Sons, 2011.

[14] H. Gavin. The levenberg-marquardt method for nonlinear least squares curve-fitting problems. *Department of Civil and Environmental Engineering, Duke University*, pages 1–15, 2011.

[15] S. Gilchrist and E. Zakrajšek. Credit spreads and business cycle fluctuations. *American Economic Review*, 102(4):1692–1720, June 2012.

[16] L. A. Grzelak and C. W. Oosterlee. From arbitrage to arbitrage-free implied volatilities. *Journal of Computational Finance, Forthcoming*, 2016.

[17] A. Gupta and M. G. Subrahmanyam. An empirical examination of the convexity bias in the pricing of interest rate swaps. *Journal of Financial Economics*, 55(2):239–279, 2000.

[18] P. S. Hagan, D. Kumar, A. Lesniewski, and D. Woodward. Arbitrage-free sabr. *Wilmott*, 2014(69):60–75, 2014.

[19] P. S. Hagan, D. Kumar, A. S. Lesniewski, and D. E. Woodward. Managing smile risk. *The Best of Wilmott*, 1:249–296, 2002.

[20] P. S. Hagan, A. S. Lesniewski, G. Skoufis, and D. E. Woodward. Convexity without replication. *Wilmott, this issue*, 2019.

[21] P. S. Hagan, A. S. Lesniewski, G. Skoufis, and D. E. Woodward. Explicit pricing of quadratic derivatives under sabr. *Wilmott, this issue*, 2019.

[22] J. M. Harrison and S. R. Pliska. A stochastic calculus model of continuous trading: complete markets. *Stochastic processes and their applications*, 15(3):313–316, 1983.

[23] M. Henrard. The irony in derivatives discounting part ii: The crisis. *Wilmott Journal*, 2(6):301–316, 2010.

[24] M. Henrard. Interest rate instruments and market conventions guide. *OpenGamma Quantitative Research,*, 2012.

[25] S. L. Heston. A closed-form solution for options with stochastic volatility with applications to bond and currency options. *The review of financial studies*, 6(2):327–343, 1993.

[26] J. Hull. *Options, Futures, and Other Derivatives*. Pearson Education, 2017.

[27] J. Hull and A. White. Pricing interest-rate-derivative securities. *The review of financial studies*, 3(4):573–592, 1990.

[28] P. Hunt and J. Kennedy. *Financial derivatives in theory and practice*. John Wiley & Sons, 2004.

[29] P. Jäckel and A. Kawai. The future is convex. *Wilmott Magazine*, 15, 2005.

[30] G. Kirikos and D. Novak. Convexity conundrums: Presenting a treatment of swap convexity in the hall-white framework. *Risk magazine*, 10:60–61, 1997.

[31] A. Lyashenko and F. Mercurio. Looking forward to backward-looking rates: A modeling framework for term rates replacing libor. *Available at SSRN 3330240*, 2019.

[32] J. Mayle and S. I. Association. *Standard Securities Calculation Methods: Fixed Income Securities Formulas for Price, Yield, and Accrued Interest*. Number v. 1 in Standard Securities Calculation Methods: Fixed Income Securities Formulas for Price, Yield, and Accrued Interest. Securities Industry Association, 1993.

[33] F. Mercurio. The present of futures: valuing eurodollar-futures convexity adjustments in a multi-curve world. *Available at SSRN 2987832*, 2017.

[34] F. Mercurio. A simple multi-curve model for pricing sofr futures and other derivatives. 2018.

[35] M. Morini. *Understanding and Managing Model Risk: A practical guide for quants, traders and validators*. John Wiley & Sons, 2011.

[36] M. Musiela and M. Rutkowski. Martingale methods in financial modelling, 2005, 2005.

[37] A. Pelsser. *Efficient methods for valuing interest rate derivatives*. Springer Science & Business Media, 2013.

[38] V. Piterbarg. Funding beyond discounting: collateral agreements and derivatives pricing. *Risk*, 23(2):97, 2010.

[39] V. Piterbarg and M. Renedo. Eurodollar futures convexity adjustments in stochastic volatility models. *Available at SSRN 610223*, 2004.

[40] V. Pozdnyakov and J. M. Steele. On the martingale framework for futures prices. *Stochastic Processes and their Applications*, 109(1):69–77, 2004.

[41] S. Shreve. *Stochastic calculus for finance I: the binomial asset pricing model*. Springer Science & Business Media, 2012.

[42] S. E. Shreve. *Stochastic calculus for finance II: Continuous-time models*, volume 11. Springer Science & Business Media, 2004.

[43] J. Sidenius. Libor market models in practice. *Journal of Computational Finance*, 3(3):5–26, 2000.

[44] M. L. Stigum and F. L. Robinson. *Money market and bond calculations*. Irwin Professional Publ., 1996.

[45] N. Vaillant. Convexity adjustments between futures and forward rates using a martingale approach. *Probability tutorials*, 1999.

[46] R. White and I. Yukinori. Eight ways to strip your caplets: An introduction to caplet stripping. *OpenGamma Quantitative Research*, 2014.

Chapter A

Appendix

A.1 Black's formula

Lemma A.1.1 (Black's formula)**.** Let L_T be a spot Libor rate with accruing period $[T, M]$, let L_t be the corresponding forward rate specified by the dynamics:

$$dL_t/(L_t + \theta) = \sigma_t dW_t^M.$$

Where θ is chosen such that $L_t+\theta$ is strictly positive. Then the M-forward expectation of the corresponding Libor caplet is given by:

$$\mathbb{E}^M[((L_T + \theta) - (K + \theta))^+ | \mathscr{F}_t] = (L_t + \theta)\Phi(d_+) - (K + \theta)\Phi(d_-) = Black(L_t + \theta, K + \theta, v, T - t).$$

With $d_\pm = \dfrac{\ln\left(\frac{L_t+\theta}{K+\theta}\right) \pm v^2(T-t)/2}{v\sqrt{T-t}}$ and $v = \sqrt{\dfrac{1}{T-t}\int_t^T \sigma_u^2 du}$.

Proof. See [7] or [2] for proof. □

A.2 One factor short rate model examples

A.2.1 Ho-Lee

We will start with the Ho-Lee model, which assumes $\sigma_f(t, T)$ is a positive deterministic function of time $\sigma_f(t)$ independent of the maturity T. After imposing $\sigma_P(t, t) = 0$ we get $\sigma_P(t, T) = \int_t^T \sigma_f(t, u)du = \sigma_f(t)(T - t)$. This gives short rate dynamics:

$$dr_t = \theta_t dt + \sigma_t dWt^{\mathbb{Q}}. \tag{A.1}$$

Here $\theta_t =$ Where θ_t depends on σ_t due to martingale relationships, note:

$$\begin{aligned} v^2 &= \frac{1}{T}\int_0^T (\sigma_P(u, M) - \sigma_P(u, T))^2 du \\ &= \frac{1}{T}\int_0^T (\sigma_f(u)(M - u) - \sigma_f(u)(T - u))^2 du \\ &= \frac{\tau^2}{T}\int_0^T \sigma_f(u)^2 du \end{aligned} \tag{A.2}$$

and

$$\begin{aligned} \Omega(0, T) &= \int_0^T (\sigma_P(u, M) - \sigma_P(u, T))\sigma_P(u, M)du \\ &= \int_0^T \sigma_f(u)\tau\sigma_f(u)(M - u)du \end{aligned}$$

$$= \int_0^T \sigma_f(u)^2 \tau(M) du - \int_0^T \sigma_f(u)^2 \tau u du$$
$$= \int_0^T \sigma_f(u)^2 du \tau(M) - \int_0^T \sigma_f(u)^2 u du \tau \tag{A.3}$$

This implies for the Futures rate using the Ho-Lee model:

$$Fut_0 = \frac{1}{\tau}\Big(\frac{P(0,T)}{P(0,M)} \exp\Big(\int_0^T \sigma_f(u)^2 du \tau(M) - \int_0^T \sigma_f(u)^2 u du \tau\Big) - 1\Big). \tag{A.4}$$

Choosing $\sigma_f(t) = \sigma_f$ constant gives us for the caplet lognormal volatility, Ω and the futures rate:

$$v = \sigma_f \tau. \tag{A.5}$$

$$\Omega(0,T) = \frac{\sigma_f^2}{2} T\tau(T + 2\tau). \tag{A.6}$$

$$Fut_0 = \frac{1}{\tau}\Big(\frac{P(0,T)}{P(0,M)} \exp\Big(\frac{\sigma_f^2}{2} T\tau(T + 2\tau)\Big) - 1\Big). \tag{A.7}$$

Giving convexity adjustment:

$$C_0 = \frac{1}{\tau}\frac{P(0,T)}{P(0,M)}\Big(\exp\Big(\frac{\sigma_f^2}{2} T\tau(T + 2\tau)\Big) - 1\Big). \tag{A.8}$$

Using (A.5), the corresponding forward rate L_0 converted to Libor discount factors using Equation (2.4.1), T the starting date of the underlying spot Libor and the corresponding θ-shift at the money caplet volatility $\sigma_T^{(\theta)}(L_0)$ the resulting convexity adjustment is given by:

$$\begin{aligned} C_{HL}(T, \sigma_T^{(\theta)}(L_0), L_0) &= \frac{1}{\tau}\frac{P(0,T)}{P(0,M)}\left(\exp\left(\frac{\sigma_T^{(\theta)}(L_0)^2}{2\tau}\left(\frac{L_0 + \theta}{L_0 + \frac{1}{\tau}}\right)^2 T(T + 2\tau)\right) - 1\right) \\ &= \frac{1}{\tau}\frac{P(0,T)}{P(0,M)}\left(\exp\left(\frac{\sigma_T^{(\theta)}(L_0)^2}{2\tau}\left((1 - (1 - \tau\theta)\frac{P(0,M)}{P(0,T)}\right)^2 T(T + 2\tau)\right) - 1\right) \end{aligned} \tag{A.9}$$

Analogously an expression for the convexity under the Hull-White model can be obtained.

A.2.2 Hull-White

The Hull-White model is specified by:

$$\sigma_f(t,T) = \sigma(t) \exp(-\lambda(t)(T - t)),$$

$\sigma(t)$ and $\lambda(t)$ are positive deterministic functions and intuitively the Hull-White model volatility $\sigma_f(t,T)$ captures the tendency of the instantaneous forward rate volatility to increase close to the start of the accruing period. After imposing $\sigma_P(t,t) = 0$ we get

$$\sigma_P(t,T) = \int_t^T \sigma_f(t,u) du = \frac{\sigma(t)}{\lambda(t)}[1 - \exp(-\lambda(t)(T - t))].$$

Which leads to:

$$\begin{aligned} v^2 &= \frac{1}{T}\int_0^T (\sigma_P(u,M) - \sigma_P(u,T))^2 du \\ &= \frac{1}{T}\int_0^T \Big(\frac{\sigma(u)}{\lambda(u)}[1 - \exp(-\lambda(u)(M - u))] - \frac{\sigma(u)}{\lambda(u)}[1 - \exp(-\lambda(u)(T - u))]\Big)^2 du \\ &= \frac{1}{T}\int_0^T \frac{\sigma^2(u)}{\lambda^2(u)}[\exp(-\lambda(u)(T - u)) - \exp(-\lambda(u)(M - u))]^2 du \end{aligned} \tag{A.10}$$

and

$$\Omega(0,T) = \int_0^T (\sigma_P(u,M) - \sigma_P(u,T))\sigma_P(u,M) du$$

$$= \int_0^T \frac{\sigma(u)^2}{\lambda(u)^2}[\exp(-\lambda(u)(T-u)) - \exp(-\lambda(u)(M-u))][1-\exp(-\lambda(u)(M-u))]du. \quad (A.11)$$

For constant λ and σ we get the following caplet lognormal volatility, Ω and futures rate:

$$v = \sqrt{\frac{\sigma^2}{2\lambda^3 T}(1-\exp(-2\lambda T))(1-\exp(-\lambda\tau))^2}. \quad (A.12)$$

$$\Omega(0,T) = \frac{\sigma^2}{\lambda^3}[1 - \frac{1}{2}(1+\exp(-\lambda T))\exp(-\lambda\tau)](1-\exp(-\lambda T))(1-\exp(-\lambda\tau)). \quad (A.13)$$

$$Fut_0 = \frac{1}{\tau}\Big(\frac{P(0,T)}{P(0,M)}\exp\Big(\frac{\sigma^2}{\lambda^3}[1-\frac{1}{2}(1+\exp(-\lambda T))\exp(-\lambda\tau)](1-\exp(-\lambda T))(1-\exp(-\lambda\tau))\Big) - 1\Big). \quad (A.14)$$

$$C_0 = \frac{1}{\tau}\frac{P(0,T)}{P(0,M)}\left(\exp\Big(\frac{\sigma^2}{\lambda^3}[1-\frac{1}{2}(1+\exp(-\lambda T))\exp(-\lambda\tau)](1-\exp(-\lambda T))(1-\exp(-\lambda\tau))\Big) - 1\right). \quad (A.15)$$

A.3 Change of numeraire

Due to market completeness the value of any $\mathscr{F}_T$-measurable payoff $B(T)V(T)$ is unique, therefore:

$$B(t)\mathbb{E}_t^B\left[\frac{B(T)Y(T)}{B(T)}|\mathscr{F}_t\right] = A(t)\mathbb{E}_t^A\left[\frac{B(T)Y(T)}{A(T)}|\mathscr{F}_t\right]. \quad (A.16)$$

Which implies:

$$\mathbb{E}_t^B\left[Y(T)|\mathscr{F}_t\right] = \mathbb{E}_t^A\left[Y(T)\frac{B(T)A(t)}{B(t)A(T)}|\mathscr{F}_t\right]. \quad (A.17)$$

Which proves the result. Theorem 1.4.2 of [2].

A.4 Penalty matrices

Given the optimization problem (2.46) we chose our penalty matrices to be: $\lambda P = \lambda_1^2 A_1^\top A_1 + \lambda_2^2 A_2^\top A_2$

With $\lambda_1 A_1 = \lambda_1 \begin{pmatrix} 0 & ... & ... & 0 \\ & & \vdots & \\ -1 & 1 & & 0 \\ \vdots & \ddots & \ddots & 0 \\ 0 & ... & -1 & 1 \end{pmatrix}$ and $\lambda_2 A_2 = \lambda_2 \begin{pmatrix} 0 & ... & ... & ... & 0 \\ 0 & ... & ... & ... & 0 \\ 1 & -2 & 1 & ... & 0 \\ 0 & \ddots & \ddots & \ddots & 0 \\ 0 & ... & 1 & -2 & 1 \end{pmatrix}$.

Here $\lambda_1 = \lambda_2 = 0.0003$, such that both volatility surfaces reprice the corresponding caps within 1 basis-point, the choice of these weighing constants is completely arbitrary and depends on the stability of the underlying optimization problem and depends on the tradeoff between repricing error and smoothness. λ_1 penalizes high second order derivatives, while λ_2 penalizes high first order derivatives, in order to ensure a smooth termstructure in the time direction. See [46] for more details.

A.5 Shift transformation

Black's formula is given in A.1. The present value of the caplet is given by:

$$P(0,M)\tau Black(L_0+\theta, \sigma_T^{(\theta)}(L_0), L_0+\theta, T).$$

The $1/\tau$ caplet volatility is given by the equation:

$$Black(L_0+\theta, \sigma_T^{(\theta)}(L_0), L_0+\theta, T) = Black(L_0+1/\tau, \sigma_T^{(1/\tau)}(L_0), L_0+1/\tau, T).$$

Writing out Black's formula gives:

$$(L_0 + 1/\tau)(N(d_+(x, 1/\tau) - N(d_-(x, 1/\tau)) = (L_0 + \theta)(N(d_+(x_2, \theta) - N(d_-(x_2, \theta))$$

With $x = \sigma_T^{(\theta)}(L_0)$ and $x_2 = \sigma_T^{(1/\tau)}(L_0)$ and with $d_\pm(x, \theta) = \dfrac{\ln\left(\frac{L_0+\theta}{L_0+\theta}\right) \pm x^2(T)/2}{x\sqrt{T}} = \pm x\sqrt{T}/2$. With N the standard normal cummulative distribution function. Note this further gives for $x > 0$:

$$\left(2N\left(\frac{x\sqrt{T}}{2}\right) - 1\right) = \frac{L_0 + \theta}{L_0 + 1/\tau}\left(2N\left(\frac{x_2\sqrt{T}}{2}\right) - 1\right).$$

Note the following holds for $x > 0$:

$$\begin{aligned}
2N(x) - 1 &= 2\int_0^x \frac{1}{\sqrt{2\pi}} \exp\left(-\frac{1}{2}u^2\right) du \\
&= \frac{2}{\sqrt{2\pi}} \sum_{i=0}^{\infty} \int_0^x \frac{\left(-\frac{1}{2}u^2\right)^i}{i!} du \\
&= \frac{2}{\sqrt{2\pi}} \sum_{i=0}^{\infty} \left(-\frac{1}{2}\right)^i \frac{x^{2i+1}}{i!(2i+1)} \\
&= \frac{1}{\sqrt{2\pi}}(x - \frac{1}{6}x^3 + O(x^5))
\end{aligned}$$

Using the approximation $2N(x) - 1 = \frac{1}{\sqrt{2\pi}}x$ proves the result.

A.6 Cubic spline interpolation

A.6.1 Curve cubic spline interpolation

Let $0 < T_0 < ... < T_N$, with discount curve spine point vector given by $(1, P(0, T_0), ..., P(0, T_N))$. Let y given by Equation (2.3.3) be the corresponding yield curve with spine-point vector $\mathbf{y} = (y(0), .., y(T_N))$. Let $\mathbf{y}'$ and $\mathbf{y}''$ be the corresponding derivative vectors at the spine points. Cubic-splines interpolation rests on imposing a second order differentiable yield curve with continuous second order derivatives:

$$y''(T) = \left(y''(T_i)\frac{T_{i+1} - T}{T_{i+1} - T_i} + y''(T_{i+1})\frac{T - T_i}{T_{i+1} - T_i}\right) \text{ if } T \in [T_i, T_{i+1}]. \tag{A.18}$$

After integrating twice and imposing continuity at the spine points of $\mathbf{y}'$ and $\mathbf{y}$ we get the known equation for the yield curve on $[0, T_N]$:

$$\begin{aligned}
y(T) = \frac{(T_{i+1}-T)^3}{6h_i}y_i'' + \frac{(T-T_i)^3}{6h_i}y_{i+1}'' + (T_{i+1} - T)\left(\frac{y_i}{h_i} - \frac{h_i}{6}y_i''\right) \\
+ (T - T_i)\left(\frac{y_{i+1}}{h_i} - \frac{h_i}{6}y_{i+1}''\right),
\end{aligned} \quad \text{if } T \in [T_i, T_{i+1}], \tag{A.19}$$

with $h_i = T_{i+1} - T_i$, $\mathbf{y}''$ is obtained from $\mathbf{y}$ by equations for $i \in \{0, ..., N-1\}$:

$$\frac{h_{i-1}}{6}y_{i-1}'' + \frac{h_{i-1} + h_i}{3}y_i'' + \frac{h_i}{6}y_{i+1}'' = \frac{1}{h_{i-1}}y_{i-1} - \left(\frac{1}{h_{i-1}} + \frac{1}{h_i}\right)y_i + \frac{1}{h_i}y_{i+1}. \tag{A.20}$$

Cubic spline interpolation fully determines the yield curve on $[0, T_N]$ after specifying $\mathbf{y}$, y_{-1}, y_{-1}'' and y_N''. The choice of $y_{-1}'' = y_N'' = 0$ corresponds to 'natural' cubic splines, which make sense from the perspective that at points 0 and T_N there should be no instantaneous change of the underlying yield curve slope.

y_{-1} corresponds to the virtual yield curve point such that $\exp(-y_{-1}0) = P(0, 0) = 1$ and can be chosen freely. Choosing y_{-1} correctly is not obvious, but what can be denoted in the below plot that by choosing $y_{-1} = 0$ we get oscillations in the initial parts of the forward curves, as visible in Figures A.1 and A.2:

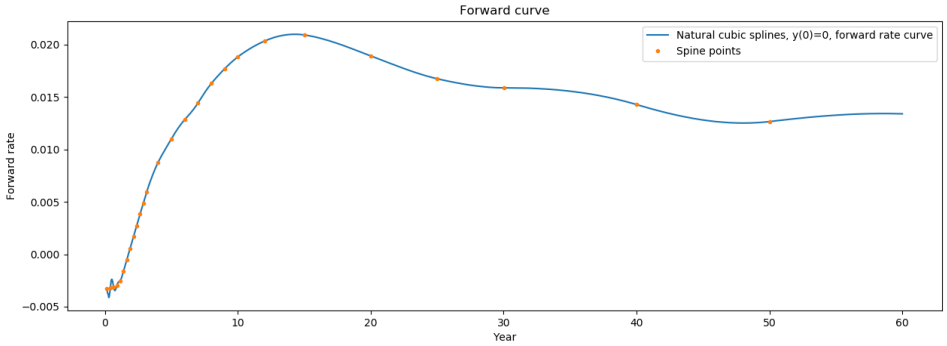

Figure A.1: 3MEUR forward curve.

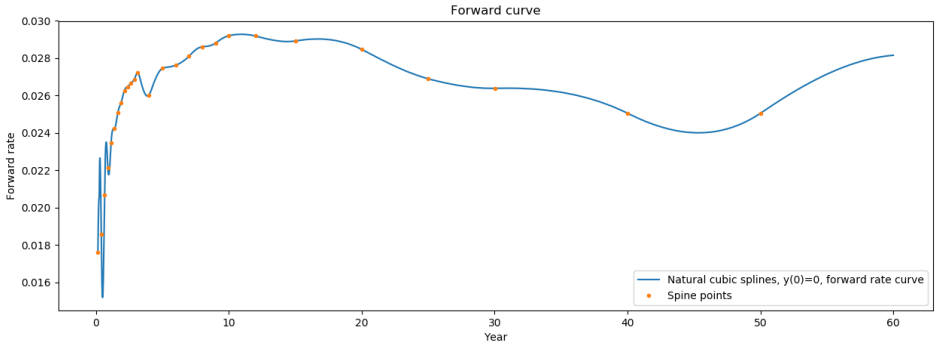

Figure A.2: 3MUSD forward curve.

The effect is moderate for the European curve, but much worse for the USD curve. This effect can be explained by looking at the corresponding yield curves:

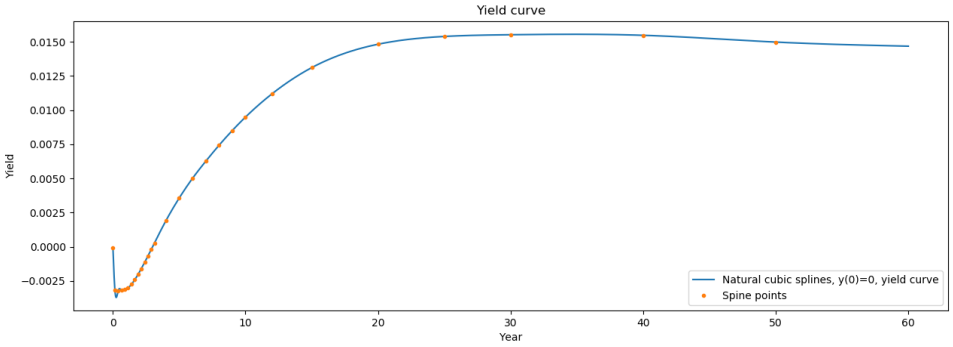

Figure A.3: 3MEUR yield curve.

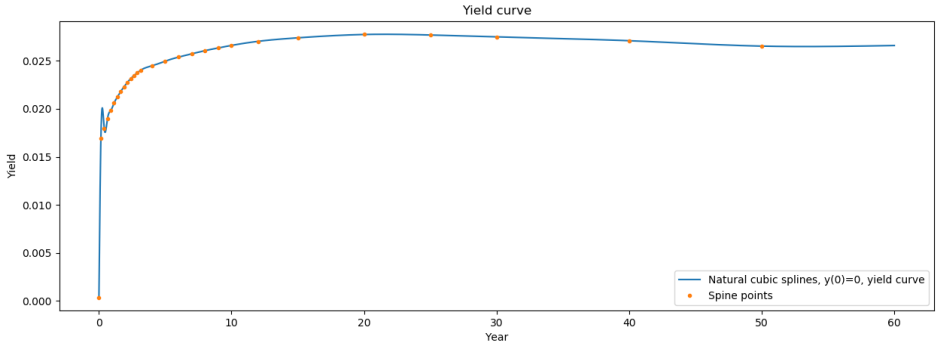

Figure A.4: 3MUSD yield curve.

and denoting due to the differing levels of y_0 and y_{-1} imposing $y_{-1} = 0$ creates a yield curve interpolation procedure with a very high first order derivative on $[0, T_0]$, which sticks initially on the interval $[T_0, T_1]$ creating an oscillation because y_1 and y_0 are on very similar levels unlike y_0 and y_{-1}. This problem can be solved by imposing a straight line through the yield curve on $[0, T_1]$, giving the following condition for y_{-1}:

$$y_{-1} = y_0 - h_{-1}\frac{y_1 - y_0}{h_0}. \tag{A.21}$$

Resulting in the forward curves visible in Figure 3.6 and the corresponding non-oscillating yield curves:

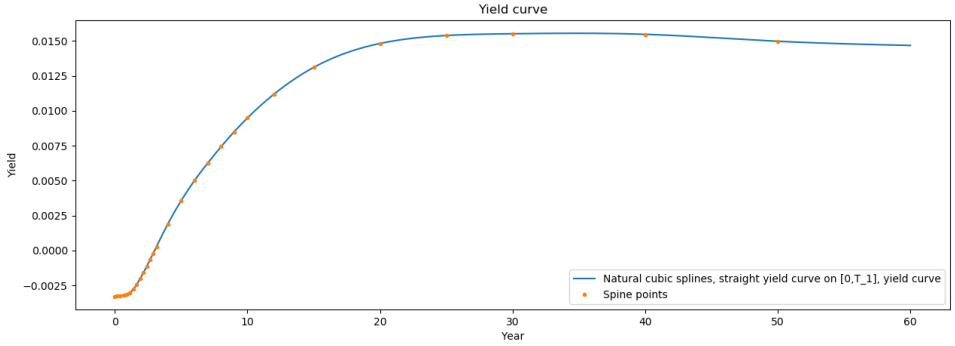

(a) 3MEUR yield curve

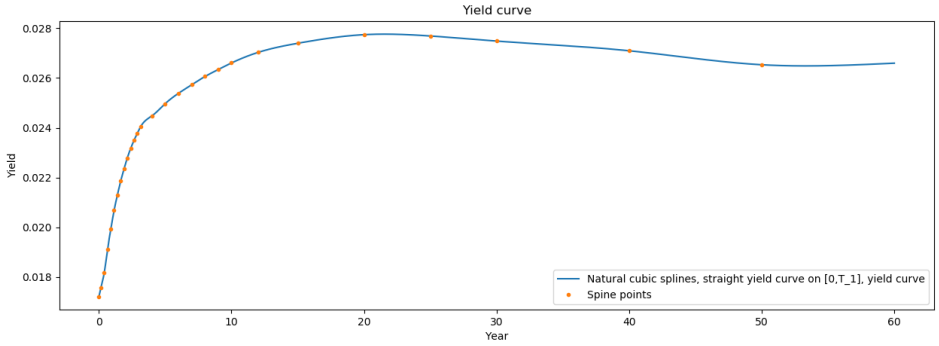

(b) 3MUSD yield curve.

Figure A.5: 25th of January 2018, yield curves, cubic spline interpolation with $y(0)$ given by (A.21).

A.6.2 Smile cubic spline interpolation

Provided a volatility smile like the one given in Figure 2.15, with known strike vector $(K_1, ..., K_{n-1})$ and smile spine-point vector $(\sigma_1, .., \sigma_{n-1})$ we introduce ghost points σ_0 at $K_0 = a$ and σ_n at $K_n = b$, such that $\sigma_n'' = \sigma_0'' = 0$ and σ_0 extends such that both the sets $(K_0, \sigma_0), (K_1, \sigma_1)$ and (K_2, σ_2) lay on a straight line in the (K, σ) plane, see (A.21). Doing the same for $(K_{n-2}, \sigma_{n-2}), (K_{n-1}, \sigma_{n-1})$ and (K_n, σ_n) gives an unfeasible smile where $\sigma(K)$ blows up for $K > K_n$ depending on σ_{n-1} and σ_{n-2}. We induce a slope penalizer $p = 5$ such that $\sigma_K = \frac{K-K_{n-1}}{p}\frac{\sigma_{n-1}-\sigma_{n-2}}{K_{n-1}-K_{n-2}} + \sigma_{n-1}$ for $K \geq K_{n-1}$.

A.7 Curve uniqueness

The Banach fixed point theorem states:

Lemma A.7.1 (Banach fixed point theorem)**.** Given some function $F : \mathbb{R}^n \to \mathbb{R}^n$. Given the existence of some domain $\Sigma \subset \mathbb{R}^n$ such that for any $P_1, P_2 \in \Sigma$ the following holds:

$$||P_1 - P_2|| \leq q||F(P_1) - F(P_2)||,$$

with $q \in [0, 1)$ then for any norm $||\cdot||$ the Picard iteration scheme: $P_n = F(P_{n-1})$ gives a converging sequence with unique solution P given any starting point P_0 in Σ.

Proof. Firstly we show the existence of a limit. Note: $||P_n - P_{n-1}|| \leq q||F(P_n) - F(P_{n-1})|| = q||P_{n-1} - P_{n-2}|| \leq q^{n-1}||P_1 - P_0||$. Given that $q \in [0, 1)$ the sequence P_n clearly converges to some limit P. Using different initial values $\hat{P}_0$ and P_0 uniqueness follows from noting $\lim_{n\to\infty} ||\hat{P}_n - P_n|| = \lim_{n\to\infty} ||F(\hat{P}_n) - F(P_n)|| \leq q \lim_{n\to\infty} ||\hat{P}_n - P_n||$. Which only holds if $\lim_{n\to\infty} ||\hat{P}_n - P_n|| = 0$. □

Assuming linear discount factor interpolation we can denote that the discount spine point vector solution of (4.5) is given implicitly by:

$$\mathbf{P} = \mathbf{A}(\mathbf{C}(\mathbf{P}), \mathbf{Q})^{-1}\mathbf{b} = \mathbf{F}(\mathbf{P}),$$

analogously to Equation (3.9). We will limit our attention to the discount curve determined by the first deposit and futures rate, which will be generalised at the end of this appendix, giving the system[1]:

$$\begin{pmatrix} 1 + \tau_{-1}dep_1 & 0 \\ -1 & 1 + \tau_0(Fut_1 - C_1(\mathbf{P})) \end{pmatrix} \begin{pmatrix} P(0, T_1) \\ P(0, T_2) \end{pmatrix} = \begin{pmatrix} 1 \\ 0 \end{pmatrix},$$

with:

- $\mathbf{P} = (P(0, T_0), P(0, T_1))$.
- $\mathbf{C}(\mathbf{P}) = (C_1(\mathbf{P}), C_2(\mathbf{P}))$.
- $\mathbf{b} = \begin{pmatrix} 1 \\ 0 \end{pmatrix}$.
- $\mathbf{A}(\mathbf{C}(\mathbf{P}), \mathbf{Q}) = \begin{pmatrix} 1 + \tau_{-1}dep_1 & 0 \\ -1 & 1 + \tau_0(Fut_1 - C_1(\mathbf{P})) \end{pmatrix}$.

We define $\mathbf{F}$ such that:

$$\mathbf{F}(\mathbf{P}) = \mathbf{A}(\mathbf{C}(\mathbf{P}), \mathbf{Q})^{-1}\mathbf{b}$$

Note $\mathbf{F}(\mathbf{P}) =$
$\begin{pmatrix} \frac{1}{1+\tau_{-1}dep_1} & 0 \\ \frac{1}{(1+\tau_{-1}dep_1)[1+\tau_0(Fut_1 - C_1(\mathbf{P}))]} & \frac{1}{[1+\tau_0(Fut_1 - C_1(\mathbf{P}))]} \end{pmatrix} \begin{pmatrix} 1 \\ 0 \end{pmatrix} = \begin{pmatrix} \frac{1}{1+\tau_{-1}dep_1} \\ \frac{1}{(1+\tau_{-1}dep_1)[1+\tau_1(Fut_1 - C_1(\mathbf{P}))]} \end{pmatrix}$

Existence and uniqueness of the curve resulting from the nested calibration routine given by (4.6) now follows from the Banach fixed point theorem if we can prove:

$$||\mathbf{F}(\mathbf{P_1}) - \mathbf{F}(\mathbf{P_2})|| \leq q||\mathbf{P_1} - \mathbf{P_2}|| \tag{A.22}$$

for some $q \in [0, 1)$ for all $\mathbf{P_i}$ in some feasible domain Σ for the spine-point vector.
Now note:

$$||\mathbf{F}(\mathbf{P_1}) - \mathbf{F}(\mathbf{P_2})||_1$$

[1] Assuming the deposit maturity equals the futures rate starting date, if the starting date is earlier, little changes in this proof.

$$= \frac{1}{1+\tau_{-1}dep_1} \left\| \frac{1}{1+\tau_0(Fut_1 - C_1(\mathbf{P_2}))} - \frac{1}{1+\tau_0(Fut_1 - C_1(\mathbf{P_1})} \right\|_1 . \tag{A.23}$$

Be the mean value theorem we can rewrite the criterium (A.22) to:

$$\left\| \frac{1}{1+\tau_{-1}dep_1} \frac{\tau_0}{[1+\tau_0(Fut_1 - x)]^2} \right\|_1 (C_1(\mathbf{P_2}) - C_1(\mathbf{P_1})) \leq q \|\mathbf{P_2} - \mathbf{P_1}\|_{\mathbf{1}}, \tag{A.24}$$

which is implied by:

$$\frac{|\nabla C_1(\mathbf{P_1}) \cdot (\mathbf{P_2} - \mathbf{P_1})|}{||\mathbf{P_2} - \mathbf{P_1}||_{\mathbf{1}}} \leq q[1+\tau_0(Fut_1 - x)]^2(1+\tau_{-1}dep_1)/\tau_0$$

for some x between $C_1(\mathbf{P_2})$ and $C_1(\mathbf{P_1})$. Which is again implied by:

$$\max(|\nabla C_1(\mathbf{P_1})|) \leq q[1+\tau_0(Fut_1 - x)]^2(1+\tau_{-1}dep_1)/\tau_0$$

$|\mathbf{v}|$ is the corresponding vector $\mathbf{v}$ with absolute values of the corresponding scalars. Given feasible values for $(1+\tau_{-1}dep_1)(1+\tau_0(Fut_1 - x))$, in very unrealistic scenarios for deposit rates and forward rates of -10%, provided $\tau_i \approx 1/4$ when calibrating the 3-month curve, the condition is implied by $\max(|\nabla C_1(\mathbf{P_1})|) \leq 4q \cdot 0.975^3$.

Which gives very crude criterium: $|\frac{\partial C_1}{\partial P_i}(\mathbf{P})| < 4a^3 q$, for any $\mathbf{P} \in \Sigma$ and any $i \in \{1,2\}$ that guarantees (A.22), with $a = 0.975$ and some $q < 1$.
Using n futures rates with tenor-structure $T_1 < ... < T_n$ and deposit rate with maturity T_0 in calibration the criterium can be generalised to: $n|\frac{\partial C_j}{\partial P_i}(\mathbf{P})| < 4a^{n+2}q$ any $j \in \{1,...,n\}$ and $i \in \{1,...,n+1\}$ that guarantees convergence and unicqueness of the curve, with $a = 0.975$. Using some feasible subset of $\mathbb{R}^{n+1}$ for the spine point vector, we choose $(0,2]^{n+1}$. Finally the criterium can be summarized as:

$$\left| \frac{\partial C_j}{\partial P_i} \right| (\mathbf{P}) < 4a^{n+2}q/n \text{ for any } j \in \{1,...,n\}, i \in \{1,...,n+1\}, \tag{A.25}$$

for any $\mathbf{P} \in \Sigma = (0,2]^{n+1}$ with $q < 1$ and $a = 0.975$. Criterium can be relaxed by choosing Σ smaller or a larger.

A.8 Libor forward rate density

$$\begin{aligned}
\frac{\partial}{\partial K}\mathbb{E}^M\left[(L_t - K)^+ | \mathscr{F}_t\right] &= \lim_{\Delta K \to 0} \frac{\int_{K+\Delta K}^{\infty} (x - (K+\Delta K)) f(x)dx - \int_K^{\infty} (x-K)f(x)dx}{\Delta K} \\
&= \lim_{\Delta K \to 0} \frac{-\Delta K \int_{K+\Delta K}^{\infty} f(x)dx - \int_K^{K+\Delta K} (x-K)f(x)dx}{\Delta K} \\
&= -\int_K^{\infty} f(x)dx.
\end{aligned} \tag{A.26}$$

from which follows:

$$\begin{aligned}
\frac{\partial^2}{\partial K^2}\mathbb{E}^M\left[(L_t - K)^+ | \mathscr{F}_t\right] &= -\frac{\partial}{\partial K}\int_K^{\infty} f(x)dx \\
&= \lim_{\Delta K \to 0} \frac{-\int_{K+\Delta K}^{K} f(x)dx}{\Delta K} \\
&= f(K)
\end{aligned} \tag{A.27}$$

Result follows analogously using a put payoff.

A.9 Out of the money choice for density functions

Carr and Madan have derived, see [9], for any κ:

$$f(L_T) = f(\kappa) + f'(\kappa)((L_T-\kappa)^+ - (\kappa - L_T)^+) \quad + \int_\kappa^\infty f(x)(L_T - x)^+ dx + \int_{-\infty}^\kappa f(x)(x - L_T)^+ dx. \tag{A.28}$$

Which implies, after choosing $\kappa = L_0$:

$$\mathbb{E}^M[f(L_T)] = f(L_0) + \int_{L_0}^\infty f(x)P_0(L_0,x)dx + \int_{-\infty}^{L_0} f(x)P_0(L_0,x)dx. \tag{A.29}$$

$$\approx f(L_0) + \int_{L_0}^b f(x)P_0(L_0,x)dx + \int_a^{L_0} f(x)P_0(L_0,x)dx \tag{A.30}$$

Such that: $\left|\mathbb{E}^M[f(L_T)] - \left(f(L_0) + \int_{L_0}^b f(x)P_0(L_0,x)dx + \int_a^{L_0} f(x)P_0(L_0,x)dx\right)\right| < \epsilon_2$.
Given an upper bound ϵ_1 for the induced error in approximation (4.27). Combining Equations (4.29) and (A.30) finally gives

$$\left|f(b)\frac{\partial}{\partial K}C(L_0,b) - f(a)\frac{\partial}{\partial K}P(L_0,a) + f'(a)P(L_0,a) - f'(b)C(L_0,b)\right| < \epsilon_1 + \epsilon_2 \tag{A.31}$$

This means that both the values aswell as strike derivatives of the calls and puts have to be negligible at the boundaries for arbitrary choices of f, which is the case when choosing out of the money calls and puts for the density ψ^{L_0}.

A.10 Ho-Lee M-forward measure correlation

Let $(\mathbb{Q}, D)$ and $(\mathbb{Q}, P(\cdot, M))$ be the risk neutral and M-forward numeraire pairs given by Equations (2.2.2) and (2.1.2). We assume the induced drift after measure change is given by (4.16). We know from Equations (4.10) and (4.12):

$$r_s = f(s,s) = f(0,s) + \int_0^s \sigma_f(u,s)\sigma_P(u,s)du + \int_0^s \sigma_f(u,s)dW_u^{\mathbb{Q}} \tag{A.32}$$

$f(0,\cdot)$ depends on the Libor curve $P(0,\cdot)$. This gives after imposing $D_0 = 0$:

$$\begin{aligned}
D_T &= \exp\left(\int_0^T r_s ds\right) \\
&= \exp\left(\int_0^T f(0,s) + \int_0^s \sigma_f(u,s)\sigma_P(u,s)duds + \int_0^T\int_0^s \sigma_f(u,s)dW_u^{\mathbb{Q}}ds\right) \\
&= \exp\left(\int_0^T f(0,s) + \int_0^s \sigma_f(u,s)\sigma_P(u,s)duds + \int_0^T\int_u^T \sigma_f(u,s)dsdW_u^{\mathbb{Q}}\right) \\
&= \exp\left(\int_0^T f(0,s) + \int_0^s \sigma_f(u,s)\sigma_P(u,s)duds + \int_0^T \sigma_P(u,T)dW_u^{\mathbb{Q}}\right) \\
&= \exp\left(\int_0^T f(0,s) + \int_0^s \sigma_f(u,s)\sigma_P(u,s)duds - \int_0^T \sigma_P(u,T)\sigma_P(u,M)du + \int_0^T \sigma_P(u,T)dW_u^M\right)
\end{aligned} \tag{A.33}$$

We choose:

$$A_D = \exp\left(\int_0^T f(0,s) + \int_0^s \sigma_f(u,s)\sigma_P(u,s)duds - \int_0^T \sigma_P(u,T)\sigma_P(u,M)du\right)$$

and

$$A_L = (L_0 + 1/\tau)\exp\left(-\frac{1}{2}\int_0^T [\sigma_P(u,M) - \sigma_P(u,T)]^2 du\right).$$

Such that, see Equation (4.19):

$$L_T + 1/\tau = A_L \exp\left(\int_0^T \sigma_P(u,M) - \sigma_P(u,T)dW_u^M\right)$$

and

$$D_T = A_D \exp\left(\int_0^T \sigma_P(u,T)dW_u^M\right)$$

Using Equations (A.33) and Equation (4.19) we can now derive:

$$\begin{aligned}
\mathrm{Cov}^M(L_T, D_T) &= \mathrm{Cov}^M(L_T, D_T) \\
&= \mathbb{E}^M[L_T D_T] - \mathbb{E}^M[L_T]\,\mathbb{E}^M[D_T] \\
&= A_D A_L \mathbb{E}^M\left[\exp\left(\int_0^T \sigma_P(u,M)dW_u^M\right)\right] \\
&- A_D A_L \mathbb{E}^M\left[\exp\left(\int_0^T \sigma_P(u,M) - \sigma_P(u,T)dW_u^M\right)\right]\mathbb{E}^M\left[\exp\left(\int_0^T \sigma_P(u,T)dW_u^M\right)\right] \\
&= A_D A_L \exp\left(\frac{1}{2}\int_0^T \sigma_P(u,M)^2 du\right) - A_D A_L \exp\left(\frac{1}{2}\int_0^T \sigma_P(u,M) - \sigma_P(u,T)]^2 + \sigma_P(u,T)^2 du\right)
\end{aligned} \tag{A.34}$$

Further notice:

$$\begin{aligned}
\sigma_L &= \sqrt{\mathbb{E}^M[L_T^2] - \mathbb{E}^M[L_T]^2} \\
&= A_L \sqrt{\mathbb{E}^M\left[\exp\left(2\int_0^T \sigma_P(u,M) - \sigma_P(u,T)dW_u^M\right)\right] - \mathbb{E}^M\left[\exp\left(\int_0^T \sigma_P(u,M) - \sigma_P(u,T)dW_u^M\right)\right]^2} \\
&= A_L \sqrt{\exp\left(2\int_0^T [\sigma_P(u,M) - \sigma_P(u,T)]^2 du\right) - \exp\left(\int_0^T [\sigma_P(u,M) - \sigma_P(u,T)]^2 du\right)} \\
&= A_L \exp\left(\frac{1}{2}\int_0^T [\sigma_P(u,M) - \sigma_P(u,T)]^2 du\right)\sqrt{\left(\exp\left(\int_0^T [\sigma_P(u,M) - \sigma_P(u,T)]^2 du\right) - 1\right)}
\end{aligned} \tag{A.35}$$

and

$$\begin{aligned}
\sigma_D &= \sqrt{\mathbb{E}^M[D_T^2] - \mathbb{E}^M[D_T]^2} \\
&= A_D \sqrt{\mathbb{E}^M\left[\exp\left(2\int_0^T \sigma_P(u,T)dW_u^M\right)\right] - \mathbb{E}^M\left[\exp\left(\int_0^T \sigma_P(u,T)dW_u^M\right)\right]^2}
\end{aligned}$$

$$= A_D \sqrt{\exp\left(2\int_0^T \sigma_P(u,T)^2 du\right) - \exp\left(\int_0^T \sigma_P(u,T)^2 du\right)}$$
$$= A_D \exp\left(\frac{1}{2}\int_0^T \sigma_P(u,T)^2 du\right) \sqrt{\left(\exp\left(\int_0^T \sigma_P(u,T)^2 du\right) - 1\right)} \tag{A.36}$$

This gives:

$$Corr^M(L_T, D_T) = \frac{\mathrm{Cov}^M(L_T, D_T)}{\sigma_D \sigma_L}$$
$$= \frac{\exp\left(\frac{1}{2}\int_0^T \sigma_P(u,M)^2 du - \frac{1}{2}\int_0^T [\sigma_P(u,M) - \sigma_P(u,T)]^2 du - \frac{1}{2}\int_0^T \sigma_P(u,T)^2 du\right) - 1}{\sqrt{\left(\exp\left(\int_0^T [\sigma_P(u,M) - \sigma_P(u,T)]^2 du\right) - 1\right)\left(\exp\left(\int_0^T \sigma_P(u,T)^2 du\right) - 1\right)}} \tag{A.37}$$

A.11 Stressed vega profiles

Here we show, analogously to Section 4.6 the vega profiles of instruments depending on the 3M Euro Libor curve under stressed rates and volatilities, see Figures 4.10 for clarification.

A.11.1 Cash deposits

Firstly cash deposits:

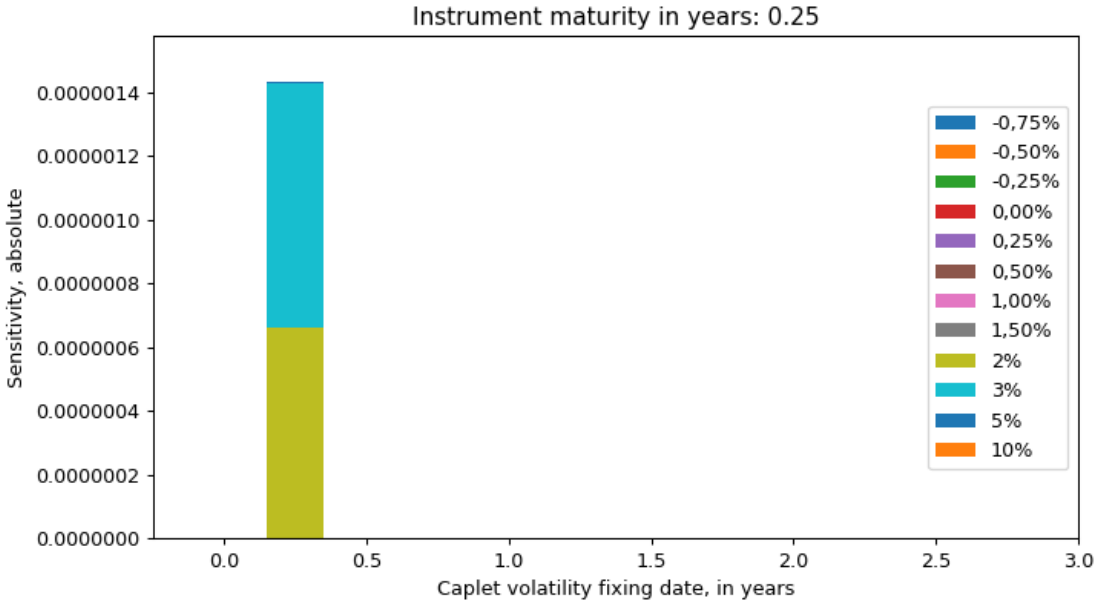

Figure A.6: Individual vegas, replication method model.

	0.25	0.5	0.75	1.0	1.25	1.5	1.75	2.0	2.25	2.5	2.75	3.0
-0,75%	0	0	0	0	0	0	0	0	0	0	0	0
-0,50%	0	0	0	0	0	0	0	0	0	0	0	0
-0,25%	0	0	0	0	0	0	0	0	0	0	0	0
0,00%	0	0	0	0	0	0	0	0	0	0	0	0
0,25%	0	0	0	0	0	0	0	0	0	0	0	0
0,50%	0	0	0	0	0	0	0	0	0	0	0	0
1,00%	0	0	0	0	0	0	0	0	0	0	0	0
1,50%	0	0	0	0	0	0	0	0	0	0	0	0
2%	0	6,6E-07	0	0	0	0	0	0	0	0	0	0
3%	0	7,71E-07	0	0	0	0	0	0	0	0	0	0
5%	0	1,81E-09	0	0	0	0	0	0	0	0	0	0
10%	0	0	0	0	0	0	0	0	0	0	0	0

Table A.1: Individual vegas, replication method model. Table

Here we display the vega profiles implied by a constant parameter Ho-Lee model and the replication method model:

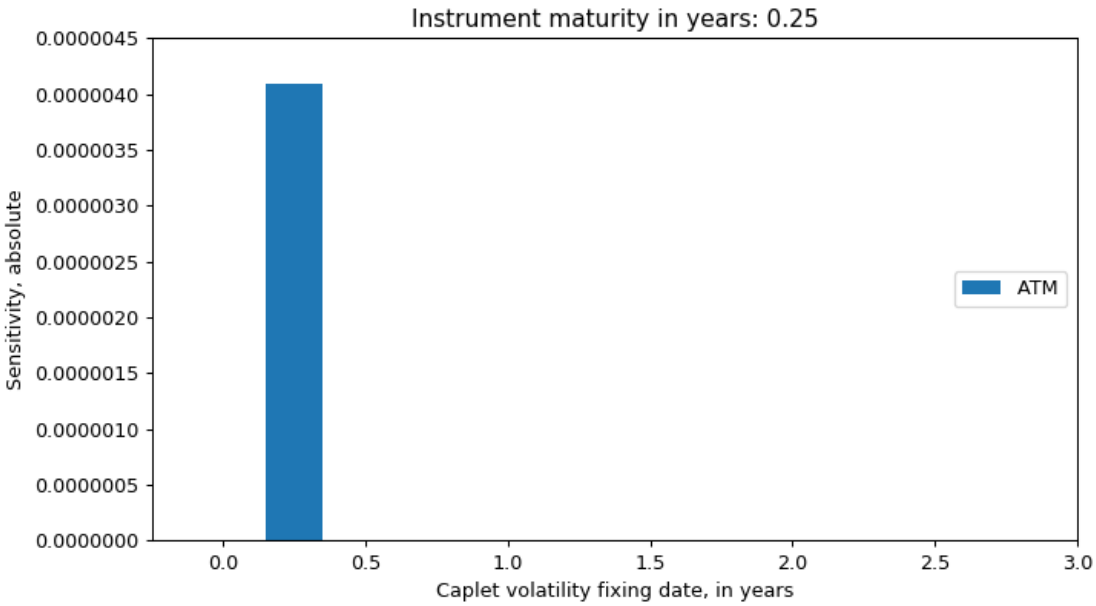

Figure A.7: Parallel smile vegas, Ho-Lee model.

	0.25	0.5	0.75	1.0	1.25	1.5	1.75	2.0	2.25	2.5	2.75	3.0
ATM	0	4,09E-06	0	0	0	0	0	0	0	0	0	0

Table A.2: Individual vegas, Ho-Lee model. Table

A.11.2 FRAs

Secondly Receiver-FRAs:

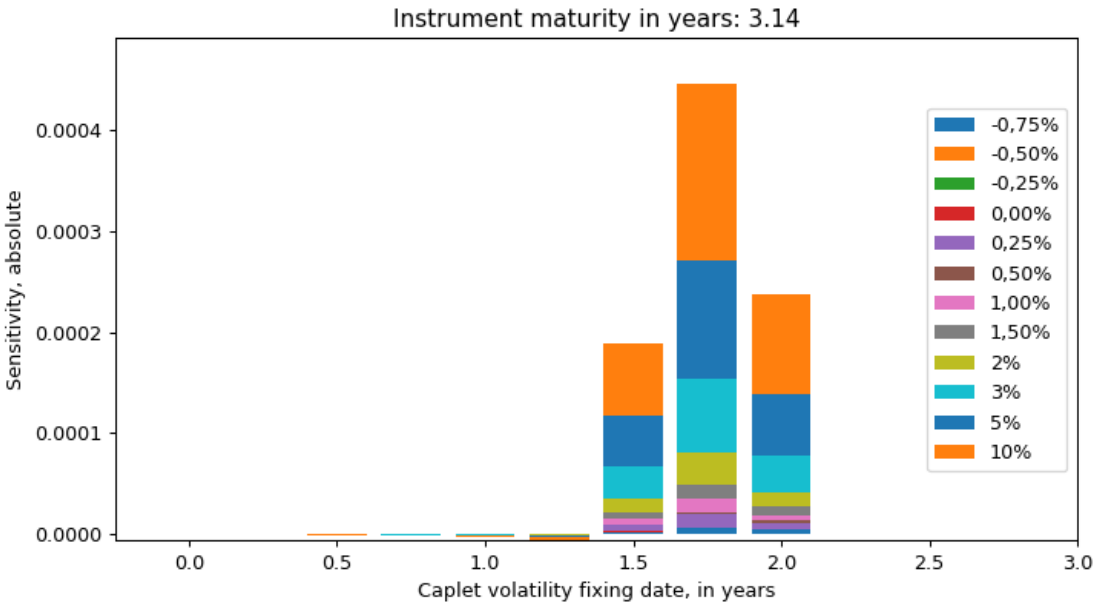

Figure A.8: Individual vegas, replication method model.

	0.25	0.5	0.75	1.0	1.25	1.5	1.75	2.0	2.25	2.5	2.75	3.0
-0,75%	0	9,99E-11	8,88E-11	-1E-09	-5,4E-09	-2,7E-08	1,89E-06	5,21E-06	3,46E-06	9,99E-11	1,01E-10	1,01E-10
-0,50%	0	9,99E-11	1,01E-10	1,01E-10	9,99E-11	9,99E-11	1,01E-10	1,01E-10	9,99E-11	9,99E-11	1,01E-10	1,01E-10
-0,25%	0	9,99E-11	-2,7E-10	-4,4E-10	9,99E-11	9,99E-11	1,01E-10	1,01E-10	9,99E-11	9,99E-11	1,01E-10	1,01E-10
0,00%	0	9,99E-11	-2,8E-09	-2,5E-08	-5,6E-08	-8,6E-08	3,77E-07	6,33E-07	9,99E-11	9,99E-11	1,01E-10	1,01E-10
0,25%	0	9,99E-11	1,01E-10	4,77E-11	-1E-08	-8,3E-08	6,35E-06	1,4E-05	6,75E-06	9,99E-11	1,01E-10	1,01E-10
0,50%	0	-8,4E-11	-5,2E-09	-1,1E-08	-5,3E-09	9,99E-11	1,01E-10	1,72E-06	2,4E-06	9,99E-11	1,01E-10	1,01E-10
1,00%	0	-1,2E-09	-4,3E-08	-1,4E-07	-2E-07	-3,2E-07	6,26E-06	1,29E-05	5,04E-06	9,99E-11	1,01E-10	1,01E-10
1,50%	0	-1,6E-08	-6,8E-08	-1,1E-07	-1,1E-07	-1,7E-07	5,54E-06	1,47E-05	9,17E-06	9,99E-11	1,01E-10	1,01E-10
2%	0	-6,3E-08	-1,8E-07	-2,5E-07	-3E-07	-5,3E-07	1,45E-05	3,16E-05	1,43E-05	9,99E-11	1,01E-10	1,01E-10
3%	0	-1,6E-07	-5E-07	-7E-07	-7,7E-07	-1,2E-06	3,17E-05	7,27E-05	3,64E-05	9,99E-11	1,01E-10	1,01E-10
5%	0	-4,9E-08	-3E-07	-7E-07	-9,5E-07	-1,7E-06	5,01E-05	0,000117	6,07E-05	9,99E-11	1,01E-10	1,01E-10
10%	0	-1,2E-09	-1,4E-07	-5,8E-07	-9,9E-07	-1,9E-06	7,17E-05	0,000175	9,87E-05	9,99E-11	1,01E-10	1,01E-10

Table A.3: Individual vegas, replication method model. Table

Here we display the vega profiles implied by a constant parameter Ho-Lee model and the replication method model:

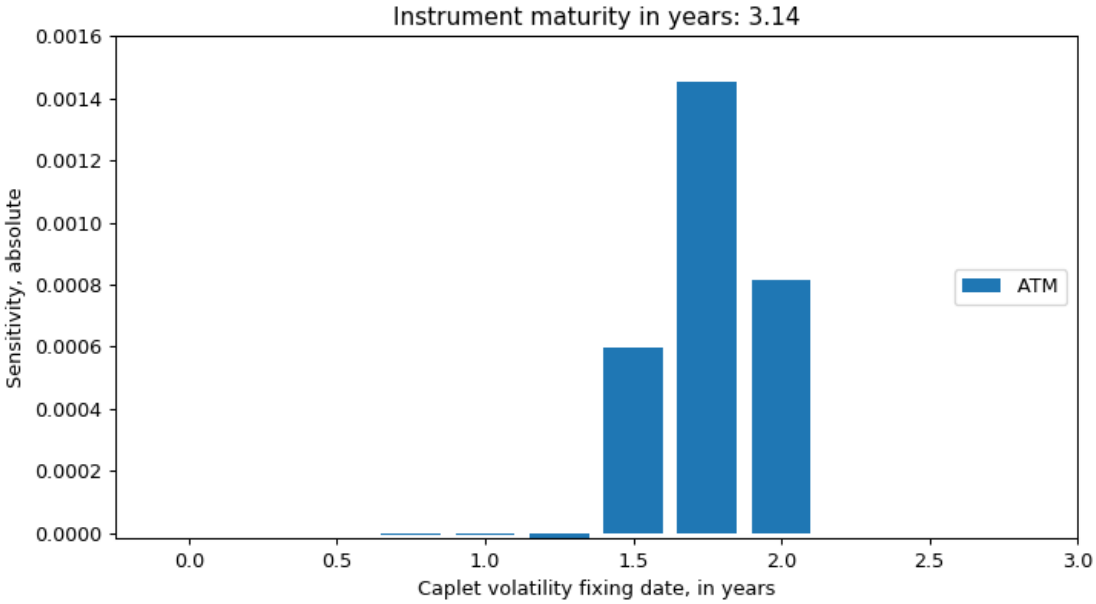

Figure A.9: Parallel smile vegas, Ho-Lee model.

	0.25	0.5	0.75	1.0	1.25	1.5	1.75	2.0	2.25	2.5	2.75	3.0
ATM	0	-4,7E-07	-2,1E-06	-4,8E-06	-7,5E-06	-1,6E-05	0,000596	0,001454	0,000814	-2,2E-12	-2,2E-12	-2,2E-12

Table A.4: Individual vegas, Ho-Lee model. Table

A.11.3 Swaps

Finally fixed-for-floating swaps:

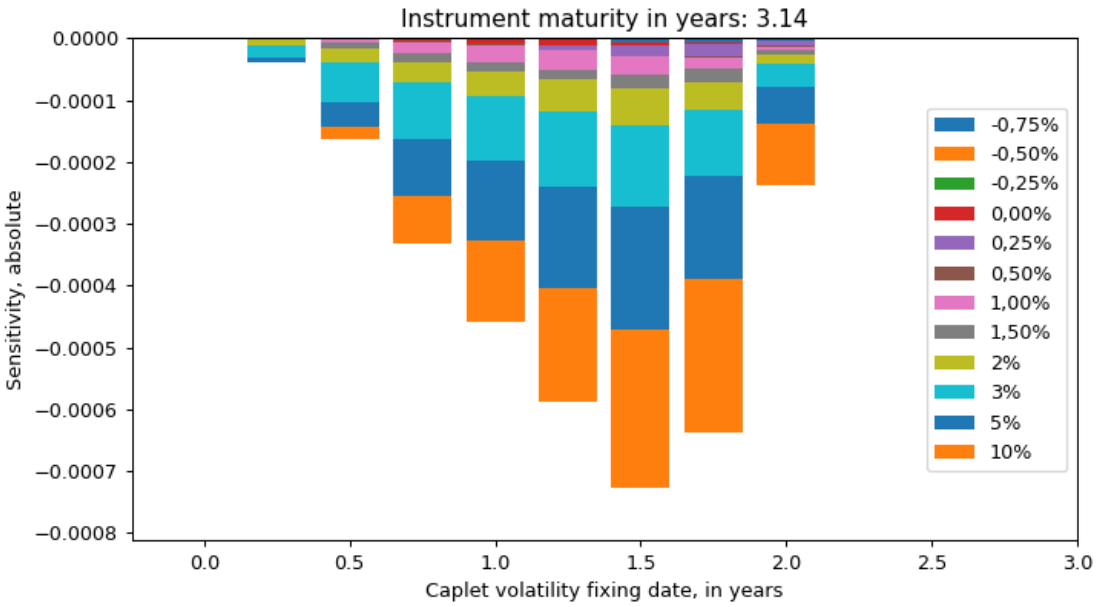

Figure A.10: Individual vegas, replication method model.

	0.25	0.5	0.75	1.0	1.25	1.5	1.75	2.0	2.25	2.5	2.75	3.0
-0,75%	0	-1,5E-10	-1,7E-09	-1,5E-07	-7,5E-07	-2,3E-06	-5,5E-06	-7,1E-06	-3,5E-06	-1,5E-10	-1,5E-10	-1,5E-10
-0,50%	0	-1,5E-10	-1,5E-10	-1,5E-10	-1,5E-10	-1,5E-10	-1,5E-10	-1,5E-10	-1,5E-10	-1,5E-10	-1,5E-10	-1,5E-10
-0,25%	0	-1,5E-10	-4,8E-08	-7,1E-08	-1,5E-10	-1,5E-10	-1,5E-10	-1,5E-10	-1,5E-10	-1,5E-10	-1,5E-10	-1,5E-10
0,00%	0	-1,5E-10	-3,8E-07	-3,4E-06	-7,6E-06	-8,8E-06	-5,6E-06	-1,1E-06	-1,5E-10	-1,5E-10	-1,5E-10	-1,5E-10
0,25%	0	-1,5E-10	-1,5E-10	-7,1E-09	-1,4E-06	-7E-06	-1,8E-05	-2E-05	-6,7E-06	-1,5E-10	-1,5E-10	-1,5E-10
0,50%	0	-2,5E-08	-7E-07	-1,5E-06	-7,3E-07	-1,5E-10	-1,5E-10	-1,7E-06	-2,4E-06	-1,5E-10	-1,5E-10	-1,5E-10
1,00%	0	-1,8E-07	-5,6E-06	-1,9E-05	-2,8E-05	-3,2E-05	-3E-05	-1,9E-05	-5E-06	-1,5E-10	-1,5E-10	-1,5E-10
1,50%	0	-2,1E-06	-9E-06	-1,4E-05	-1,5E-05	-1,7E-05	-2E-05	-2E-05	-9,2E-06	-1,5E-10	-1,5E-10	-1,5E-10
2%	0	-8,4E-06	-2,3E-05	-3,3E-05	-4E-05	-5,2E-05	-6E-05	-4,6E-05	-1,4E-05	-1,5E-10	-1,5E-10	-1,5E-10
3%	0	-2,1E-05	-6,5E-05	-9,2E-05	-0,0001	-0,00012	-0,00013	-0,00011	-3,6E-05	-1,5E-10	-1,5E-10	-1,5E-10
5%	0	-6,5E-06	-4E-05	-9,2E-05	-0,00013	-0,00016	-0,0002	-0,00017	-6,1E-05	-1,5E-10	-1,5E-10	-1,5E-10
10%	0	-1,7E-07	-1,8E-05	-7,7E-05	-0,00013	-0,00018	-0,00026	-0,00025	-9,9E-05	-1,5E-10	-1,5E-10	-1,5E-10

Table A.5: Individual vegas, replication method model. Table

Here we display the vega profiles implied by a constant parameter Ho-Lee model and the replication method model:

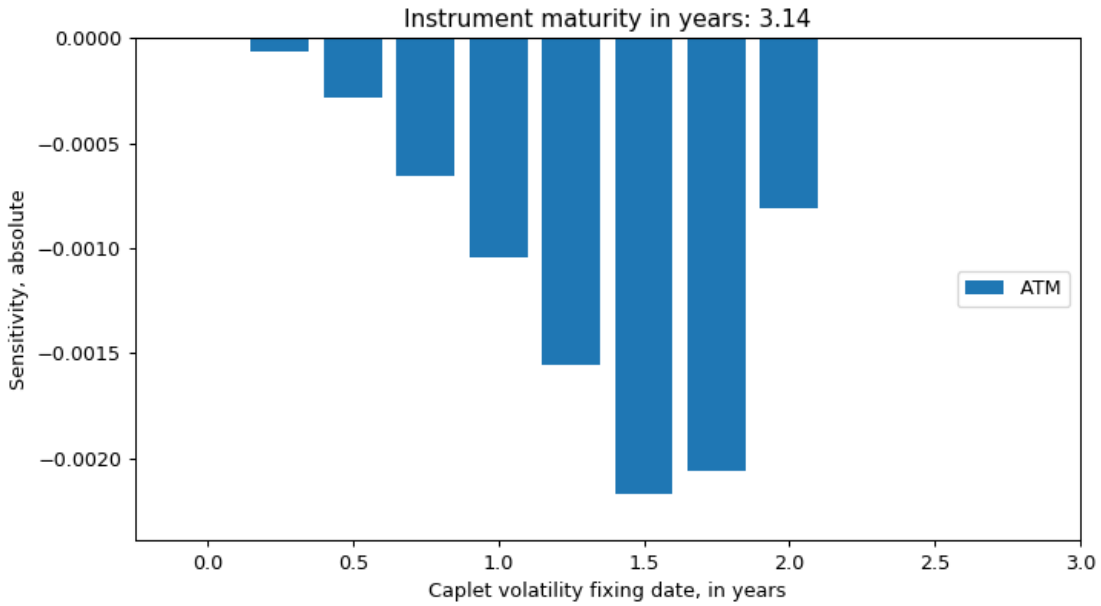

Figure A.11: Parallel smile vegas, Ho-Lee model.

	0.25	0.5	0.75	1.0	1.25	1.5	1.75	2.0	2.25	2.5	2.75	3.0
ATM	0	-6,5E-05	-0,00028	-0,00065	-0,00104	-0,00156	-0,00217	-0,00206	-0,00081	2,08E-12	2,08E-12	2,08E-12

Table A.6: Individual vegas, Ho-Lee model. Table

Chapter B

Market data

Instrument	Rates, with futures	Rates, with implied FRA	Start	Maturity	Test spine points	Convexity	
Cash 21Mar18	-0,327	-0,33	29-1-2018	21-3-2018	1.0	MAR18	0,0000
MAR18	100,3225	-0,32	21-3-2018	21-6-2018	1,0005	JUN18	0,0000
JUN18	100,3125	-0,31	20-6-2018	20-9-2018	1,0013	SEP18	0,0000
SEP18	100,2975	-0,30	19-9-2018	19-12-2018	1,0021	DEC18	0,0000
DEC18	100,2525	-0,25	19-12-2018	19-3-2019	1,0029	MAR19	0,0000
MAR19	100,1625	-0,16	20-3-2019	20-6-2019	1,0035	JUN19	0,0000
JUN19	100,0525	-0,05	19-6-2019	19-9-2019	1,0039	SEP19	0,0000
SEP19	99,9425	0,06	18-9-2019	18-12-2019	1,0040	DEC19	0,0000
DEC19	99,8325	0,17	18-12-2019	18-3-2020	1,0039	MAR20	0
MAR20	99,7275	0,27	18-3-2020	18-6-2020	1,0035	JUN20	0
JUN20	99,6175	0,38	17-6-2020	17-9-2020	1,0028	SEP20	0
SEP20	99,5125	0,49	16-9-2020	16-12-2020	0,1002	DEC20	0
DEC20	99,4075	0,59	16-12-2020	16-3-2021	1,0006		
4Y	0,1905	0,19	29-1-2018	25-1-2022	0.9991		
5Y	0,3545	0,35	29-1-2018	25-1-2023	0.9923		
6Y	0,4965	0,50	29-1-2018	25-1-2024	0.9821		
7Y	0,6205	0,62	29-1-2018	27-1-2025	0.9700		
8Y	0,7345	0,73	29-1-2018	27-1-2026	0.9565		
9Y	0,839	0,84	29-1-2018	26-1-2027	0.9415		
10Y	0,934	0,93	29-1-2018	25-1-2028	0.9253		
12Y	1,0965	1,10	29-1-2018	25-1-2030	0.9083		
15Y	1,277	1,28	29-1-2018	25-1-2033	0.8727		
20Y	1,437	1,44	29-1-2018	26-1-2038	0.8192		
25Y	1,494	1,49	29-1-2018	27-1-2043	0.7402		
30Y	1,5115	1,51	29-1-2018	27-1-2048	0.6767		
40Y	1,5185	1,52	29-1-2018	25-1-2058	0.6235		
50Y	1,489	1,49	29-1-2018	25-1-2068	0.5333		
60Y	1,471	1,47	29-1-2018	25-1-2078	0.4673		
					0.4088		

Table B.1: 25th of January 2018, 3M Euribor

Instrument	Rates, with futures	Rates, with implied FRA	Start	Maturity	Test spine points	Convexity	
Cash 21Mar18	1,76031	1,76031	29-1-2018	21-3-2018	1		
MAR18	98,1425	1,85	21-3-2018	21-6-2018	0,9973	MAR18 SP	0,0214
JUN18	97,9325	2,06	20-6-2018	20-9-2018	0,9926	JUN18 SP	0,0824
SEP18	97,7875	2,19	19-9-2018	19-12-2018	0,9874	SEP18 SP	0,1720
DEC18	97,6525	2,35	19-12-2018	19-3-2019	0,9820	DEC18 SP	0,2895
MAR19	97,5775	2,42	20-3-2019	20-6-2019	0,9763	MAR19 SP	0,4344
JUN19	97,4925	2,49	19-6-2019	19-9-2019	0,9702	JUN19 SP	0,6061
SEP19	97,4375	2,56	18-9-2019	18-12-2019	0,9641	SEP19 SP	0,8038
DEC19	97,3725	2,62	18-12-2019	18-3-2020	0,9580	DEC19 SP	1,0270
MAR20	97,3525	2,63	18-3-2020	18-6-2020	0,9517	MAR20 SP	1,2751
JUN20	97,3325	2,67	17-6-2020	17-9-2020	0,9453	JUN20 SP	1,5474
SEP20	97,3125	2,68	16-9-2020	16-12-2020	0,9391	SEP20 SP	1,8435
DEC20	97,2775	2,70	16-12-2020	16-3-2021	0,9328	DEC20 SP	2,1628
4Y	2,472	2,472	29-1-2018	25-1-2022	0,9266		
5Y	2,521	2,521	29-1-2018	25-1-2023	0,9054		
6Y	2,562	2,562	29-1-2018	25-1-2024	0,8810		
7Y	2,596	2,596	29-1-2018	27-1-2025	0,8568		
8Y	2,628	2,628	29-1-2018	27-1-2026	0,8328		
9Y	2,655	2,655	29-1-2018	26-1-2027	0,8092		
10Y	2,68	2,68	29-1-2018	25-1-2028	0,7862		
12Y	2,72	2,72	29-1-2018	25-1-2030	0,7635		
15Y	2,755	2,755	29-1-2018	25-1-2033	0,7196		
20Y	2,788	2,788	29-1-2018	26-1-2038	0,6590		
25Y	2,788	2,788	29-1-2018	27-1-2043	0,5693		
30Y	2,776	2,776	29-1-2018	27-1-2048	0,4950		
40Y	2,753	2,753	29-1-2018	25-1-2058	0,4328		
50Y	2,721	2,721	29-1-2018	25-1-2068	0,3321		
60Y	2,721	2,721	29-1-2018	25-1-2078	0,2593		
					0,19711631		

Table B.2: 25th of January 2018, 3M USD Libor

Maturity \ Strike	-0,75%	-0,50%	-0,25%	0,00%	0,25%	0,50%	1,00%	1,50%	2%	3%	5%	10%	ATM strikes	ATM volatilities
25-1-2019	6,33	4,26	5,37	8,43	10,77	12,74	15,97	18,59	20,8	24,39	29,91	42,11	-0,3	4,55
25-7-2019	7,19	5,06	5,67	8,12	10,11	11,81	14,64	16,93	18,85	21,97	26,46	33,19	-0,25	5,68
25-1-2020	8,79	6,3	6,44	8,81	10,62	12,19	14,8	16,92	18,7	21,57	25,67	31,76	-0,16	7,39
25-1-2021	11,63	9,03	8,41	10,41	11,75	12,84	14,71	16,31	17,7	20	23,34	28,33	0,03	10,59
25-1-2022	13,62	11,14	10,16	11,65	12,65	13,46	14,89	16,2	17,38	19,39	22,4	26,95	0,22	12,53
25-1-2023	14,89	12,7	11,62	12,67	13,41	14,02	15,09	16,06	16,94	18,48	20,85	24,55	0,38	13,73
25-1-2024	15,68	13,79	12,75	13,47	14,02	14,47	15,25	15,94	16,56	17,63	19,32	22,13	0,51	14,5
25-1-2025	16,34	14,66	13,65	14,11	14,51	14,84	15,42	15,93	16,39	17,21	18,53	20,81	0,63	15
25-1-2026	16,81	15,28	14,3	14,57	14,84	15,07	15,49	15,86	16,2	16,82	17,89	19,82	0,74	15,28
25-1-2027	17,14	15,71	14,76	14,9	15,06	15,21	15,48	15,73	15,96	16,4	17,22	18,86	0,84	15,4
25-1-2028	17,33	16	15,08	15,11	15,19	15,27	15,42	15,56	15,68	15,94	16,51	17,82	0,94	15,4
25-1-2030	17,47	16,29	15,43	15,32	15,28	15,25	15,22	15,19	15,16	15,16	15,33	16,15	1,09	15,21
25-1-2033	17,4	16,37	15,58	15,35	15,2	15,08	14,87	14,69	14,54	14,32	14,21	14,66	1,27	14,77
25-1-2038	17,09	16,21	15,5	15,18	14,93	14,72	14,38	14,08	13,84	13,49	13,19	13,39	1,42	14,13
25-1-2043	16,8	15,99	15,33	14,96	14,67	14,42	14	13,66	13,38	12,98	12,63	12,73	1,47	13,68
25-1-2048	16,53	15,77	15,13	14,74	14,42	14,14	13,69	13,32	13,02	12,6	12,22	12,29	1,49	13,33

Table B.3: Flat 3M Euribor shifted lognormal cap volatility surface, 25th of January 2018, ICAP. shifting parameter is 3 percent.

Maturity \ Strike	-0,50%	-0,25%	0,00%	0,25%	0,50%	0,75%	1,00%	2%	2%	3%	3%	4%	ATM strikes	ATM volatilities
25-1-2019	93,6	85,9	78,5	71,5	57,35	45,08	36,46	23,72	13,51	13,51	15,87	21,55	2,11	13,42
25-1-2020	68,4	65	63,5	61,8	48,83	40,09	34,05	25,29	17,84	16,36	15,78	16,39	2,31	16,73
25-1-2021	69,2	68,7	67,8	66,5	52,4	43,25	37,01	28,2	21,28	19,15	18,65	19,73	2,42	19,34
25-1-2022	72,2	71,9	71,3	70,2	55,69	46,04	39,55	30,57	23,87	21,28	20,53	21,14	2,48	21,34
25-1-2023	74,7	74,5	74	73,1	58,53	48,35	41,58	32,39	25,79	22,89	21,91	22,15	2,52	22,83
25-1-2024	76	76	75,6	74,8	60,35	49,8	42,86	33,59	27,1	24,01	22,81	22,71	2,55	23,81
25-1-2025	75,9	76,1	75,8	75,1	61	50,29	43,33	34,13	27,8	24,6	23,24	22,83	2,58	24,29
25-1-2026	75,7	75,9	75,7	75,1	61,34	50,52	43,55	34,42	28,23	24,97	23,48	22,81	2,61	24,54
25-1-2027	75,3	75,6	75,5	75	61,51	50,58	43,6	34,54	28,48	25,17	23,57	22,69	2,63	24,62
25-1-2028	74,9	75,2	75,1	74,7	61,49	50,48	43,51	34,52	28,56	25,23	23,53	22,46	2,66	24,57
25-1-2030	74,1	74,5	74,5	74,1	61,66	50,39	43,37	34,44	28,62	25,24	23,4	22,07	2,69	24,4
25-1-2033	73,2	73,5	73,4	73,1	62,1	50,29	43,11	34,15	28,43	25	23,03	21,45	2,72	23,97
25-1-2038	71	71,2	71	70,6	62,28	49,65	42,25	33,27	27,69	24,23	22,15	20,38	2,75	23,05

Table B.4: Flat 3M USD Libor shifted lognormal cap volatility surface, 25th of January 2018, ICAP. shifting parameter is 0 percent.